THE ASTROPHYSICAL JOURNAL

AN INTERNATIONAL REVIEW OF SPECTROSCOPY AND ASTRONOMICAL PHYSICS

VOLUME 91 APRIL 1940 NUMBER 3

SOME PROBLEMS CONCERNING THE STRUCTURE AND DYNAMICS OF THE GALACTIC SYSTEM AND THE ELLIPTICAL NEBULAE NGC 3115 AND 4494[1]

J. H. OORT

ABSTRACT

After a general introduction, in which some features of the density distribution and velocity distribution are discussed in connection with the possibility that the galaxy may have a spiral-like structure, the author attempts in the third section to elucidate the relation between density distribution and distribution of peculiar velocities. It is shown that if the large-scale unevenness in density found in a recent study is accepted, it is natural to expect a deviation of the stream vertex from the longitude of the galactic center of similar order as the deviation actually observed.

The distribution of light in the nearly spherical nebula NGC 4494 and in the strongly flattened elliptical nebula NGC 3115 has been investigated with the aid of plates taken by Dr. Oosterhoff with the 60-inch reflector on Mount Wilson. The results, as shown in Table 1 and Figures 3 and 4, can be fairly well represented by Hubble's formula $I = I_0/(1 + r/a)^2$, though some small but probably real deviations are indicated. The isophotes in NGC 3115, of which a few typical ones are shown in Figure 5, deviate markedly from ellipses and show remarkably sharp points at the equator. The ratio of the axes varies with the distance from the center; it has a minimum for a semimajor axis of 1′ (see Fig. 6). The space distribution of light in NGC 3115 has been calculated; a section with isophotal surfaces is shown in Figure 7, while the run of space density in the equatorial plane may be found in the last column of Table 1 and in the dotted curve in Figure 4. The light density near the center is of the same order as that in the center of the globular cluster M 3.

In the last section these data are considered in relation to Humason's measures of the rotation of NGC 3115. It is found that beyond about 10″ from the center in the equatorial plane the mass density must be about constant. The actual density depends on the unknown flattening of the attracting mass, but it should be at least of the order of 140 solar masses per cubic parsec (10^{-20} gm/cm^3), or 2000 times that near the sun. In this region of constant mass density the light-density diminishes with a factor of at

[1] This paper was presented at the symposium on galactic and extragalactic structure, held in connection with the dedication of the McDonald Observatory on May 5–8, 1939.

least 10; the distribution of mass in the system appears to bear almost no relation to that of light. The total mass of the system cannot yet be estimated; it should be at least 5.10^{10} solar masses but may be much larger. Expressing both mass and light in the sun as unit, one finds the ratio of mass to light in the outer parts of NGC 3115 to be about 250; this contrasts sharply with the value of 1.8 found in the neighborhood of the sun and suggests an extreme relative density of very faint dwarfs or interstellar material. The analysis further indicates that the peculiar velocities of the material (stellar or other) responsible for the light of the nebula must be high, between 100 and 200 km/sec for the parts within $a = 20''$, between 175 and 300 km/sec near $a = 45''$, the actual values depending again primarily upon the flattening assumed for the attracting mass. The distribution of velocities perpendicular to the equatorial plane indicates a remarkably strong deviation from a normal Gaussian law (cf. Table 5). The results of this section should be regarded as quite tentative, the main uncertainty being due to the possible existence of important absorption and diffusion of light within the nebula.

I. THE GALACTIC SYSTEM

STRUCTURE

About the beginning of this century the outstanding problem for the explorer of the universe was that of the size and general shape of the galactic system. The *Plan of Selected Areas* initiated by Kapteyn in 1906 was proposed principally with a view to this problem. The *Plan* has been successful in that it has helped to obtain a fairly reliable picture of the general features of the density distribution within a sphere of, roughly, 1500 parsecs radius around the sun. On account of the strong absorption of light near the galactic plane it has not yet been possible to make much use of it in outlining the dimensions of the system in the plane of the Milky Way, which, however, could be derived from other data, notably those on the distribution of globular clusters, and recently also of cluster-type variables, gathered by Shapley and others.

Though it can hardly be said that our knowledge concerning the general shape of the system is anything like final, yet some of the interest is shifting gradually to another phase, namely, that of detecting an eventual spiral structure. As has been pointed out by several authors, it can hardly be doubted that in all observable characteristics (such as extreme flatness, occurrence of many highly luminous stars, existence of a well-defined center) the galactic system resembles most strongly that class of extragalactic systems which invariably show a more or less well-defined spiral structure.

The view that the galaxy might have a spiral structure has been expressed almost since the first discoveries of spiral structure in nebulae. The oldest explicit reference to this seems to be in a paper

by Stephen Alexander.[2] Both he and Proctor,[3] seventeen years later, tried to find support for their spiral theory and to construct to some extent the galactic spiral from the appearance of the Milky Way as inferred mainly from the observations of the Herschels. In 1900, and more completely again in 1913, Easton,[4] apparently quite independently and unaware of these earlier suggestions, made a very careful study of the Milky Way as shown by modern visual and photographic observations, especially with a view to delineating the course of the possible spiral arms of the galactic system; he placed the center of the spiral in the direction of Cygnus.

Later developments have made it clear that this representation can hardly resemble the real structure of the galaxy, the main cause of its failure and of the failure of all attempts to find spiral-like structure being the strong and uneven absorption near the galactic plane; for there is little doubt that many of the features of the apparent Milky Way structure are determined rather by the distribution of absorbing material than by that of the stars.

With the data at present available the difficulty (which, as indicated, is essentially that of separating the effects of absorption and of real structure) can be overcome more or less satisfactorily only in regions at some distance from the Milky Way, where the total amount of absorption may be estimated from the numbers of extragalactic nebulae (and, in some cases, also from color excesses). The procedure involves two assumptions, which it has been possible to verify only to a certain extent: (1) the assumption that the distribution of faint nebulae presents no large-scale irregularities and (2) the supposition that the absorbing material is mainly confined to regions within a few hundred parsecs from the galactic plane. The available evidence on these two points is still unsatisfactory.

[2] "On the Origin of the Forms and the Present Condition of Some of the Clusters of Stars and Several of the Nebulae," *A.J.*, **2**, 101, 1852.

I am indebted to Dr. Rosseland for this reference as well as for that to Proctor's paper. Dr. Rosseland has also drawn my attention to the possibility that Lord Rosse himself may have had the idea that the galaxy had a spiral structure, but so far no direct published reference to this by Lord Rosse has been found.

[3] "A New Theory of the Milky Way," *M.N.*, **30**, 50, 1869.

[4] "A New Theory of the Milky Way," *Ap. J.*, **12**, 136, 1900, and "A Photographic Chart of the Milky Way and the Spiral Theory of the Galactic System," *ibid.*, **37**, 105, 1913.

The results of a study of the Selected Areas along these lines, if accepted at their face value, show that the sun is situated in a relatively sparse region, surrounded in practically all the longitudes covered by the observations by large regions where the star density within 500 parsecs of the galactic plane is higher than that near the sun. These results are certainly very tentative, and it is probable that more extensive and more adequate subsequent studies may in several regions yield considerably different densities. But the general trend of the density distribution would seem to be fairly well established. Naturally, then, the thought presents itself that the density variations found bear some relation to the spiral structures observed in extragalactic systems; but the indications are still vague and entirely qualitative.

In a flat system like the galaxy, the main results of such density analyses as the one described can be most easily represented by comparing the counted numbers of stars in a given region to the number which would be found in a standard system in which the equidensity layers are planes parallel to the galactic plane and are so arranged that they conform to the density distribution perpendicular to the galactic plane as found in the vicinity of the sun.[5] The true density distribution in space can later be easily derived from the residuals found. I believe that in the present preliminary stage of this type of investigation the procedure of starting with this simple comparison has considerable advantage, because it does not involve the use of any other data than those directly observed, and at the same time it brings out the essentials of the density phenomena studied.

It has been found by several astronomers that the arms in spiral nebulae have a color corresponding to a fairly early spectral class.[6] A large-scale survey of faint B- and A-type stars in our galaxy, accompanied by a systematic and precise investigation of their colors, might accordingly furnish a good opportunity for a further search for such a structure in the galactic system. Radial velocities and studies of differential galactic rotation would furnish a necessary check on

[5] See Vashakidse, *Bull. Abastumani Obs.*, No. 1, p. 87, 1937, and No. 2, p. 109, 1938; Oort, *Ann. d'ap.*, **1**, 71, 1938, and *B.A.N.*, No. 308, 1938.

[6] Seares, *Proc. Nat. Acad.*, **2**, 553, 1916, and Carpenter, *Pub. A.S.P.*, **43**, 294, 1931; compare also an unpublished article by Seyfert on relative colors of arms and nuclei.

the average total absorptions. Beside color excesses and galactic-rotation effects, proper motions of faint stars of known spectral type may become an important help in evaluating the absorption.

MOTIONS

It may be in place here to mention a few points concerning stellar motions, which would seem to have a bearing on the problem of the internal structure of the galactic system.

So far, the most important information derived from proper motions of faint stars has been concerned with the velocity distribution, as it has been shown that this distribution remains practically identical over a large region in the galactic plane, extending to about 1500 parsecs in the northern Milky Way. Not only do the motions of stars over this entire region follow the same ellipsoidal law, but they also appear to show the same lengths for the axes of the velocity ellipsoid and thus to indicate that the "temperature" of the stellar system does not vary perceptibly throughout the region investigated.

The extremely valuable study of radial velocities of faint δ Cephei variables recently published by Joy[7] adds important evidence to that already in existence on the relative motions of different parts of the galactic system. All available data concerning these motions can be adequately interpreted as indicating that the motions of the various parts are closely perpendicular to the direction of the material center of the system, as found from globular clusters ($l = 325° \pm 2°$ p.e.) and independently also from the distribution of stars at large distances from the galactic plane[8] ($l = 324° \pm 3°$). From a comprehensive study of the "rotation-effects" in the radial velocities Plaskett and Pearce[9] found $l = 325°.4 \pm 1°.1$ (p.e.); Joy[7] obtained $325°.3 \pm 1°.3$ (p.e.), while Merrill and Sanford's recent study of velocities from interstellar lines[10] yielded 329°. The asymmetry of high velocities and our systematic motion with respect to globular clusters and near-by extragalactic systems also point in a direction roughly 90° away from the center. Considering these data together, there appears to be pretty strong evidence that the motions in the

[7] *Ap. J.*, **89**, 356, 1939; *Mt. W. Contr.*, No. 607.

[8] *B.A.N.*, No. 308, p. 263, 1938. [9] *Victoria Pub.*, **5**, 281, 1936.

[10] *Ap. J.*, **87**, 118, 1938; *Mt. W. Contr.*, No. 585.

galactic system, at least in our surroundings, are circular around the center. If systematic motions along spiral arms exist, the arms must be very nearly circular. The data for differential rotation now extend over a disk of nearly 2500 parsecs radius around the sun, except for longitudes between 193° and 271°, where only a few observations are available. Apart from a (probably) local effect in the bright, relatively near-by B-type stars, the data show no evidence of a systematic expansion or contraction; Joy, for instance, finds a quite negligible value of -3.8 km/sec for the K-term in his distant Cepheids.

In the bright Cygnus cloud Joy has observed two faint Cepheids, GL and V343 Cygni, which, judging from unpublished color measures recently obtained by Oosterhoff, appear to be situated at distances of about 6000 and 10000 parsecs and are yet not more than 350 and 600 parsecs from the galactic plane; MZ Cygni, at $-10°$ latitude, likewise seems to have suffered but moderate absorption and to be about 5000 parsecs distant. If Joy's velocities for these three stars may be considered as representative for the regions in which they are situated, they show that also in this very distant part of the galactic system the motions can be satisfactorily represented by a simple rotation of this system. Computing the distances from the radial velocities, on the assumption that the residual velocities are wholly due to rotation of the galaxy, I find for GL Cygni 6700, for V343 Cygni 9100, and for MZ Cygni 5500 parsecs, in very good agreement with the values just quoted, which were derived from the apparent magnitudes.

The available data seem as yet to be unsuited for a significant determination of the distance to the center and still less of the arrangement of mass within the galactic system. Berman,[11] and, more recently, Camm[12] have published evidence which they interpreted as indicating that the smallest planetary nebulae are situated at distances comparable to that of the galactic center, and some even considerably farther. They conclude that the velocities of these nebulae give, therefore, information about the dynamics of the system in regions near the center. The evidence, however, is not convincing.[13]

[11] *Lick Obs. Bull.*, **18**, 57, 1937.

[12] *M.N.*, **99**, 71, 1938.

[13] Cf. Oort, *M.N.*, **99**, 376, 1939.

The large-scale irregularities indicated in the density distribution do not seem to modify the gravitational field to any observable extent, at least there is no sign of this in the differential motions. This need not cause surprise, for it can be inferred from the available data that as much as 85 per cent of the total gravitational force in our neighborhood may be considered as due to a central mass and as varying approximately as the inverse square of the distance from the center, while the rest can be adequately ascribed to a homogeneous mass extending beyond the sun.

THE DEVIATION OF THE VERTEX

Though the systematic motions of stars with small peculiar motions may be almost uninfluenced by local unevenness in the density, circumstances are quite different with regard to the *peculiar* velocities. It can easily be seen that a close relationship must exist between the distribution of peculiar velocities and the distribution of density in the surroundings of the sun. To simplify, let us consider stars moving exactly in the galactic plane. Size and shape of a stellar orbit may then be characterized by two quantities, for which we may take the mean distance from the center, $\bar{\omega}_0$, and the velocity Π_0 with which the star will pass the circle with radius $\bar{\omega}_0$ (these parameters are evidently equivalent to the parameters I_1 and I_2, the energy integrals and the momentum integrals, used so extensively by Lindblad). As long as there is no instability and as long as Π_0 is fairly small compared to the rotational velocity of the system, the motion of a star can be described approximately as following an elliptical epicycle, the center of which moves with uniform velocity over a circle of radius $\bar{\omega}_0$ around the center of the system.[14] Suppose, for simplicity, that the frequency distribution of Π_0 is the same over the whole region considered and also that the phases of the motions of the stars along the epicycles are distributed uniformly. The distribution of the centers of the epicycles will then evidently be directly related to the density distribution, while it also determines the velocity distribution at any given point.

It is well known that in a system having rotational symmetry the

[14] This description was first used by Lindblad in 1927; cf. *Arkiv f. mat., astr. o. fysik*, **20A**, No. 17, and *Upsala Medd.*, No. 26.

resulting distribution of velocities should be symmetrical with respect to an axis pointing to the center of the system, and this axis should be the major axis of the velocity ellipsoid.

The observations, especially those of bright stars, show, however, that the longitude of the major axis of the velocity ellipsoid deviates between 15° and 20° from the direction of the center. For the faint stars a deviation in the same direction is indicated, although there seems to be some evidence that it would be less pronounced for these stars.

In the representation of the system just given the most direct interpretation of the vertex deviation is that it indicates a lack of rotational symmetry in the density distribution. The assumption of an asymmetry in the density distribution of the right order to explain the deviation of the vertex is quite in line with the unevenness in the density discussed in the first section. Inversely, it might be said that the existence of the vertex deviation indicates large-scale density deviations. The relation between the two can best be illustrated by considering a simple hypothetical case.

Consider the motion of a star whose velocity is small compared to the rotational velocity of the galactic system. Let $\bar{\omega}$ be the distance from the center of the system and $\bar{\omega}_0$ the mean distance. If Θ is the transverse velocity and Θ_0 the same velocity at $\bar{\omega}_0$, then the equations of motion can, in first approximation, be written as

$$\Theta\bar{\omega} = \Theta_0\bar{\omega}_0 , \qquad \ddot{\bar{\omega}} = K_{\bar{\omega}_0} + \frac{(\bar{\omega} - \bar{\omega}_0)\partial K_{\bar{\omega}}}{\partial\bar{\omega}} + \frac{\Theta^2}{\bar{\omega}} .$$

Restricting ourselves again to first-order terms in $(\bar{\omega} - \bar{\omega}_0)/\bar{\omega}_0$, we can put

$$K_{\bar{\omega}_0} = -\frac{\Theta_0^2}{\bar{\omega}_0}$$

and

$$\frac{\partial K_{\bar{\omega}}}{\partial\bar{\omega}} = -2\frac{\Theta_0}{\bar{\omega}_0}\frac{\partial\Theta_0}{\partial\bar{\omega}_0} + \frac{\Theta_0^2}{\bar{\omega}_0^2} ,$$

so that the second equation may be reduced to

$$\ddot{\bar{\omega}} = - n^2(\bar{\omega} - \bar{\omega}_0) ,$$

where

$$n^2 = 2\left(\frac{\Theta_0^2}{\bar{\omega}_0^2} + \frac{\Theta_0}{\bar{\omega}_0}\frac{\partial\Theta_0}{\partial\bar{\omega}}\right) = - 4B(A - B) ,$$

A and B denoting the usual constants of differential galactic rotation. We obtain, accordingly,

$$\bar{\omega} - \bar{\omega}_0 = a \sin nt ,$$

while the difference between the star's actual angular velocity, ω, and the angular velocity, ω_0, of the center of the epicycle described by the star, is evidently given by

$$\omega - \omega_0 = \frac{\Theta}{\bar{\omega}} - \frac{\Theta_0}{\bar{\omega}_0} = - \frac{2a}{\bar{\omega}_0}\frac{\Theta_0}{\bar{\omega}_0} \sin nt .$$

In a system of co-ordinates rotating with an angular velocity ω_0, the orbit of the star is, therefore, given by

$$x = \bar{\omega} - \bar{\omega}_0 = a \sin nt ,$$

$$y = \frac{2a}{n}(A - B) \cos nt ,$$

y being the transverse co-ordinate reckoned from the center of the epicycle in the direction of the rotation.

Assuming $A = +0.018$ km/sec·parsec, $B = -0.013$ km/sec · parsec,[15] and, accordingly, $n = +0.040$ km/sec·parsec, we obtain an orbit as shown in Figure 1. Let us now consider a point S situated in a longitude differing by φ from that of the galactic center. We are

[15] *M.N.*, **99**, 374, 1939.

interested in the "peculiar velocity" at S or, more precisely, in the difference between the original star's velocity Π, Θ in the point S and the velocity corresponding to circular motions at S. Denoting this circular velocity by $\Theta_{c,S}$, we have

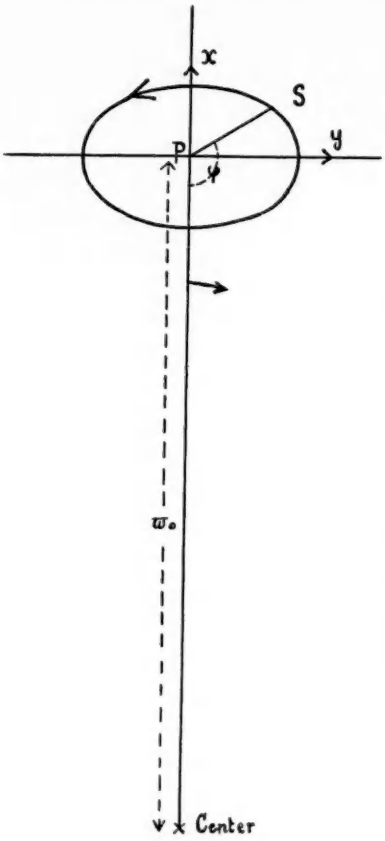

FIG. 1

$$\Theta_{c,S} = \Theta_0 + \frac{x\partial\Theta_0}{\partial\bar{\omega}},$$

and

$$\Theta = \Theta_0 - \frac{x\,\Theta_0}{\bar{\omega}_0},$$

so that

$$\Theta - \Theta_{c,S} = Bx,$$

while

$$\Pi = an\cos nt = 2By.$$

If α is the angle between the peculiar velocity at S and the direction of the galactic center, we thus have

$$\operatorname{tg}\alpha = -\frac{(\Theta - \Theta_{c,S})}{\Pi} = \frac{x}{y} = -\operatorname{ctg}\varphi.$$

Suppose now, for an illustration, that, as seen from the sun, the density of centers of epicycles between 248° and 271° galactic longitude and from 1400 to 1900 parsecs distance were twice that in the corresponding longitudes at the other side of the galactic center (between 19° and 42°). At an average longitude of 260° ($\varphi = 115°$) the distance limits considered would correspond to $x = 560$ and 730 parsecs, respectively. As $\Pi = an\cos nt = 2Bx\operatorname{tg}\varphi = -0.056x$, those stars near the sun whose epicycle centers lie in the region con-

sidered would have peculiar velocities in the Π-direction between 33 and 44 km/sec. With the aid of the foregoing equation, we find that the angles a corresponding to the limits of φ are 193° and 216°, so

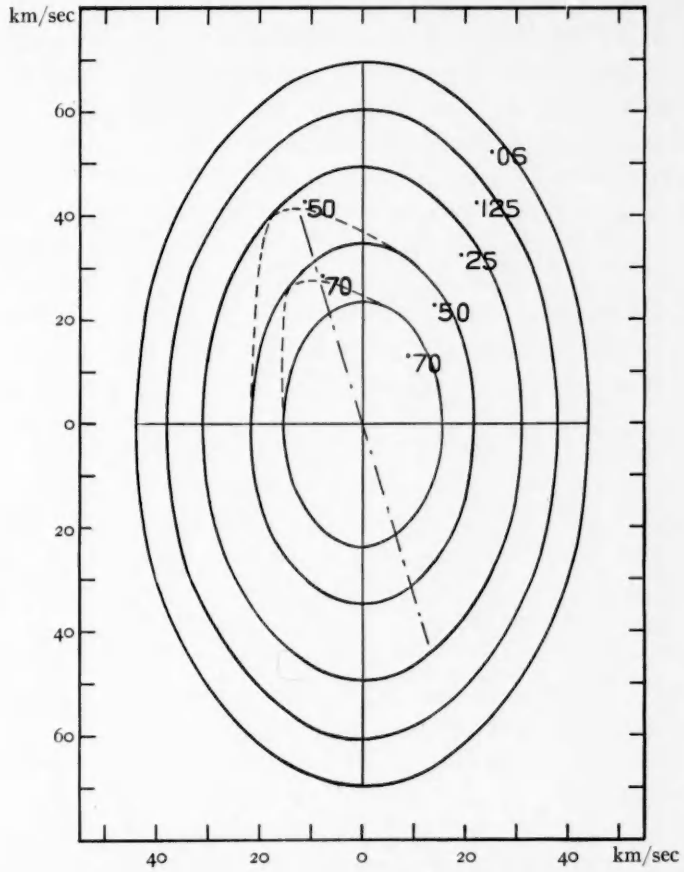

FIG. 2.—Velocity ellipsoids. The numbers attached to the ellipses indicate frequencies relative to that in the center.

that the double star density in the region considered entails a doubling of the frequency of peculiar velocities in the neighborhood of the sun between, roughly, 35 and 50 km/sec in position angles between 193° and 216° as reckoned from the direction of the galactic center. The corresponding changes in the velocity distribution are roughly pictured in Figure 2. Ordinates are peculiar velocities in the

Π-direction, abscissas those in the Θ-direction. The full-drawn ellipses, with their major axes pointing to the galactic center, represent lines of equal frequency in a symmetrical stellar system; the accompanying numbers indicate the relative frequencies expressed in terms of that at the center of the figure as unity. The local increase of star density considered causes the lines of equal frequency to bulge out, as shown roughly by the dotted curves, the bulges having been smoothed so as to avoid sudden transitions. The bulge extends over the range of curves with frequencies between about 0.40 and 0.16. A similar bulge for the inner curves may be obtained by an increase of the star density between 700 and 1400 parsecs in the same longitude interval by 50 per cent. Though we cannot make a very certain estimate of the vertex deviation which would be caused by the bulges considered, it is probable that it would come out at least of the same order as that observed; at the same time, it need not entail a very noticeable effect on the systematic motion of the stars considered.

The foregoing example does not pretend to resemble the actual conditions in the galactic system. It is evident that a relative excess of density in a sector opposite to the one considered would produce the same deviation in the vertex. It is also possible, and even probable, that conditions are complicated by the fact that any unevenness in the density distribution is likely to be accompanied by an unevenness in the distribution of the phases of the motions.

Available density data are still insufficient to indicate whether density deviations in the required sense exist; all that can be said, I believe, is that the data do not contradict the interpretation suggested. The only purpose of the present discussion was to illustrate the relation between velocity distribution and density distribution and to indicate the order of the deviations in the density required to explain the deviation observed in the velocity distribution. It may be well to point out, in this connection, that rather different interpretations are possible, such as, for instance, that proposed by Lindblad.[16] He suggests that the orbits of the stars responsible for the deviation of the vertex extend to a region where circular motions are unstable. The orbits of these stars would then be of a different character from those considered, starting in a spiral-like manner in the

[16] *Stockholms Obs. Ann.*, **12**, No. 4, 1936; *Östen Bergstrand Festskrift*, 1938.

unstable region; it is easily conceivable how, on this model, a slight difference could occur between the velocities of outgoing and of incoming stars, which would give rise to a deviation of the vertex.

Lindblad has pointed out that the more or less sudden appearance of the strong asymmetry in the velocity distribution which is found to occur at peculiar velocities of about 65 km/sec can also find explanation in his model. The most direct interpretation of the sudden appearance of the asymmetry would, however, seem to be that it is caused by the way in which the density in the galactic system varies in its outer regions. If considered in the same way that we considered the vertex deviation, it would mean that, after remaining roughly constant up to about 1600 parsecs in the direction of the anticenter, the density would rapidly fall off beyond this distance. Such a variation could certainly be reconciled with the available data.

II. EXTRAGALACTIC SYSTEMS

Accurate knowledge of the density distribution in extragalactic systems is evidently one of the prerequisites for a study of the dynamics of these systems. Apart from a few color measurements, as reported above, little or no quantitative work has yet been done on spiral nebulae proper. For the elliptical nebulae quite interesting results have been obtained by Hubble, and more recently studies on the same subject have been published by Redman and Shirley. A number of these nebulae have been studied in some detail in Leiden, with the aid of plates taken by Dr. Oosterhoff at the Mount Wilson Observatory and by the author at the Perkins Observatory. The measurements and reductions were carried out in collaboration with Mr. Kleibrink. In the following pages a report will be given on the results for two of the nebulae, NGC 4494 and NGC 3115. The results given are provisional in several ways, and some further measurements and reductions are contemplated.

The most interesting outcome of Hubble's original investigation of the elliptical nebulae[17] was that, except for differences in flattening, all these nebulae appeared to be built on the same model. In each of the 15 objects studied the surface intensity could be well represented by the formula $I = I_0/(1 + r/a)^2$; and this is not all: it ap-

[17] *Ap. J.*, **71**, 231, 1930; *Mt. W. Contr.*, No. 398.

peared also that the "central" intensity, or rather, the parameter I_o, was nearly identical for the various nebulae; the same may hold approximately for the linear diameters. No satisfactory reason has yet been found why these nebulae should all be built on this particular model, but it is evidently a result of the greatest interest.[18]

PHOTOMETRY OF NGC 4494

Figure 3 shows detailed results of the intensity measures on NGC 4494 as studied at Leiden. Four plates taken by Dr. Oosterhoff with the Mount Wilson 60-inch reflector were used, with altogether six exposures ranging from 1 to 60 minutes. The nebula had been classified as E0 by Hubble, but the measures indicate a ratio of 0.83 for the shortest and the longest axes. For the plot in Figure 3 various position angles were simply averaged (for most exposures tracings were made through 12 different position angles). The ordinates in Figure 3 show logarithms of surface intensity I, this being expressed in stars of magnitude 25.0 per square second of arc as unit.[19] The intensity scale was determined by means of sensitometer marks; on two of the plates it was also determined from measurements of surface brightness in the rings of far interfocal images of a Selected Area exposure superimposed on the field of the nebula. These Selected Area exposures were also used for obtaining the zero points of surface brightness. The two independent determinations of the intensity scale agree very well. A partial third test is furnished by the intercomparison of the various exposures. Zero-point corrections have been applied to the different exposures in order to fit the curves together. It will be seen from the diagram that, with these corrections applied, the various exposures agree quite satisfactorily. Significant differences are found only for points derived from the faint

[18] It should be mentioned that Redman (*M.N.*, **96**, 588, 1936; see also *ibid.*, **98**, 613, 1938) has recently found somewhat deviating results for some of the nebulae measured by Hubble. On the other hand, Miss Patterson, working at Harvard, has in an unpublished study obtained data which generally confirmed Hubble's earlier measures. The results for NGC 4494 and 3115 can be represented quite well by Hubble's formula.

[19] The surface brightness expressed in magnitudes per square second of arc (H) is related to I by the formula $H = 2.5\ (10 - \log I)$. The relation between the surface intensity I', expressed as the number of stars of 10.0 photographic magnitude per square degree (as has also been used in recent work) and that used in the present note, I, is $I' = 13.0\ I$.

and ill-defined part of the toe of the reduction curve. Observations corresponding to these uncertain parts have been indicated by reduced size of the characters in the figure. Abscissas in the graph are logarithms of the distance to the center in seconds of arc. The surface brightnesses plotted have not yet been corrected for the effect of

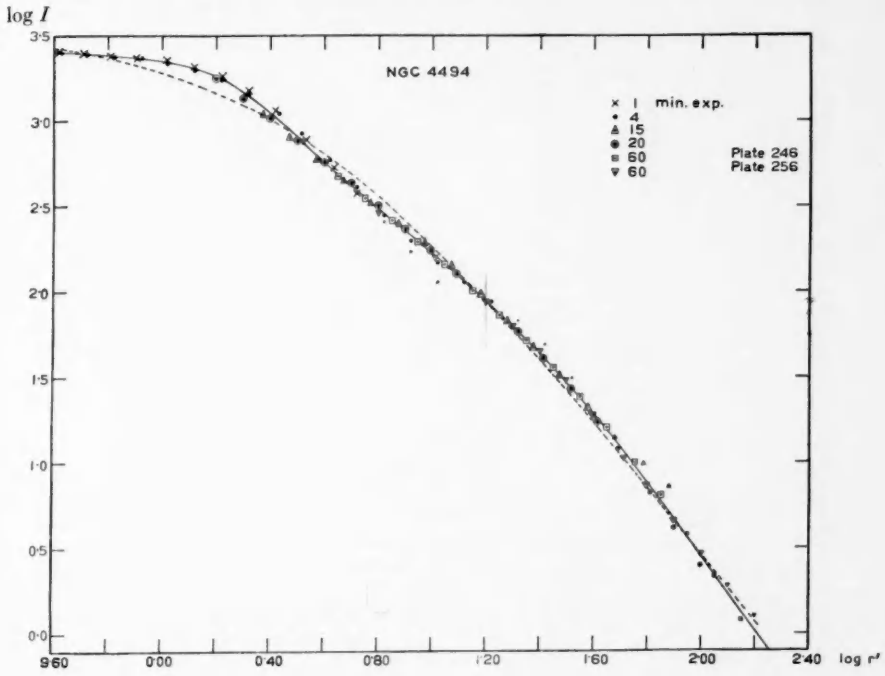

FIG. 3.—Distribution of light in NGC 4494. Ordinates are logarithms of surface intensity, expressed in stars of $25^{m}0$ per square second of arc. Abscissas are logarithms of the distance from the center in seconds. The dotted curve represents Hubble's formula $\log I = \log I_0 - 2 \log (1 + r/a)$, with $\log I_0 = 3.41$ and $a = 3''.0$ ($1''$ is roughly 12 parsecs).

atmospheric and instrumental diffusion of the light; this must have had a pronounced effect upon the curve to the left of $\log r = 0.5$, but it is believed to have been of relatively little importance for the rest of the curve.[20]

[20] Redman and Shirley have recently shown (*M.N.*, **98**, 614, 1938) that on their plates a measurable fraction of the light is dispersed to distances of several minutes from the source of light. Qualitatively, this has been confirmed on the Mount Wilson plates

As will be seen from the dotted curve in Figure 3 as well as from the numbers in Table 1, the main features of the density distribution in this nebula (which has not been measured by Hubble) can be quite well represented by Hubble's formula, with $a = 3''.0$ and

TABLE 1

DISTRIBUTION OF SURFACE BRIGHTNESS IN NGC 4494 AND 3115

r	log r	NGC 4494		NGC 3115				
				Major Axis		Minor Axis		Major Axis
		log I_{obs}*	O−C†	log I_{obs}*	O−C†	log I_{obs}*	O−C†	log φ‡
0".0	−∞	3.28	−0.13	3.61	+0.26	3.61	+0.06	+3.26
1.0	0.0	3.20	+ .04	3.48	+ .21	3.46	+ .17	+2.91
2.5	0.4	2.92	+ .04	3.18	+ .02	3.07	+ .07	+2.19
4.0	0.6	2.65	− .03	3.03	− .03	2.83	+ .04	+1.83
6.3	0.8	2.38	− .05	2.89	− .04	2.56	+ .03	+1.51
10.0	1.0	2.11	− .03	2.73	− .03	2.24	.00	+1.19
15.8	1.2	1.83	+ .01	2.55	+ .01	1.85	− .07	+0.87
25.1	1.4	1.51	+ .04	2.31	+ .04	1.47	− .09	+0.48
39.8	1.6	1.16	+ .06	2.04	+ .07	1.16	− .04	+0.01
63.1	1.8	0.78	+ .05	1.71	+ .07	0.85	+ .03	−0.50
100.0	2.0	0.34	0.00	1.29	+ .01	0.51	+0.08	−1.06
158.0	2.2	.....	.....	0.86	− .06	.....	.....	−1.65
251.0	2.4	.....	.....	0.44	−0.09	.....	.....	−2.27

* The symbols I and φ are expressed in stars of photographic magnitude 25.0 per square, or cubic, second of arc as unit.

† The columns O−C contain the differences between the observed distributions and those computed from the formula $\log I = \log I_0 - 2 \log (1 + r/a)$. The constants used are NGC 4494, $\log I_0 = 3.41$; $a = 3''.0$; NGC 3115 major axis, $\log I_0 = 3.35$, $a = 10''.2$; NGC 3115 minor axis, $\log I_0 = 3.55$, $a = 2''.84$.

‡ The last column shows the distribution of light in space along the equatorial plane.

$\log I_0 = 3.41$. There are, however, some minor deviations which are probably real; between 4″ and 8″ the computed values are about 0.06, or $0^m.15$, brighter than the observed intensities, while between 25″

used in this article by tracings through the stars BD+26°2359 ($8^m.4$, A0) situated only 6′ from NGC 4494, and BD−6° 3066 ($10^m.2$ pg, K2), 19′ from NGC 3115. The magnitude of the effect may be illustrated by stating that 3 per cent of the light is dispersed to distances between ½′ and 2′ from the star. The percentage is found to be practically the same on all four long-exposure plates measured; it appears to be independent of seeing conditions and might well be due to dispersion in the plate. The amount is about four times less than that found by Redman and Shirley at the same angular distances. The effect upon the outer contours is small, even for the very condensed nebula NGC 4494. In order to correct for it, the value of log I for $r = 100''$ should be diminished by 0.04, that for $r = 63''$ by about 0.02.

and 50″ they are about the same amount fainter. It should be mentioned that, on account of the uncertainty as to the true distribution of light near the center, the parameters a and I_0 cannot be separated with much accuracy. A value of $a = 4''.0$, for instance (with $\log I_0 = 3.20$), would fit the well-observed part of the intensity distribution quite as well as the values adopted.

The distance of NGC 4494 may be estimated from its radial velocity, which was kindly communicated to me by Humason, in advance of publication. As corrections to the center of the galactic system are negligible in this case, the distance can at once be obtained by the aid of the velocity-distance relation. Using Hubble's value of 530 km/sec per million parsecs[21] for the coefficient of expansion and Humason's velocity of +1350 km/sec, we find 2.5×10^6 parsecs. The nebula is only 14° away from the nucleus of the Virgo cluster; if it is a member of the nuclear part of this cluster, its distance should be 2.2×10^6 parsecs.[22] Assuming, provisionally, a distance of $2.4\times10_9$ parsecs, 1″ at the distance of NGC 4494 is equivalent to 12 parsecs, and we find $a = 36$ parsecs.

PHOTOMETRY OF NGC 3115

Of NGC 3115, three 60-inch Mount Wilson plates taken likewise by Dr. Oosterhoff were measured, containing altogether five exposures of 60, 50½, 15, 4, and 1 minutes, respectively. Details of measurements and reductions will be more fully published elsewhere in combination with the results for the other nebulae studied; we shall discuss only the main results of this study.

Several circumstances appear to make this elliptical nebula especially interesting for thorough investigation. The object is the brightest of the nebulae classified as E7 by Hubble. Its flattening, corresponding to a ratio of about 3 to 1 between the two axes, is the strongest observed among the nebulae classified as elliptical; this indicates that it is an extreme case, which, in the current thoughts on spiral formation, may mark the point of transition to an unstable system; it also indicates that the nebula must be seen practically edge on, and this knowledge enables us to derive the space distribution from the distribution of light as seen projected on the sky. Fur-

[21] *The Realm of the Nebulae*, p. 170. [22] *Ibid.*, p. 163.

thermore, the rotation has been measured by Humason, the measurements extending to about 45″ from the center.

Figure 4 and Table 1 show the results of the measures of the distribution of light in the nebula as projected on the sky, along the major and minor axes, respectively. The various exposures have

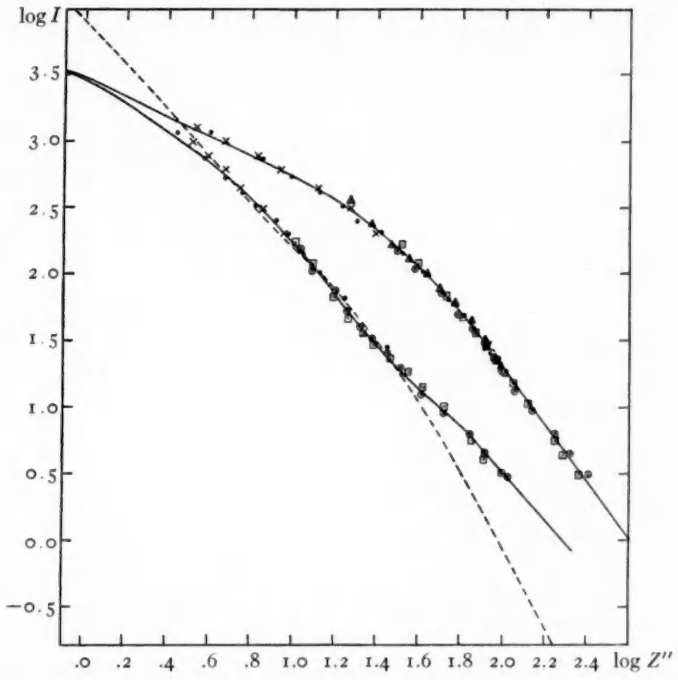

FIG. 4.—Distribution of light in NGC 3115. The full-drawn curves show the variation of surface intensity I along the major and minor axes. The 1-minute exposure is represented by crosses, the 4-minute by dots, the 15-minute by triangles, the 50½-minute by circles, and the 60-minute by squares. The dashed curve shows the variation of the space density of light, φ, along the equatorial plane. Abscissas are logarithms of the distance from the center in seconds, ordinates are logarithms of the light-intensity expressed in stars of $25^{m}0$ per square second for I (numbers on the left) and per cubic second for φ (numbers on the right).

again been fitted together by applying zero-point corrections. In this case a provisional correction has been applied in the region near the nucleus for the dispersion of light caused by atmosphere, instrument, and plate. This dispersion, as determined from registrograms

through a focal star image 80″ from the center of the nebula on the one-minute exposure, is ±0.04 mm on the plate, or ±1″.0. The corrections applied to log I range from about +0.18 in the center to −0.08 at 3″ distance, becoming negligible beyond about 4″. No claim is made for the numerical accuracy of these corrections; the most that can be said is that they indicate the order of the uncertainty arising from the light dispersion. It would seem that the shape of the isophotal contours (as shown in Fig. 5) and the results for the concentration of the light near the major axis (except in the central

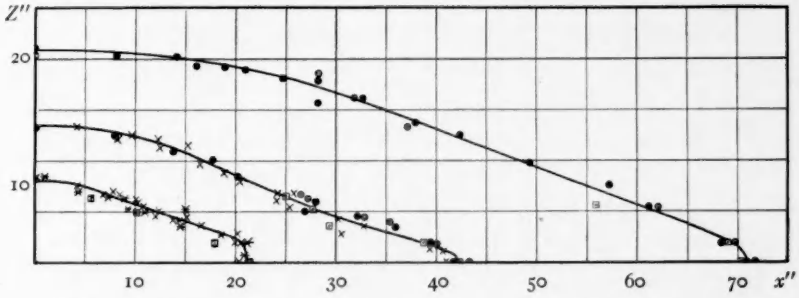

FIG. 5.—Isophotes in NGC 3115. The isophotes correspond to log I 2.4, 2.0, and 1.6, I being expressed in stars of 25^{m}.0 per square second. The co-ordinates are given in seconds (1″ is roughly 7 parsecs). The 1-minute exposure is represented by asterisks, the 4-minute by crosses, the 15-minute by squares, the 50½-minute by dots, and the 60-minute by circles.

nucleus) can have been but little disturbed by the small observational dispersion.

The distributions in Table 1 can again be fairly well represented by Hubble's simple formula, though there are some deviations which appear to be real. The differences from the values computed by this formula, using Hubble's results for the parameters a (viz., 10″.2 for the major axis and 2″.84 for the minor axis), are as shown in Table 1; the values of log I_0 used for fitting the formula to the present observations are 3.35 for the major axis and 3.55 for the minor.

Isophotes for log I = 2.4, 2.0, and 1.6 are shown in Figure 5. They were obtained from a considerable number of tracings in directions parallel with and perpendicular to the principal axis. Special care was taken to obtain tracings near the equatorial plane and accurately parallel to it, in order to get as reliable data as possible on

the run of the isophotes near the major axis; for this purpose each exposure was traced along the equatorial plane as well as at 0.07 and 0.20 mm (or 1".9 and 5".4) distance on either side of it. The exact situation of the major axis had been ascertained by micrometer measures and had been indicated on the plates by dots; in this way the error of centering in the microphotometer has been reduced to something of the order of 0".1, while the probable error of the orientation will not have exceeded 0°.1. The various exposures have been indicated by separate signs; the corresponding isophotes were reduced to exactly the same size by applying factors derived by equating the average of the minor and major axes of the isophotes considered to the standard values of the axes for the surface brightness concerned as read from Figure 4.

The most remarkable features of the isophotes are the remarkable sharpness with which they run into the major axis and the long, straight portions which lead down to these sharp edges—features that have also previously been remarked upon by Hubble;[23] his data, however, show a little less detail in the parts near the axis. There is an indication that for the inner isophote, with semimajor axis $a = 21''$, and especially for isophotes still nearer to the center, the sharpness of the edge disappears, while at the same time the ratio c/a of minor to major axis increases. The ratio reaches a minimum of 0.29 near $a = 60''$; it increases again for the outer isophotes. The variation of c/a with log a between $a = 4''$ and $a = 300''$ is shown in Figure 6, in which the ratios for various exposures have been plotted separately. Both the innermost isophotes (say for a below $10''$) and the outermost isophotes (beyond $a = 100''$) are somewhat uncertain on account of the instrumental and atmospheric dispersion of light. The effect upon the outer isophotes has been determined on the long-exposure plates 460 and 467 by measures on the near-by tenth-magnitude star BD $-6°$ 3066 (cf. also n. 20, p. 287); the curve gives the corrected values, while the crosses have been plotted without correction. In order to strengthen the part of the curve for large values of a, a number of registrograms were made of a fine 100-minute exposure taken by Ritchey on December 25, 1911, which was kindly put at my disposal during a stay at the Mount Wilson

[23] *Ap. J.*, **71**, 264, 1930; *Mt. W. Contr.*, No. 398.

Observatory in the summer of 1939. The results, again uncorrected for dispersion, have been plotted as asterisks in Figure 6. Hubble's earlier determinations of the axial ratio[24] for the brighter parts of the nebula have also been indicated in the figure (as squares); they are slightly higher than the values derived here. No attempt has yet been made to correct the inner isophotes for the effect of light-dispersion.

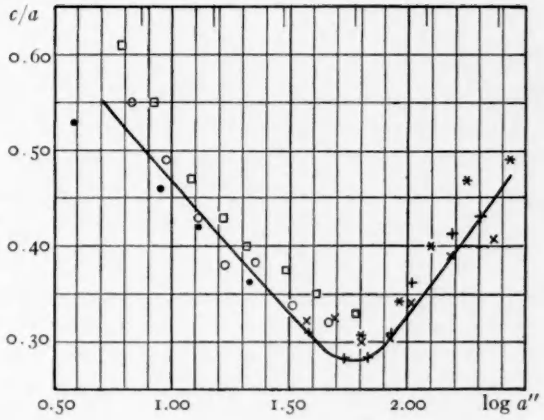

FIG. 6.—Axial ratio of isophotes in NGC 3115. Dots represent results from 1-minute exposure, circles from 4-minute, and crosses from 50½- and 60-minute exposures. The asterisks have been derived from a 100-minute exposure by Ritchey. The squares have been copied from results of short 100-inch exposures previously published by Hubble. The curve has been approximately corrected for the effect of light-dispersion over great distances (see text).

SPACE DISTRIBUTION OF THE LIGHT IN NGC 3115

In order to obtain at least some rough insight into the true structure and possible dynamics of NGC 3115, the admittedly provisional isophotes discussed in the foregoing section were used to determine the space density φ. Let z denote the distance from the equatorial plane of the system; let $\varphi_z(\bar{\omega})$ define the space density of light at distances $\bar{\omega}$ and z from the minor and major axes, respectively, expressed as the number of stars of 25.0 photographic magnitude per "cubic second of arc" at the distance of the nebula. Let $I_z(x)$ be the surface brightness at a distance x from the minor, and z from the

[24] *Ap.J.*, **71**, 264, 1930; *Mt. W. Contr.*, No. 398.

major axis. If it is assumed that the system considered has rotational symmetry around an axis perpendicular to the line of sight and that there is no absorption of light within the system, it can be shown that in any plane of constant z

$$\varphi_z(\bar{\omega}) = -\frac{1}{\pi}\int_{\bar{\omega}}^{\infty} \frac{\frac{dI_z(x)}{dx}}{\sqrt{x^2-\bar{\omega}^2}}\,dx\,,^{25}$$

In most of the actual integration, which was carried out by Mr. Pels, it proved easiest to determine first, graphically, the derivative of log I with respect to log x and then to compute dI/dx from these quantities. The extrapolation over the unknown outer regions is of little importance. If, in rough accordance with the observations, it is assumed that for large values of x (say, beyond X) I becomes of the form cx^{-2} and if this formula is assumed to hold to infinity, the part of the integral expression for φ beyond X is easily seen to be

$$\frac{c}{\pi\bar{\omega}^3}\left(-\frac{\bar{\omega}}{X}\sqrt{1-\frac{\bar{\omega}^2}{X^2}}+\arcsin\frac{\bar{\omega}}{X}\right).$$

If X is taken to correspond to the outer isophotes measured, the extrapolated part is usually only a small fraction of the total. The calculations were carried out for 8 values of z and were roughly checked by the inverse calculation of I from φ.

Figure 7 shows a section through the isophotal surfaces as provisionally found from these calculations. The curves resemble, in general, the isophotes in the projected image, but the ratio between minor and major axis comes out somewhat larger; between $a = 30''$ and $a = 100''$, c/a is found to be approximately 0.40, as against 0.30 in the projected image. However, it should be remembered that the true flattening may well be somewhat stronger, as the line of sight may be slightly inclined to the true equatorial plane. The values of log φ corresponding to the various surfaces are indicated in the figure. In the center we find, approximately, log $\varphi = 3.26$. Taking

[25] The formula was first given by Von Zeipel (*Ann. de l'obs. de Paris, Mém.*, **25**, p. F30, 1908); see also Smart, *Stellar Dynamics*, pp. 297–302; it is easily seen to apply to any surface of revolution the axis of which is perpendicular to the line of sight.

the photographic light of the sun per cubic parsec as unit of density of light[26] and estimating the distance of the nebula as $1\frac{1}{2}$ million parsecs[27] (therefore, $1'' = 7.3$ parsecs and $m - M = 25.9$), we find that a star of $25^{m}.0$ per cubic second corresponds to 0.74 units; if the true distance is κ times larger, the corresponding light per cubic parsec will be κ times smaller. The central intensity corresponds to

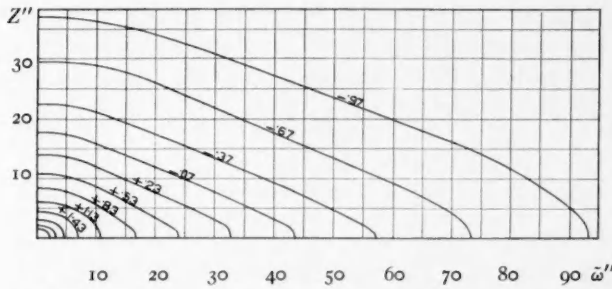

FIG. 7.—Section of isophotal surfaces in NGC 3115. The numbers in the figure are logarithms of the light-density φ corresponding to the respective curves, φ being expressed in stars of $25^{m}.0$ per cubic second. For the three inner curves log φ is, respectively, 2.33, 2.03, and 1.73; in the center log φ is estimated to be 3.27. Co-ordinates are in seconds ($1''$ is roughly 7 parsecs).

1400 units. This is 30,000 times the total density of light in the part of the galactic system in which the sun is situated and is of the same order as that in the center of Messier 3.[28]

[26] The photographic absolute magnitude of the sun was assumed to be +5.26, in accordance with a recent discussion by Kuiper (*Ap. J.*, **88**, 429, 1938).

[27] This distance is still very uncertain. The only criteria from which it can be estimated are the radial velocity, the apparent magnitude, and the size. The radial velocity, corrected to the center of the galaxy, is +450 km/sec, corresponding to a distance of 0.8 million parsecs; however, the smallness of the velocity makes this result doubtful. From the apparent magnitude, 9.8 according to Shapley and Miss Ames, combined with Hubble's value of −15.2 for the average absolute magnitude of this class of nebulae (*The Realm of the Nebulae*, p. 176), a distance of 1.0 million parsecs is derived. The apparent dimensions, on the other hand, indicate a much larger distance: the average of a_{max} and a_{min} for NGC 3115 is $6''.5$, while the average linear value of a for the 7 elliptical nebulae measured by Hubble in the core of the Virgo cluster amounts to 66 parsecs; if we suppose that the average a for NGC 3115 is the same, we find 2.1 million parsecs for the distance. The foregoing value is thus a compromise; it should be kept in mind that the true distance may well differ from it by a factor as large as 2 in either direction.

[28] Hertzsprung, *A.N.*, No. 4952, 1918.

The run of log φ with $\bar{\omega}$ in the equatorial plane of the nebula has been plotted as a dotted curve in Figure 4. The curve for log φ runs considerably steeper than that for log I; from $\bar{\omega} = 80''$ on, φ can be expressed as $\bar{\omega}^{-3.1}$. The smallest light density recorded is approximately $\varphi = 0.01$, or 0.007 units as previously defined, or one-sixth of the light-density in the region surrounding the sun.

DYNAMICS OF NGC 3115

It was hoped, originally, that the distribution of the light in extragalactic nebulae would bear resemblance to the distribution of mass and that investigations of the light-distribution might give some

TABLE 2

$\bar{\omega}$	$\bar{\omega}$ (Parsecs)	Φ (Cm²/Sec²)	$-K_{\bar{\omega}}$ (Cm/Sec²)	Θ_c (Km/Sec)	Θ_0 (Km/Sec)	$\frac{\partial \log \varphi}{\partial \log \bar{\omega}}$
4.″0.....	29 κ	$70.8 \times 10^{12} \kappa f$	$17.9 \times 10^{-8} f$	$40.2\sqrt{\kappa f}$	.....	−1.69
8.1.....	59	58.7	10.1	42.7	79	1.60
16.1.....	117	44.6	6.43	48.1	158	1.76
32.2.....	234	28.9	2.70	44.1	316	2.36
45.5.....	331	22.5	1.59	40.2	447	2.50
64.5.....	470	17.6	0.89	36.1	.....	2.59
129.0.....	939	9.9	0.31	30.0	.....	−2.98

insight into the question of how far the most flattened elliptical nebulae and the regular cores of early-type spirals approach unstable configurations which could give rise to the formation of spiral arms. Humason's results on the rotation of NGC 3115 seem to indicate, however, that there is not much prospect in this direction; not, at least, for this nebula.

Table 2 shows the values of the potential Φ and the acceleration $K_{\bar{\omega}}$ for points in the equatorial plane of the nebula, computed on the assumption that the distribution of density is the same as that of the light. The factor by which the true distance is larger than the distance of 1.5 million parsecs provisionally assumed is κ; f is the unknown ratio of mass density to light-density, the former being expressed in the mass of the sun per cubic parsec, the latter in the photographic light of the sun per cubic parsec as a unit (in the direct vicinity of the sun f is about 2). The potential was assumed to be zero at infinity.

The values of Φ and $K_{\bar{\omega}}$ were obtained by numerical integration with the aid of the equidensity surfaces given in Figure 7, and with rough estimates about the more outlying surfaces. The surface corresponding to $\log \varphi = -2.17$ ($a = 233''$) was arbitrarily taken as the boundary of the nebula, the density being supposed to become zero outside this surface. The neglect of the material outside this surface is not likely to have had an appreciable influence on $K_{\bar{\omega}}$, but the values given for the potential will be too low. Accepting the approximate values given, the velocity of escape for $\bar{\omega} = 4''.0$ is found to be $119\sqrt{\kappa f}$ km/sec; with $\kappa = 1$ and f of the order of 100, it may roughly be estimated to be of the order of 1200 km/sec.

It is evident from the run of the values of Φ in Table 2 that, if the mass distribution in a system like NGC 3115 is assumed to be like that of the light, such a system would be very stable. The condition for the appearance of dynamical instability is that at some place the force varies more rapidly than $\bar{\omega}^{-3}$, or the potential more rapidly than $\bar{\omega}^{-2}$. With the numbers given in Table 2, the steepest variation of $\log \Phi$ with respect to $\log \bar{\omega}$ occurs in the outer parts of the nebula, but even at $\bar{\omega} = 120''$ we have only $\Phi \sim \bar{\omega}^{-0.86}$, that is, an even slower variation than in the case of a Newtonian field, so that the system would be very far from a state in which it could begin to develop spiral structure.

However, the spectrographic measures of rotation indicate that the distribution of mass is probably very different from that of the light; in such a case the stability cannot, of course, be judged from the distribution of the light. Humason's rotational velocities are given under Θ_0 in the sixth column of Table 2.[29] The measures represent the average radial velocity of the various parts of the nebula seen projected on top of each other; it is easily seen, however, that in a case like the present, where the rotational velocity increases linearly with the distance to the center, the observed radial velocity will be equal to the true rotational velocity at the corresponding point. Humason's measures extend to $45''$ from the center; on account of the small scale the measured velocity for $\bar{\omega} = 8''.1$ is likely to have a considerable percentage of uncertainty.

It is interesting to compare the run of the rotational velocities with

[29] *Report of the Director of Mt. W. Obs., 1936–37*, p. 31.

the entirely different run of the "circular" velocities (velocities corresponding to circular orbits) computed on the assumption that the mass distribution is the same as that of the light; these are given in the preceding column under Θ_c and appear to remain practically constant over the range in $\bar{\omega}$ considered. As Θ_0 will, in general, be lower than Θ_c, we infer from the data for $\bar{\omega} = 45''.5$ that, if $\kappa = 1$ (that is, if the distance is $1\frac{1}{2}$ million parsecs), f must be at least of the order of 150. Furthermore, if f were taken constant, the circular velocity at $8''.1$ and $16''.1$ would come out many times larger than the rotational velocity. On the other hand, if we should assume that the rotational velocities are of the same order as the circular velocities, we should find that f varies with $\bar{\omega}$ and that the distribution of the density differs radically from that of the light.

I believe it can be shown that the first alternative is very improbable. Let us assume for a moment that it were true; suppose, therefore, that f be constant and, for instance, equal to 200.[30]

The general relation between Θ_0 and Θ_c in systems which are in a dynamically steady state may be written[31]

$$\Theta_c^2 - \Theta_0^2 = \overline{\Pi^2}\left[-\frac{\partial \log \varphi}{\partial \log \bar{\omega}} - \frac{\partial \log \overline{\Pi^2}}{\partial \log \bar{\omega}} - \left\{ 1 - \frac{\overline{(\Theta - \Theta_0)^2}}{\overline{\Pi^2}} \right\} \right] . \quad (1)$$

Here Π and Θ denote the velocities in the direction of $\bar{\omega}$ and in that of the rotation; bars denote average values, thus $\overline{\Theta} = \Theta_0$. In the case of NGC 3115, where the angular velocity of rotation is approximately constant, the term $\{1 - \overline{(\Theta - \Theta_0)^2}/\overline{\Pi^2}\}$ is probably small; in the accompanying tentative calculations it has been neglected.

The seemingly perfect regularity and symmetry of the system suggests an approximately steady state. Jeans[32] has shown that in the case of strict dynamical equilibrium the velocity distribution in the Π-direction must be identical with that in the Z-direction (parallel to the axis of rotation), so that

$$\overline{Z^2} = \overline{\Pi^2} . \quad (2)$$

[30] The total mass of the system would then be 7×10^{10} solar masses.

[31] The equation can, for instance, be derived directly from equation (10) given by Jeans in *M.N.*, **82**, 122, 1922.

[32] See, for instance, *M.N.*, **76**, 81, 1915.

Although it is by no means clear how such an equality of the two distributions would be established[33]—for during an interval of 10^{10} or 10^{11} years the transfer of energy between individual stars in NGC 3115 must have been negligible—I shall nevertheless use the above equation as a tentative working hypothesis for the following calculations. It should be noted that, as far as an estimate of the line width can be made, it indicates, according to information from Humason, that the dispersion of the H-velocities cannot be much larger than about 100 km/sec—an amount, therefore, which is of the same order as that computed for the velocities in the Z-direction (see Table 5).

If the gravitational force is known, the distribution of velocities in the Z-direction can be derived from the density distribution. In the computations I have assumed that the distribution of velocities could be represented as the sum of a number of exponential distributions, as follows:

$$f(Z) = \sum \theta_i \frac{l_i}{\sqrt{\pi}} e^{-l_i^2 Z^2}, \tag{3}$$

in which $\sum \theta_i = 1$. We have then the following equation,[34] in which K_z represents the gravitational acceleration

$$\frac{\varphi_z(\tilde{\omega})}{\varphi_0(\tilde{\omega})} = \sum \theta_i e^{2l_i^2 \int_0^z K_z dz}. \tag{4}$$

The mean square velocity for a point near the equatorial plane is given by

$$\overline{Z^2} = \sum \frac{\theta_i}{2l_i^2}. \tag{5}$$

The computation of this mean square velocity might also have been made with the aid of the more general formula

$$\overline{Z^2} = -\frac{1}{\varphi_0} \int_0^\infty \varphi_z K_z dz, \tag{6}$$

which, however, would have necessitated extrapolations to infinity.

[33] I am indebted to Dr. Woltjer for a discussion on some of the difficulties involved in introducing this equation. Cf. *B.A.N.*, No. 238, p. 253.

[34] Cf. *ibid.*

In the hypothetical case considered above, where the distribution of mass is the same as that of light and the ratio of mass to light is 200, K_z can be directly computed from the known light-distribution. Somewhat approximate[35] calculations were made for two regions of the nebula, namely, at $\bar{\omega} = 16''.1$ and $32''.2$, respectively. The results are shown in Table 3 (units cm/sec² and cm²/sec², respectively; κ was assumed to be 1).

From these data it was found that the velocity distribution for $\bar{\omega} = 16''.1$ could be well represented as the sum of two Gaussian distributions with mean square velocities of 160 and 335 km/sec and

TABLE 3

z	$\bar{\omega} = 16''.1 = 117$ PARSECS			$\bar{\omega} = 32''.2 = 234$ PARSECS		
	$\frac{\varphi_z}{\varphi_0}$	$-K_z$	$-\int_0^z K_z dz$	$\frac{\varphi_z}{\varphi_0}$	$-K_z$	$-\int_0^z K_z dz$
4''.0.....	0.62	4.21×10^{-6}	1.90×10^{14}	0.69	1.20×10^{-6}	0.54×10^{14}
8.1.....	.295	6.54	7.06	.40	2.04	2.03
16.1.....	.081	6.14	18.9	.174	2.72	6.46
32.2.....	.019	3.65	35.8	.051	2.46	16.2
64.5.....	0.003	1.72	54.5	0.013	1.53	30.4

with $\theta_1 = 0.52$ and $\theta_2 = 0.48$, so that the total mean square velocity $\sqrt{\overline{Z^2}} = 259$ km/sec. For $\bar{\omega} = 32''.2$ we obtain also a sum of two Gaussian distributions, corresponding to mean square velocities of 95 and 280 km/sec with $\theta_1 = 0.60$ and $\theta_2 = 0.40$; the total mean square velocity is 192 km/sec.

We can now insert these values of $\overline{Z^2}$ in formulae (2) and (1) and compute Θ_c from the latter. As has been explained, the last term in the parentheses was neglected. From the values of $\overline{Z^2}$ just found, $\partial \log \overline{\Pi^2} / \partial \log \bar{\omega}$ was estimated to be about -0.86; $\partial \log \varphi / \partial \log \bar{\omega}$, which has been computed from the data on the light-distribution, is given in the last column of Table 2. In this way we find $\Theta_c = 448$ and 468 km/sec for $\bar{\omega} = 16''.1$ and $32''.2$, respectively. These values differ very considerably from the values 676 and 620 km/sec computed

[35] The approximation consisted in replacing the real equidensity surfaces by spheroids, which were so chosen that their volumes as well as axial ratios equaled those of the corresponding equidensity surfaces.

from the light-distribution. Such high values for the circular velocity could have been obtained only by using very much larger values (between 400 and 500 km/sec) for the mean square peculiar velocities, values which would have been in contradiction with the distribution of light in the z-direction. Probably such high values as 400 or 500 km/sec for the mean peculiar velocities could likewise be dismissed on the ground that the widths of the spectral lines would then have had to be greater than those observed. It may be concluded that the distribution of mass in the system must be considerably different from that of the light. A study of the light-distribution does not, therefore, enable us to draw conclusions regarding such problems as stability or the total mass of the system.

The question now arises: How must the distribution of mass density be in order that both the observed distribution of light and the measured rotational velocities as well as the conditions for dynamical equilibrium can be satisfied? The available data are not sufficient to permit a complete answer. We can start from attracting masses of various degrees of flattening. Detailed calculations have been made only for a model in which the equidensity surfaces in the attracting body are ellipsoids of axial ratio $c/a = 2/3$. The high value $2/3$ was selected in order to be safely above the limit 0.552, where the instability of a homogeneous mass sets in. The computations were made for three points, at $\bar{\omega} = 8''.1$, $16''.1$, and $45''.5$, respectively; the gravitating mass was supposed to consist of an ellipsoid shell I with semimajor axis $a = 10''$, an ellipsoidal shell II extending from $a = 10''$ to $a = 20''$, and another shell III from $a = 20''$ to $a = 70''$, outside of which the density was assumed to be zero. The densities in the inner ellipsoid and in the two shells were now determined in such a way that for the three points mentioned the equations (1), (2), and (4) were satisfied. The results are in Tables 4 and 5.

The mass densities and light-densities are expressed in terms of the sun per cubic parsec. It will be noted that throughout the nebula the mass density is extremely high. Beyond $a = 10''$ a value of 140 solar masses per cubic parsec is found, roughly equivalent to 10^{-20} gm/cm^3, or nearly 2000 times the density near the sun. The total mass of the system would become 5×10^{10} solar masses. As the extent of the outer ellipsoid is entirely arbitrary, the real mass may differ

considerably from this figure; the system may easily be as massive as the galactic system, the mass of which is estimated to be between 10^{11} and 2×10^{11}.

The most remarkable feature is that the mass density appears to remain practically constant outside $a = 10''$, though the light-in-

TABLE 4*

DISTRIBUTION OF MASS AND LIGHT IN NGC 3115

Shell	a	Mass Density	Light-Density at $z=0$	$\frac{\text{Mass}}{\text{Light}}=f$
I	$0''$–$10''$	$365/\kappa^2$	$a=7''.5$ $18.6/\kappa^3$	19.6κ
II	10 –20	$144/\kappa^2$	$a=15.0$ $6.02/\kappa^3$	23.9κ
III	20 –70	$138/\kappa^2$	$a=45.0$ $0.56/\kappa^3$	249.0κ

* The symbol κ is the factor by which the true distance differs from the assumed distance of 1.5×10^6 parsecs.

TABLE 5

	$\bar{\omega}=8'.1=59$ PARSECS		$\bar{\omega}=16'.1=117$ PARSECS		$\bar{\omega}=45'.5=331$ PARSECS	
	$1/l\sqrt{2}$ Km/Sec	θ	$1/l\sqrt{2}$ Km/Sec	θ	$1/l\sqrt{2}$ Km/Sec	θ
	52	0.46	45	0.49	43	0.30
	104	.50	91	.38	85	.25
	209	.035	182	.087	170	.27
	418	0.005	364	0.034	340	0.18
$\sqrt{\overline{Z^2}}$	94	.....	106	.....	175	.....
Θ_0	79	.....	158	.....	447	.....
Θ_c	137	.....	197	.....	481	.....
$\frac{\partial \log \overline{Z^2}}{\partial \log \bar{\omega}}$	+0.19		+0.52		+1.46	

tensity falls off steeply. The strongly condensed luminous system appears imbedded in a large and more or less homogeneous mass of great density. This is a feature which, to some extent, might be expected at once from a superficial consideration of Humason's result that the nebula rotates like a solid body; for, if the peculiar velocities are moderate, so that, except near the center, the measured rotational velocity resembles the circular velocity, Humason's re-

sult means that the attracting mass must approximately be a homogeneous ellipsoid enveloping the measured region.

It may be noted that the mean square velocities, as shown in the fourth line from the bottom of Table 5, are still high, though they are considerably smaller than in the model considered previously. A notable feature is the pronounced non-Gaussian character of the distribution of the velocities Z, which suggests that we are looking at a mixture of very different types of stars, or of stars and interstellar material. Though the particular velocity distributions found depend to a considerable extent on the assumptions concerning the mass distribution, we have seen that the non-Gaussian character remains, even if the mass distribution is supposed to be the same as the light-distribution.

A very rough calculation along the same lines as that described but assuming axial ratios of $\frac{1}{3}$ instead of $\frac{2}{3}$ for the attracting ellipsoids indicates that in this case also the densities in the outer ellipsoids would come out nearly equal; the absolute densities as well as the values of f, however, would become more than twice as high as those found previously, while the peculiar velocities would also increase by a factor of nearly 2. The mean square velocity at $\bar{\omega} = 45''.5$ would become of the order of 300 km/sec, a value so large that it could probably be verified from observations.

In the outer parts of the nebula the ratio f of mass density to light-density is found to be very high; and this conclusion holds for whatever dynamical model we consider. The spectrum of the nebula shows the characteristics of G-type dwarfs. Since f cannot be much larger than 1 for such stars, they can account for roughly only $\frac{1}{2}$ per cent of the mass; the remainder must mainly consist either of extremely faint dwarfs having an average ratio of mass to light of about 200 to 1 or else of interstellar gas or dust.

Let us first consider these latter two possibilities. If the mass consisted mainly of gas, the optical thickness for rays coming from the nucleus would be of the order of 1000 times the average optical thickness traversed by the light of a star at 1000 parsecs distance in the galactic plane. The presence of layers of gas of such thickness might be verified from suitable spectra.

Many objects of the apparently more or less related type of Sa

spirals show strong evidence of absorption effects. Though no direct trace of such effects can be found in NGC 3115, the possibility cannot be excluded that there would be considerable amounts of solid interstellar material distributed evenly through the nebula. At the same time, however, it must be observed that if this matter is at all like the absorbing matter in the galactic system, it can at most account for a negligible fraction of the total density in NGC 3115, which is at least 3000 times that of the interstellar material in the galaxy. For, if the great density in the nebula were due to such absorbing matter, the transparency would be so low that we could not penetrate more than a very few parsecs into the system.[36]

The high value of f found stands in sharp contrast to what is found in the galactic system. In the vicinity of the sun f is about 2; it may rise to, at most, 7 at large distances from the galactic plane.[37] The ratio for the bulk of the galactic system can hardly be very much larger. A minimum value for the total amount of light contained in the part within the sun's distance from the center may be estimated by assuming that the light-density within an ellipsoid having a semimajor axis equal to the distance of the sun from the center (adopted as 8000 parsecs) and an axial ratio $c/a = 1/20$, is everywhere the same as that observed near the sun, i.e., 0.048 times the photographic light of the sun per cubic parsec. The total amount of light thus found is 0.51×10^{10} units. From the rotation of the galaxy the total mass within the sun's distance from the center may be estimated as 9.1×10^{10}, so that we should find $f = 18$. The true value of f must be expected to be considerably smaller, as the light will probably be concentrated toward the center, so that the above estimate would give too small a value for the total light. We may conclude that the ratio between mass and light for the galactic sys-

[36] It is conceivable that an absorption might exist which is sufficiently powerful to reduce the light of the stars in the system by a considerable factor and that, thus, the real ratios f for the undimmed light would be much smaller than those inferred from the present discussion. Such absorption would, however, also affect the central regions and, if called in to explain the high f-values in the outer region, would give impossibly low values for the central parts.

[37] Cf. *B.A.N.*, No. 238, p. 285, 1932. It should be noted that the unit of light in that article was a star of +6.0 photographic absolute magnitude; the light densities given should therefore be multiplied by a factor of 0.506 to be reduced to the present units.

tem as a whole is probably not much larger than that found in our surroundings, and is certainly very much smaller than that in NGC 3115.

The smallness of the dispersion in the radial velocities of nebulae in the Large Magellanic Cloud[38] indicates that the mass of this system can hardly exceed 2×10^9; since the luminosity is about 3×10^8 times that of the sun, f would be 6 at most—again very much smaller than the values found in the outer regions of NGC 3115.

No reliable data for other systems have yet been published. It should be noted, however, that measures by Horace Babcock[39] of the rotational velocity in the outer regions of the great Andromeda nebula indicate that the average value of f for this system would be about 55.

The dynamical models discussed do not give a direct explanation of the sharp edges of the isophotal surfaces of NGC 3115 near its equatorial plane. The most probable explanation would seem to be that these are due to the admixture of a relatively small fraction of stars with low velocities.

In concluding this reconnaissance of the possible dynamical peculiarities of NGC 3115, it is well to emphasize its hypothetical character. Of the hypotheses underlying the analysis the most uncertain is no doubt the neglect of absorption within the nebula and the supposition that the light we observe comes directly from stars. If important absorption and dispersion of light has occurred, this would probably have tended to lessen the light-gradients; the true disparity between the distribution of luminous stars and of mass would then be still greater than that indicated. The numerical results for the velocity distributions would, however, lose their significance. The possibility that the equatorial plane of the nebula may be somewhat inclined to the line of sight also introduces some uncertainty; however, the sharpness of the edges of the isophotes near the equator shows that the inclination can hardly exceed 5°. The principal excuse for attempting an analysis in the present stage is that it may give some indication of what kind of additional observations would seem most promising for a better understanding of the struc-

[38] R. E. Wilson, *Lick Obs. Pub.*, **13**, 189, 1917.

[39] To be published in the *Lick Obs. Bull.*

ture of a system of this kind. There cannot be any doubt that an extension of the measures of rotation to greater distances from the nucleus would be of exceptional interest. Also, our knowledge of the system could certainly be greatly advanced if it were possible to obtain spectroscopic estimates of the true mean peculiar velocities.

I am greatly indebted to Dr. Adams, who permitted the use of the 60-inch telescope for the work on the light-distribution in nebulae. Likewise, my sincere thanks are due to Dr. Oosterhoff for his willingness to take the plates. To Mr. Humason I am indebted for showing me unpublished details of his measures of the rotation of NGC 3115. Professor Ornstein kindly permitted us to use the Moll registering photometer of the physical laboratory at Utrecht. Throughout, Messrs. Kleibrink and Pels have most efficiently co-operated in the measurements and computations.

Astronomical Observatory
Leiden, Holland
October 23, 1939

PHYSICAL PROCESSES IN GASEOUS NEBULAE

IX. ON THE EXCITATION OF FRACTIONAL MULTIPLETS BY ELECTRON CAPTURE

GEORGE H. SHORTLEY AND DONALD H. MENZEL

ABSTRACT

Observations show that certain permitted multiplets of *O* III and *N* III are not completely represented in the spectra of gaseous nebulae. Some mechanism apparently acts to give selective excitation of certain levels of a term, without exciting other levels. Bowen attributes the phenomenon to resonance absorption, principally of the ultimate line of *He* II, which happens to coincide with an ultimate line of *O* III. The absorptions originate from the highest, instead of the lowest, levels of the ground terms. Since these levels have mean lifetimes of the order of several hours, Bowen's theory requires the operation of some additional mechanism to maintain a sufficient population in the levels involved in the fluorescence process. Another method of excitation of fractional multiplets, direct electron capture by an ion in the ground level of a term (e.g., $^2P_{1/2}$ of *O* IV), is examined. The components predicted by quantum mechanics do not, however, agree with those observed in the nebulae. The conclusion is reached that Bowen is probably right, although a few discrepancies still remain unexplained. His method apparently requires inelastic electron impacts to be sufficiently frequent to maintain approximately a thermodynamic equilibrium population of atoms in the levels of the ground term. This paper includes the relevant quantum mechanical analysis of the relative probabilities of capture into the different levels of a configuration.

Several years ago William H. Wright[1] identified a number of lines in the far ultraviolet spectrum of the planetary nebulae with certain permitted lines of doubly ionized oxygen. A most striking feature of the identification was the fact that the complete multiplet $2p3p\ ^3P - 2p3d\ ^3P^o$ does not appear, but only the lines arising from the level $^3P^o_2$.

In Table 1 are given the lines of two significant transition arrays of *O* III. The lines observed in the gaseous nebulae are shown in boldface type. Nebular spectra to the violet of about λ 3200 are only incompletely observed. With the exception of the lines λ 3122 and λ 5592, all of the observed lines would emanate from initial excitation of the level $2p3d\ ^3P^o_2$, with subsequent cascadings to lower levels.

Bowen[2] has suggested a possible mechanism for the selective excitation of this single atomic level. He has noted that a very close coincidence exists between the frequencies of the ultimate lines $1s\ ^2S - 2p\ ^2P^o$ of *He* II and $2p^2\ ^3P_2 - 2p3d\ ^3P^o_2$ of *O* III. Most of the

[1] *Pub. A.S.P.*, **46**, 142, 149, 280, 1934. [2] *Pub. A.S.P.*, **46**, 146, 1934.

nebulae where fractional multiplets of *O* III are observed are evidently of high excitation. The great intensity of the line λ 4686 of *He* II suggests that the ultimate line of *He* II, referred to above, is also very intense. Bowen argues that resonance absorption by *O* III of the intense *He* II radiation would lead to excitation of $2p3d\ {}^3P^o_2$

TABLE 1

TRANSITION ARRAYS 2p3d→2p3p AND 2p3p→2p3s OF *O* III

			$1s^2\,2s^2\,2p3p$									
			³D			³P			¹S	¹D	¹P	¹S
		J	3	2	1	2	1	0	1	2	1	0
$1s^2\,2s^2\,2p3d$	³F	4	3265.41	.....	.....	.....	.....	.....	.....	.....	.....	.....
		3	3284.56	3260.95	.....	.....	.....	.....	.....	.....	.....	.....
		2	3305.77	3281.92	3267.29	.....	.....	.....	.....	.....	.....	.....
	³D	3	3017.69	2997.70	.....	3715.07	.....	.....	.....	.....	.....	.....
		2	*	3004.35	2992.10	3725.29	3707.28	.....	.....	.....	.....	.....
		1	.....	3008.75	2996.49	*	3714.01	3702.70	.....	.....	.....	.....
	³P	2	2836.35	2818.80	*	**3444.15**	**3428.70**	.....	**3132.87**	.....	.....	.....
		1	.....	2809.72	2799.01	3430.66	3415.33	3405.79	**3121.71**†	.....	.....	.....
		0	.....	.....	2794.21	.....	3408.20	.....	3115.74	.....	.....	.....
	¹F	3	.....	.....	.....	.....	.....	.....	.....	2983.78	.....	.....
	¹D	2	.....	.....	.....	.....	.....	.....	.....	*	2959.68	.....
	¹P	1	.....	.....	.....	.....	.....	.....	.....	*	2390.44	5268.06
$1s^2\,2s^2\,2p3s$	³P	2	**3759.83**	3791.26	3810.99	**3047.14**	3059.31	.....	**3340.78**	.....	.....	.....
		1	.....	3754.65	3774.01	**3023.42**	3035.92	3043.01	**3312.35**	.....	.....	.....
		0	.....	.....	3757.20	.....	3024.54	.....	**3299.39**	.....	.....	.....
	P	1	.....	.....	.....	.....	.....	.....	.....	3961.58	**5592.37**‡	2454.99

* Faint unobserved or unidentified line. Triplets according to Mihul, *Ann. de phys.*, **9**, 261, 1928. Singlets according to Edlén, *Nov. Act. Reg. Soc. Sci. Upsala*, IV, **9**, No. 6, 1933. Edlén also identifies a number of faint intercombination lines not included in this table.

† Although λ 3122 does not originate in $2p3d\ {}^3P_2$, Wright and Bowen have suggested that it may arise from resonance absorption of λ 303, by atoms moving with relative velocities of 90 km/sec.

‡ Bowen and Wyse record the presence of λ 5592 in Nebulae NGC 7027 and 7662, with approximately one-half the intensity of λ 3760. We are indebted to these scientists for the communication of this information in advance of publication.

but not to excitation of the other levels of ${}^3P^o$, because the wave lengths do not coincide. As a further argument in support of his theory, Bowen points out that the line $2p3s\ {}^3P^o_1 - 2p^2\ {}^3P_2$ of *O* III, one of the end-products of the cycle of excitation and radiation, coincides in turn with the line $2p\ {}^2P^o_{3/2} - 3d\ {}^2D_{5/2}$ of *N* III. This coincidence initiates another cycle, with further excitation of fractional multiplets of *N* III.

Bowen's ingenious explanation, if true, places some definite restrictions on the physical conditions obtaining in planetary nebulae.

It does not seem to have been emphasized previously that the levels $^3P_2$ of *O* III and $^2P_{3/2}$ of *N* III, from which the original fluorescent absorption arises, *are not the ground levels* of the terms involved. Furthermore, although the mean lives of the levels $2p^2\ ^3P_2$ and $2p\ ^2P_{3/2}$ are long,[3] they are, nevertheless, much shorter than the expected time the atom must wait before being excited by the foregoing mechanism. Therefore, if only radiation processes are involved, we should expect the large majority of the atoms to be in the true ground levels, $^3P_0$ and $^2P_{1/2}$, respectively, of *O* III and *N* III. That a condition of this sort holds in interstellar space is shown by the observations of T. Dunham,[4] who points out that the only observable interstellar absorption lines of *Ti* II are those arising from the true ground level. Lines from other levels of the same term are not observed.

In view of the fact that there is an alternative method by means of which fractional multiplets may be obtained—namely, in electron capture by ions not statistically distributed—we have thought it wise to undertake the relevant quantum mechanical analysis. Although the results are apparently negative, as far as explanation of the fractional multiplets of planetary nebulae is concerned, the calculations appear to be of sufficient interest to warrant a summary here.

The problem is extremely simple to visualize. For the sake of explicitness, we shall discuss first the case of radiative electron capture by *O* IV to give directly *O* III in the configuration $1s^2\ 2s^2\ 2p3d$. Under the conditions that obtain in the nebulae we might reasonably assume that practically all the *O* IV ions are in the very lowest level $1s^2\ 2s^2\ 2p\ ^2P_{1/2}$. If the *O* IV ions were distributed between $^2P_{3/2}$ and $^2P_{1/2}$ according to the statistical weights, we should obtain (because of the sum rules) approximately a statistical distribution of the captured electrons among the levels of *O* III 2p3d. But on the assumption that all the ions are in the level $^2P_{1/2}$, we expect and obtain, large peculiarities in the distribution in 2p3d.

To make a (dipole) radiative transition into 2p3d, the electron before capture must be in either a p or an f orbit. The *O* IV ion in the level $2p\ ^2P_{1/2}$, plus the free electron in a hyperbolic orbit of energy

[3] The mean lives are: *O* III $2p^2\ ^3P_2$, 2.9 hours; *N* III $2p\ ^2P_{3/2}$, 5.3 hours.

[4] *Nature*, **139**, 246, 1937.

E, are to be considered together as forming a term of the continuous spectrum of O III, which we write as

$$2p_{1/2}Ep_{1/2}\,,\ 2p_{1/2}Ep_{3/2}\,,\ 2p_{1/2}Ef_{5/2}\,,\ 2p_{1/2}Ef_{7/2}\,, \tag{1}$$

according to whether the free electron is in a p or an f orbit and according to the total (spin+orbital) angular momentum of this free electron. These are definite terms of O III in *jj* coupling, capable of making radiative transitions to the levels of 2p3d, which are, however, in *LS* coupling. The problem is then one of obtaining the strengths of the lines in the transitions from the configurations 2pEp and 2pEf in *jj* coupling to the configuration 2p3d in *LS* coupling. This problem may be solved in all detail, but with considerable labor, by the standard methods of transformation theory; but a theorem we shall shortly prove will furnish very quickly the answers to the questions of interest here.

We are interested only in the *total* strength from all the levels comprehended in (1)[5] to a given level of 2p3d. *If* the configuration 2p3d were in *jj* coupling, the answer would be given very simply by the sum rule:[6] the total strength to any level $(2p_{1/2}\,3d_j\,J)$ in which the 2p electron has the same j value as in (1) would be proportional to $2J+1$; the strengths to all levels for which the 2p electron has the j value $\frac{3}{2}$ would vanish. The theorem below shows that with 2p3d in any other coupling, in particular Russell-Saunders, we need only express the eigenfunction of each level in terms of *jj* coupling levels, e.g.,[7]

$$\psi(pd\,^3F_2) = \left(\frac{1}{15\sqrt{2}}\right)\left[4\sqrt{21}\,\psi(p_{1/2}d_{3/2}) - \sqrt{14}\,\psi(p_{1/2}d_{5/2}) + 2\sqrt{21}\,\psi(p_{3/2}d_{3/2}) - 4\psi(p_{3/2}d_{5/2})\right],$$

$$\psi(pd\,^3P_1) = \left(\frac{1}{\sqrt{30}}\right)\left[-\sqrt{5}\,\psi(p_{1/2}d_{3/2}) + 4\psi(p_{3/2}d_{3/2}) + 3\psi(p_{3/2}d_{5/2})\right],$$

etc. We then take the sum of the squares of the coefficients of the states $p_{1/2}d_{3/2}$ and $p_{1/2}d_{5/2}$ (which sum we call the $p_{1/2}$ *parentage factor*)

[5] I.e., the levels $2p_{1/2}\,Ep_{1/2}$, $J = 0, 1$; $2p_{1/2}\,Ep_{3/2}$, $J = 1, 2$; etc.

[6] Condon and Shortley, *Theory of Atomic Spectra*, p. 279.

[7] *Ibid.* All the necessary transformation coefficients are tabulated on p. 294.

and multiply this sum by $2J + 1$ to get the relative total strengths of the capture transitions to the different levels of $2p3d$. For example, for $^3F_2$ and $^3P_1$ the $p_{1/2}$ parentage factors are

$$(1/225 \cdot 2)(16 \cdot 21 + 14) = \tfrac{7}{9},$$

$$(\tfrac{1}{30})5 = \tfrac{1}{6},$$

respectively. The relative total strengths are then $\frac{7}{9} \cdot 5 = 35/9$ and $\frac{1}{6} \cdot 3 = 1/2$.

It is in this way that the $p_{1/2}$ parentage factors and the relative total strengths of Table 2 are computed for various transition arrays of interest.[8] These values are independent of the energy and the angular momentum of the captured electron, but to get transition probabilities from these strengths requires multiplication by the cube of the wave number of the radiation emitted in the capture, averaged in a complicated way over the energy of the captured electron. The transition probability falls rapidly with increasing electron energy. Consequently, for low electron temperatures, T, such that $kT < \chi$, where χ is the ionization energy, one should get satisfactory relative transition probabilities by using the cube of the wave-length limit of the continuous radiation. For very high temperatures the averaged factors for the various continua approach equality.

The method used in these computations is a special case of a rather general theorem of matrix mechanics, which is demonstrated at the end of the paper. For the modifications necessary to handle capture into a configuration, such as p^2, involving equivalent electrons, see the discussion under this theorem. We shall proceed first to the astrophysical discussion of Table 2.

In Table 3 are given the relative strengths of the lines in the configuration arrays ps − pp and pp − pd. The relative intensities are to be obtained from these strengths by multiplication by the fourth power of the wave number and by a population factor that is unity if each upper level is populated in proportion to its statistical weight

[8] If we had been interested in the case in which the ion is in $^2P_{3/2}$, we should, by the same procedure, obtain the complementary relative strengths, which with the strengths from $^2P_{1/2}$ make up the whole $2J + 1$. These are also listed in Table 2.

$(2J + 1)$. The population of a level depends on the rates at which atoms enter and leave the level, by all processes. For the assumption of excitation of pp and pd, respectively, purely by electron capture,

TABLE 2

RELATIVE TOTAL STRENGTHS OF TRANSITIONS INVOLVED IN RADIATIVE ELECTRON CAPTURE BY AN ION IN LEVELS p $^2P_{1/2}$ AND p $^2P_{3/2}$

TRANSITION	TERM	ION IN LEVEL		SUM	$p_{1/2}$ PARENTAGE FACTOR
		$^2P_{1/2}$	$^2P_{3/2}$		
Capture of p or f electron to give pd	$^3F_4$	0	9	9	0
	$^3F_3$	28/9	35/9	7	4/9
	$^3F_2$	35/9	10/9	5	7/9
	$^1F_3$	7/3	14/3	7	1/3
	$^3D_3$	14/9	49/9	7	2/9
	$^3D_2$	35/18	55/18	5	7/18
	$^3D_1$	3/2	3/2	3	1/2
	$^1D_2$	5/3	10/3	5	1/3
	$^3P_2$	5/2	5/2	5	1/2
	$^3P_1$	1/2	5/2	3	1/6
	$^3P_0$	0	1	1	0
	$^1P_1$	1	2	3	1/3
Capture of s or d electron to give pp	$^3D_3$	0	7	7	0
	$^3D_2$	5/2	5/2	5	1/2
	$^3D_1$	5/2	1/2	3	5/6
	$^1D_2$	5/3	10/3	5	1/3
	$^3P_2$	5/6	25/6	5	1/6
	$^3P_1$	3/2	3/2	3	1/2
	$^3P_0$	2/3	1/3	1	2/3
	$^1P_1$	1	2	3	1/3
	$^3S_1$	1	2	3	1/3
	$^1S_0$	1/3	2/3	1	1/3
Capture of s or d electron to give p^2	$^3P_2$	5/3	25/3	10	1/6
	$^3P_1$	3	3	6	1/2
	$^3P_0$	4/3	2/3	2	2/3
	$^1D_2$	10/3	20/3	10	1/3
	$^1S_0$	2/3	4/3	2	1/3
Capture of p electron to give ps	$^3P_2$	0	5	5	0
	$^3P_1$	2	1	3	2/3
	$^3P_0$	1	0	1	1
	$^1P_1$	1	2	3	1/3

Table 4 takes into account solely the rate of entrance of the atoms. It is obtained from Table 3 by multiplication of the files referring to the upper levels by the $p_{1/2}$ *parentage* factors of Table 2.[9]

[9] Note also that the variation in the (wave number)^3 factor necessary to convert Table 2 into transition probabilities is neglected.

Table 4 contains only part of the story, however. Since 2p3d feeds very strongly into $2p^2$ as well as into 2p3p, only a fraction, and probably a small fraction at that, of the atoms entering 2p3d will be available for transition to 2p3p. Most of the atoms in the terms ^3D, ^3P, ^1F, ^1D, or ^1P of 2p3d will have a much higher probability,

TABLE 3

LINE STRENGTHS IN NORMAL ARRAYS

			$1s^2\ 2s^2\ 2p3p$									
			^3D			^3P			^3S	^1D	^1P	^1S
		J	3	2	1	2	1	0	1	2	1	0
$1s^2\ 2s^2\ 2p3d$	^3F	4	54	0	0	0	0	0	0	0	0	0
		3	14/3	112/3	0	0	0	0	0	0	0	0
		2	2/15	14/3	126/5	0	0	0	0	0	0	0
	^3D	3	28/3	7/6	0	63/2	0	0	0	0	0	0
		2	7/6	125/24	9/8	45/8	135/8	0	0	0	0	0
		1	0	9/8	27/8	3/8	45/8	15/2	0	0	0	0
	^3P	2	7/10	1/8	1/120	75/8	25/8	0	50/3	0	0	0
		1	0	3/8	1/8	25/8	15/8	5/2	10	0	0	0
		0	0	0	1/6	0	5/2	0	10/3	0	0	0
	^1F	3	0	0	0	0	0	0	0	42	0	0
	^1D	2	0	0	0	0	0	0	0	15/2	45/2	0
	^1P	1	0	0	0	0	0	0	0	1/2	15/2	10
$1s^2\ 2s^2\ 2p3s$	^3P	2	7	5/4	1/12	15/4	5/4	0	5/3	0	0	0
		1	0	15/4	5/4	5/4	3/4	1	1	0	0	0
		0	0	0	5/3	0	1	0	1/3	0	0	0
	^1P	1	0	0	0	0	0	0	0	5	3	1

because of the large ν-cube factor, of relapsing directly to ^3P, ^1D, or ^1S of $2p^2$ than of going to the terms of 2p3p. Atoms in any one of the levels of ^3F of 2p3d, however, can relapse only to ^3D of 2p3p. The intensity of this multiplet remains as given in Table 4, whereas all the others are diminished by a very appreciable factor. The strengths in the second part of Table 4, from the array 2p3p − 2p3s, are unaffected by any such complications. Comparison of Tables 3 and 4, even without the depletion just discussed, shows that the

relative strengths of the various multiplet lines are abnormal. Certain lines are missing or are very weak. As far as the multiplets $^3P - {}^3D$, $^3P - {}^3P$, and $^3P - {}^3S$ are concerned, the intensity distor-

TABLE 4

MODIFICATION OF TABLE 3 ON THE ASSUMPTION OF EXCITATION BY DIRECT ELECTRON CAPTURE IN THE UPPER LEVELS OF $2p3d \rightarrow 2p3p$ AND $2p3p \rightarrow 2p3s$

			^3D			^3P			^3S	^1D	^1P	^1S
		J	3	2	1	2	1	0	1	2	1	0
			$1s^2\,2s^2\,2p3p$									
$1s^2\,2s^2\,2p3d$ (excited by capture)	^3F	4	0	0	0	0	0	0	0	0	0	0
		3	56/27	448/27	0	0	0	0	0	0	0	0
		2	14/135	98/27	98/5	0	0	0	0	0	0	0
	^3D	3	56/27	7/27	0	7	0	0	0	0	0	0
		2	49/108	875/432	7/16	35/16	105/16	0	0	0	0	0
		1	0	9/16	27/16	3/16	45/16	15/4	0	0	0	0
	^3P	2	7/20	1/16	1/240	75/16	25/16	0	25/3	0	0	0
		1	0	1/16	1/48	25/48	5/16	5/12	5/3	0	0	0
		0	0	0	0	0	0	0	0	0	0	0
	^1F	3	0	0	0	0	0	0	0	14	0	0
	^1D	2	0	0	0	0	0	0	0	5/2	15/2	0
	^1P	1	0	0	0	0	0	0	0	1/6	5/2	10/3
			$1s^2\,2s^2\,2p3p$ (excited by capture)									
$1s^2\,2s^2\,2p3s$	^3P	2	0	5/8	5/72	5/8	5/8	0	5/9	0	0	0
		1	0	15/8	25/24	5/24	3/8	2/3	1/3	0	0	0
		0	0	0	25/18	0	1/2	0	1/9	0	0	0
	^1P	1	0	0	0	0	0	0	0	5/3	1	1/3

tion agrees fairly well with observation. The partial excitation of $^3P_1$ is accounted for naturally, whereas Bowen was forced to consider the extremely high velocity differential of 90 km/sec to achieve excitation of $2p3d\ ^3P_1$ by resonance absorption of the ultimate line of *He* II. But failure of at least the lines of the $^3F - {}^3D$ and $^3D - {}^3P$ multiplets to appear is definite evidence against the validity of the

mode here considered of exciting fractional multiplets. It is true that we have taken into account only the excitation of 2p3d directly by electron capture, while electrons will also be captured into higher configurations and feed down into 2p3d. But the changes occasioned by taking this into account will certainly *decrease* the intensity anomalies and will not aid matters.

Looking now at 2p3p − 2p3s in Table 4, we see that direct capture into 2p3p could not possibly account for the observed intensity anomalies. A rough computation shows that the assumption of ex-

TABLE 5

RELATIVE STRENGTHS OF OBSERVABLE LINES ON BOWEN'S HYPOTHESIS

		J	$1s^2\,2s^2\,2p3p$						
			^3D			^3P			^3S
			3	2	1	2	1	0	1
$1s^2\,2s^2\,2p3d$ . .	^3P	2	7/10	1/8	1/120	75/8	25/8	0	50/3
$1s^2\,2s^2\,2p3s$ . .	^3P	2	7/10	1/32	1/4320	225/32	125/96	0	250/27
		1	0	3/32	1/288	75/32	75/96	0	50/9
		0	0	0	1/216	0	25/24	0	50/27

citation of 2p3p principally by transitions from 2p3d does not improve the agreement.

Also, the observed anomalous intensities in the multiplet $3p\,^2P^0 - 3d\,^2D$ of *N* III cannot be accounted for by the present scheme, because the ground term of *N* IV is $^1S_0$, a single level.

We are apparently forced to return to the Bowen mechanism for the excitation of these lines, despite the fact that it does not account for the strength of the singlet line λ 5592. In Table 5 are given the relative theoretical strengths of the lines of the significant multiplets of *O* III, calculated on the basis of initial selective excitation of $^3P_2$ alone. The strengths in the two transition arrays of this table have the correct relative values and need only be multiplied by ν^4 to give the relative intensities of all the lines. The tabulated strengths show good qualitative agreement with the lines observed in the nebulae.

As was noted earlier in this paper, acceptance of the Bowen mechanism places a definite restriction on physical conditions within a

nebula. In interstellar space the high concentration of atoms occurs in the lowest level, whereas in the nebulae an appreciable population must be maintained in the levels $^3P_2$ and $^2P^o_{3/2}$ of *O* III and *N* III, respectively. The mean lifetimes of these levels are of the order of several hours,[3] and a concentration will occur only when the rate of excitation to these levels is also about once in three hours. Radiation processes, with the high dilution existing in nebulae, cannot be called on for so frequent excitations. A study of the problem indicates that collisional excitations from the ground level must be sufficiently frequent to maintain the required population. This investigation, by Hebb and Menzel, will form the subject of the next paper of the present series.

We proceed now to the proof of a theorem concerning the transformation properties of the line-strength matrix which will justify the method used in the above computations.

THEOREM.—*Consider a configuration* α *and all the levels* βJ *of a particular angular momentum* J *belonging to a configuration* β. *In a particular coupling let the levels of* α *and of* βJ *break into two groups* α', α'' *and* $\beta' J$, $\beta'' J$ *such that* $\beta'' J$ *does not combine with* α' ($\beta' J$ *may combine with both* α' *and* α''). *In this case the matrix*[10] *of* $S^{1/2}$ *connecting the levels of configuration* α *with those of* βJ *will have the form*

$$
\begin{array}{c|c|c}
 & \beta' J & \beta'' J \\
\hline
\alpha' & \begin{matrix} S_{11} & S_{12} \ldots S_{1\nu} \\ S_{21} & S_{22} \ldots S_{2\nu} \\ \ldots\ldots\ldots \\ S_{n1} & S_{n2} \ldots S_{n\nu} \end{matrix} & \begin{matrix} 0 & 0 \ldots 0 \\ 0 & 0 \ldots 0 \\ \ldots\ldots \\ 0 & 0 \ldots 0 \end{matrix} \\
\hline
\alpha'' & \begin{matrix} x & x \ldots x \\ x & x \ldots x \\ \ldots\ldots \\ x & x \ldots x \end{matrix} & \begin{matrix} x & x \ldots x \\ x & x \ldots x \\ \ldots\ldots \\ x & x \ldots x \end{matrix}
\end{array}
\qquad (2)
$$

[10] See Condon and Shortley, *op. cit.*, p. 277, for definition of this matrix, whose components are the square roots of the line strengths chosen with phases corresponding to those of the matrix components of electric moment.

Let the strength of each of the files connecting one of the levels of $\beta' J$ with all the levels of α' have the same value C_J, and let all pairs of these files be orthogonal. That is, let

$$\sum_{i=1}^{n} s_{i\xi}\, s_{i\eta} = C_J\, \delta_{\xi\eta} . \tag{3}$$

Now consider a level βJ of configuration β in any other coupling. When this level is expressed in the β', β'' scheme, let the sum of the squares of the transformation amplitudes connecting this level with the levels of $\beta' J$ be τ. Then the total strength of all transitions connecting the level βJ and the levels of the part-configuration α' will be τC_J.

To prove this statement let the level βJ be connected with those of β'J and β''J by transformation amplitudes contained in the one-column matrix

	βJ
	t_1
β'J	t_2
	. . . .
	t_ν
	x
	x
β''J	. . . .
	x

(4)

where by hypothesis

$$\sum_{\xi=1}^{\nu} t_\xi^2 = \tau \leq 1 . \tag{5}$$

Now, since α' does not combine with β''J, we may get the $S^{1/2}$ ma-

trix connecting α' and βJ by multiplying the upper left square of (2) with the upper part of (4) to get

$$\begin{array}{c|c} & \beta J \\ \alpha' & \begin{array}{|c|}\hline \sum_{\xi=1}^{\nu} s_{1\xi}\, t_\xi \\ \hline \sum s_{2\xi}\, t_\xi \\ \hline \cdots\cdots\cdots \\ \hline \sum s_{n\xi}\, t_\xi \\ \hline \end{array} \end{array}$$

The sum of the squares of these elements is

$$\sum_{i=1}^{n}\sum_{\xi=1}^{\nu}\sum_{\eta=1}^{\nu} s_{i\xi}\, t_\xi\, s_{i\eta}\, t_\eta = C_J \sum_{\xi=1}^{\nu} t_\xi^2 = \tau C_J\,,$$

where the right-hand members are obtained by carrying out first the sum over i, then that over ξ. Note that in cases where this theorem is valid, one may obtain the desired sums without knowing the relation between the phases in (2) and the phases in (4). This is sometimes a great convenience.

We may now apply this theorem explicitly to transitions from αEl to αn'l' where the electron n'l' is not equivalent to any in the parent configuration α. Let α_1 represent a given *level* of the parent configuration in the ion. Then, if we characterize the levels of αn'l' by the same parents, there will be no transitions from any level of α_1n'l' to any levels of αEl except those of α_1El. The sum of the strengths from a given level α_1n'l'J to all levels of α_1El is

$$C_J = (2J+1)\,|(\mathrm{El}\,\vdots\,P\,\vdots\,\mathrm{n'l'})|^2\,\Xi(l, l')\,, \qquad (6)^{11}$$

[11] *Ibid.*, p. 281. Here $\Xi(l, l+1) = (l+1)(2l+3)$; $\Xi(l, l-1) = l(2l-1)$; $(\mathrm{El}\,\vdots\,P\,\vdots\,\mathrm{n'l'})$ is an integral of the product of r and the radial functions of the two states as defined in *ibid.*, p. 132. Since one of the levels is in the continuum, we must consider (6) as referring to unit energy range and the radial function for the continuum normalized in the proper fashion. See Kemble, *Quantum Mechanics*, for a good discussion of this normalization.

proportional to $2J + 1$. The orthogonality conditions of the foregoing theorem are also satisfied;[11] hence, in the case of a level of $\alpha n'l'J$ in any other coupling, having a total component τ in the sense of (5) in the direction of $\alpha_1 n'l'J$, the total strength to all levels of $\alpha_1 El$ will be τC_J. Note that *the relative values of the strength sums from the different levels of a given discrete* configuration $\alpha n'l'$ to continuous states $\alpha_1 El$ is independent of whether $l = l' + 1$ or $l' - 1$, and of the energy E.

O III is just a special case of the previous paragraph, with $\alpha = 1s^2\,2s^2\,2p$; $\alpha_1 = 1s^2\,2s^2\,2p\,{}^2P_{1/2}$; hence our earlier calculations are justified except for the case $p({}^2P_{1/2})Es$ or $p({}^2P_{1/2})\,Ed \rightarrow p^2$, which violates the inequivalence specification. But in this case an examination of the $S^{1/2}$ matrices in *jj* coupling shows them to be of the form (2), if for the p^2 configuration we take $\beta' 0 = p_{1/2}p_{1/2}0$; $\beta' 1 = p_{3/2}p_{1/2}1$; $\beta' 2 = p_{3/2}p_{1/2}2$ (for the case ps, p^2 see the matrix on page 265 of Condon and Shortley). The C_J's in these cases are no longer proportional to $2J + 1$ but have the same relative values for capture of s and d electrons, namely, $C_0 : C_1 : C_2 = 2 : 3 : 5$.

MENDENHALL LABORATORY OF PHYSICS
OHIO STATE UNIVERSITY
AND
HARVARD COLLEGE OBSERVATORY

AN INVESTIGATION OF THE ROWLAND INTENSITY SCALE

DONALD H. MENZEL, LEO GOLDBERG, AND EDWARD M. COOK

ABSTRACT

A new calibration of Rowland's scale of solar intensities has been derived with the aid of the theoretical strengths of multiplets in transition arrays. The calibration takes the form of a double-entry table giving average values of log X_0, where X_0 is the optical depth at the center of an absorption line, for each Rowland intensity from -3 to $+8$ at intervals of 400 A from λ 2800 to λ 6800. A total of 37 transition arrays, representing 13 metallic elements and 1119 lines in all, was employed in the analysis. The present calibration is considerably less steep than the earlier one of Russell, Adams, and Moore.

Probably the most promising method of deducing the physical conditions in the solar reversing layer is through studies involving the curve of growth of absorption lines in the Fraunhofer spectrum. Such studies have been greatly accelerated by the wealth of equivalent widths published by C. W. Allen,[1] and further important results are to be expected on the completion of the Utrecht atlas of the solar spectrum. In the future we may expect these photometric measures to replace completely the admittedly rough estimates of intensity contained in the *Revised Rowland Tables*. Nevertheless, as ragged and approximate as the Rowland intensity estimates are, they represent a vast amount of data. The estimates are particularly important for the very faint solar lines and for lines in the region 3000–4000 A, for which measures by Allen are not available.

Before the Rowland estimates can be employed in analyses of the physical conditions in the solar reversing layer, it is necessary that the arbitrary intensity scale be calibrated, preferably in terms of a quantity related to the numbers of atoms per square centimeter above the photosphere that are active in producing the various Fraunhofer lines. Such a calibration was first carried out by Russell, Adams, and Moore[2] in their pioneering investigation of a decade ago. The important astrophysical results that have accrued from this initial investigation are so well known that there is no necessity of reviewing them here.

The Russell-Adams-Moore calibration assumed that the relative

[1] *Mem. Comm. Solar Obs.*, **1**, No. 5, 1934. [2] *Ap. J.*, **68**, 1, 1929.

strengths of the lines in a multiplet correspond to the relative numbers of atoms that are active in producing these lines. For each multiplet the lines were combined into two or three groups, for which mean values of log N and R yielded one or two values of ΔR and $\Delta \log N$ corresponding to a given value of R. The limitations of such a calibration are obvious. Confining the theoretical strengths to lines of the same multiplet meant that only a relatively small range of intensity could be covered in any one group of related lines, a procedure that increased the possibilities of systematic and accidental errors in the calibration. Also, since lines of the same multiplet do not differ widely in wave length, there is no possibility of determining whether a line in the red requires more, or fewer, atoms for its production than one of the same Rowland intensity in the violet.

We may overcome these two difficulties simultaneously by employing the theoretical strengths of different multiplets in transition arrays. Whereas a single multiplet rarely consists of more than 12 or 13 lines with approximately a 100 A wave-length range, the number of lines that can be related in a transition array may number well over a hundred and possess a wave-length dispersion of several thousand angstroms. The relative strengths of different multiplets in a transition array are calculable according to methods outlined by Krönig,[3] Shortley,[4] Condon and Ufford,[5] and Menzel and Goldberg,[6] under the assumptions that configuration interaction is negligible and that the atom obeys the rules of LS coupling. These idealized conditions are not too well fulfilled by complex atoms, and the present investigation was begun with the hope of testing the general validity of the theoretical multiplet strengths. But with the progress of this and other related solar work,[7] the evidence accumulated that the use of large numbers of multiplets tends to iron out random deviations and yields consistent results in the mean, although the theoretical strength of a single multiplet may be considerably in error. Consequently, the decision was made to employ the theoretical multiplet strengths in an independent calibration of the Rowland scale.

[3] *Zs. f. Phys.*, **33**, 261, 1925.

[4] *Phys. Rev.*, **47**, 295, 1935.

[5] *Phys. Rev.*, **44**, 740, 1933.

[6] *Ap. J.*, **84**, 1, 1936.

[7] Menzel, Baker, and Goldberg, *Ap. J.*, **87**, 81, 1938.

Menzel[8] has shown that the quantity W/λ, where W is the equivalent width of an absorption line and λ its wave length, is a simple function of X_0, the optical depth at the center of the line. The expression for X_0 is written

$$X_0 = 3.510 \times 10^{-12} \frac{N_a}{b(T)} e^{-\chi_{J'}/kT} \sqrt{\frac{\mu}{T}} \phi S \frac{s}{\Sigma s}, \qquad (1)$$

where N_a is the total number of atoms of a given element in a particular stage of ionization in a square-centimeter column above the photosphere, $b(T)$ is a partition function, k is Boltzmann's constant, $\chi_{J'}$ is the lower excitation potential, T is the temperature, μ is the atomic weight, and $s/\Sigma s$ is the fraction that a line in a given multiplet contributes to the total strength, S, of the multiplet. The strength is measured in units of σ^2, the square of the first-order electric moment between the two electronic configurations. ϕ is a dimensionless constant, defined by the relation

$$\phi = \frac{\sigma^2}{a_0^2 \epsilon^2}, \qquad (2)$$

where a_0 is the radius of the first Bohr orbit, and ϵ is the electronic charge.

In the interest of consistency with equivalent-width investigations, we have chosen to calibrate the Rowland scale in terms of X_0. The quantity ϕ is constant for a given transition array. Hence, if we set

$$\log X_0'' = \log S - \log \frac{\Sigma s}{s} - \frac{5040}{T} \chi_{J'} + \tfrac{1}{2} \log \mu, \qquad (3)$$

X_0'' proves to be proportional to X_0 for all the lines of a transition array. The quantity T is the excitation temperature governing the distribution of atoms among the various excited states. In a preliminary calibration, the value $T = 5740°$ was adopted, but later investigation[9] showed that a temperature of 4500° corresponded

[8] *Ap. J.*, **84**, 462, 1936.

[9] Menzel, Baker, and Goldberg, *op. cit.*; R. B. King, *Ap. J.*, **87**, 40, 1938.

more closely to the observations, and this value was employed in the final calibration. It will be seen later that the slope of the calibration-curve is not very sensitive to the temperature assumed.

The procedure followed in effecting the calibration may be briefly outlined. For all the lines of a transition array we calculate log X_0'' from equation (3). The quantities S and $s/\Sigma s$ are taken from Goldberg's[10] and from Russell's[11] tables, respectively. A total of 37 transition arrays, representing 13 metallic elements and 1119 lines in all, was employed in the analysis. The material is contained in Table 1, where successive columns show the element, the transition array, and the numbers of multiplets and lines in each array. Since the lines of a transition array usually extend over a considerable region of the spectrum, we have attempted to establish the variation of log X_0'' with λ for each Rowland intensity. The spectrum was divided into successive wave-length intervals and the average taken of all the values of log X_0'' for lines of the same R that fall within a particular interval. It is, of course, desirable that the wave-length interval be as small as possible, so that rapid variations in Rowland's scale may be detected. In practice, however, we are limited by the relative thinness of the distribution with wave length of the set of related lines. Accordingly, we found it most practical to choose intervals of 400 A over the region from λ 2800 to λ 6800. The calibration for each array then takes the form of a double-entry table which gives a value of log X_0'' corresponding to each value of R and λ. Table 2 provides an illustration of the procedure, showing the two-dimensional table for the transition array *Ti* I $3d^34s - 3d^34p$.

If a sufficient number of lines in each array were available, each such table would represent a two-dimensional calibration of Rowland's scale. It would then be a simple matter to obtain the final calibration by combining the various transition arrays graphically. Unfortunately, however, although the maximum possible number of entries per table is 144, the actual numbers vary from as few as 2 or 3 to only 38 for the transition array shown in Table 2. We must therefore seek to combine the various tables by some numerical

[10] *Ap. J.*, **82**, 1, 1935; *ibid.*, **84**, 11, 1936.

[11] *Ap. J.*, **83**, 129, 1936.

TABLE 1

SUMMARY OF SPECTROSCOPIC DATA

Element	Transition Array	Number of Multiplets	Number of Lines
Ca I	$4s4p-4s4d$	1	6
	$4s4p-4p^2$	3	8
	$4s4p-4s6s$	2	3
	$4s4p-4s6d$	2	5
	$4s4p-4s7s$	2	4
	$4s3d-4s5p$	2	7
	$3d4s-3d4p$	4	22
	$4s3d-4s6p$	2	5
Sc I	$3d4s^2-3d4s4p$	2	6
	$3d^24s-3d^24p$	6	21
Sc II	$3d4s-3d4p$	6	16
	$3d^2-3d4p$	8	26
Ti I	$3d^34s-3d^34p$	34	128
	$3d^24s^2-3d^24s4p$	18	57
	$3d^34s-3d^24s4p$	9	25
	$3d^24s4p-3d^24s5s$	8	31
	$3d^24s4p-3d^24s4d$	11	34
Ti II	$3d^3-3d^24p$	24	82
	$3d^24s-3d^24p$	17	68
V I	$3d^44s-3d^44p$	11	60
Cr I	$3d^54s-3d^54p$	2	6
	$3d^44s4p-3d^44s5s$	5	37
Cr II	$3d^44s-3d^44p$	3	17
Mn I	$3d^64s-3d^64p$	6	54
	$3d^54s4p-3d^54s5s$	3	11
	$3d^54s4p-3d^54s4d$	2	13
Fe I	$3d^74s-3d^74p$	11	64
	$3d^64s4p-3d^64s5s$	8	82
Ni I	$3d^94s-3d^94p$	5	14
	$3d^84s4p-3d^84s4d$	13	45
	$3d^94p-3d^94d$	16	43
	$3d^94p-3d^96s$	4	9
	$3d^94p-3d^95d$	4	7
Zr I	$4d^25s^2-4d^25s5p$	6	13
	$4d^35s-4d^35p$	5	11
Zr II	$4d^25s-4d^25p$	14	44
	$4d^3-4d^25p$	14	35

method.[12] The following method of effecting the combination appeared to be most satisfactory.

Let us denote an entry in any double-entry table by $F'(R_i\lambda_j)_n$, where R_i and λ_j are particular values of R and λ, and n refers to a given transition array or double-entry table. The corresponding

TABLE 2

MEAN VALUES OF LOG X_0'' FOR TRANSITION ARRAY *Ti* I $3d^34s-3d^34p$

R	Wave Length						
	4000–4400	4400–4800	4800–5200	5200–5600	5600–6000	6000–6400	6400–6800
+4	+0.24 (2)*	+0.32 (2)	+0.46 (2)	.....	.....	.....	.....
+3	−0.58 (1)	−0.45 (6)	−0.04 (4)	.....	.....	−0.29 (2)	.....
+2	−0.61 (7)	−0.67 (11)	−0.58 (6)	−0.62 (3)	.....	−0.46 (1)	.....
+1	−1.32 (3)	−1.12 (9)	−1.06 (3)	.....	.....	.....	−0.35 (1)
0	−1.61 (7)	−1.71 (7)	−1.38 (4)	.....	−1.24 (1)	−1.15 (1)	−0.50 (1)
−1	−1.75 (9)	−2.07 (8)	−1.69 (5)	−1.88 (3)	.....	−1.52 (1)	.....
−2	.....	−2.27 (2)	−2.19 (6)	−1.99 (3)	.....	−1.52 (1)	.....
−3	.....	−2.39 (2)	−2.18 (2)	.....	.....	.....	−1.52 (1)

* Numbers in parentheses denote number of lines comprising each average.

value of log X_0 may be written $F(R_i\lambda_j)$, since log X_0 depends only on R and λ. Equations (1) and (3) show that $F'(R_i\lambda_j)_n$ differs from $F(R_i\lambda_j)$ by a constant, which we denote by the symbol Δ_n:

$$\left.\begin{aligned}\Delta_n &= F'(R_i\lambda_j)_n - F(R_i\lambda_j) \\ &= 13.35 - \log\left[\frac{N_a}{b(T)}\,\phi\right]_n,\end{aligned}\right\} \tag{4}$$

or

$$F(R_i\lambda_j) = F'(R_i\lambda_j)_n - \Delta_n\,. \tag{5}$$

If we write equation (5) for any other transition array m, inserting the same values of R and λ, we have

$$F(R_i\lambda_j) = F'(R_i\lambda_j)_m - \Delta_m\,. \tag{6}$$

[12] We are indebted to Dr. T. E. Sterne for suggesting the proper method of approach to this problem.

Subtracting equation (5) from equation (6), we find

$$F'(R_i\lambda_j)_m - F'(R_i\lambda_j)_n = \Delta_m - \Delta_n . \tag{7}$$

Thus, any entry in one table theoretically differs from the corresponding entry in another table by a constant, and, if a single value of Δ is known, the remaining values may be calculated from equation (7). Because of errors in the theoretical strengths, however, and also in the Rowland estimates, the differences between corresponding entries in any pair of tables are not identical. Some method of averages must be employed. To calculate the Δ_n's we begin by assigning an arbitrary value of Δ_1 to array No. 1, *Ti* II $3d^3 - 3d^24p$, and then proceed to determine relative values of Δ_n. Let

$$\Delta_{mn} = \Delta_m - \Delta_n , \tag{8}$$

whereupon equation (7) becomes, for $m = 1$,

$$F'(R_i\lambda_j)_1 - F'(R_i\lambda_j)_n = \Delta_{1n} . \tag{9}$$

We can calculate a value of Δ_{1n} for every pair of values F'_1 and F'_n that occurs in the same R, λ interval. Since they are not identical, the simplest procedure, which immediately suggests itself, is first to compute the average value of Δ_{1n} for each transition array and then combine the 37 tables by a straight averaging process. Unfortunately this method fails because a great many tables have few or no entries in common with the first table. Hence, we must first endeavor to enlarge this table more nearly to completion. This result may be accomplished by combining the 6 most complete tables (Tables 1–6) by a least-squares solution.

We are required to evaluate the quantities $\Delta_{12}, \Delta_{13}, \ldots, \Delta_{16}$ by the method of least squares. If $\overline{\Delta}_{mn}$ is the mean value of Δ_{mn} as computed from pairs of tabular entries with the same values of R and λ, the Δ's are to be computed according to the following equations

of condition, weighted according to the square root of the number of values of Δ_{mn} that were employed in computing the means:

$$\left.\begin{aligned}
\Delta_{12} &= \bar{\Delta}_{12} && (\sqrt{14})\\
\Delta_{13} &= \bar{\Delta}_{13} && (\sqrt{12})\\
\Delta_{14} &= \bar{\Delta}_{14} && (\sqrt{5})\\
\Delta_{15} &= \bar{\Delta}_{15} && (\sqrt{8})\\
\Delta_{16} &= \bar{\Delta}_{16} && (\sqrt{16})\\
\Delta_{23} &= -\Delta_{12}+\Delta_{13} = \bar{\Delta}_{23} && (\sqrt{14})\\
\Delta_{24} &= -\Delta_{12}+\Delta_{14} = \bar{\Delta}_{24} && (\sqrt{3})\\
\Delta_{25} &= -\Delta_{12}+\Delta_{15} = \bar{\Delta}_{25} && (\sqrt{11})\\
\Delta_{26} &= -\Delta_{12}+\Delta_{16} = \bar{\Delta}_{26} && (\sqrt{10})\\
\Delta_{34} &= -\Delta_{13}+\Delta_{14} = \bar{\Delta}_{34} && (\sqrt{8})\\
\Delta_{35} &= -\Delta_{13}+\Delta_{15} = \bar{\Delta}_{35} && (\sqrt{15})\\
\Delta_{36} &= -\Delta_{13}+\Delta_{16} = \bar{\Delta}_{36} && (\sqrt{9})\\
\Delta_{45} &= -\Delta_{14}+\Delta_{15} = \bar{\Delta}_{45} && (\sqrt{4})\\
\Delta_{46} &= -\Delta_{14}+\Delta_{16} = \bar{\Delta}_{46} && (\sqrt{3})\\
\Delta_{56} &= -\Delta_{15}+\Delta_{16} = \bar{\Delta}_{56} && (\sqrt{9})
\end{aligned}\right\} \qquad (10)$$

The weighting factors are given in parentheses. The equations were solved in the usual way for $\Delta_{12}, \Delta_{13}, \ldots, \Delta_{16}$. The results are shown

TABLE 3

RESULTS OF LEAST-SQUARES SOLUTION FOR Δ_{1n}

Table	Element	Number of Lines	$\bar{\Delta}_{1n}$	Δ_{1n}	m.e.
1.....	*Ti* II $3d^3-3d^24p$	72	0.00	0.00	.....
2.....	*Ti* I $3d^24s^2-3d^24s4p$	57	−0.96	−0.97	±0.0095
3.....	*Ti* I $3d^34s-3d^34p$	128	−0.04	−0.10	± .0095
4.....	*Fe* I $3d^64s4p-3d^64s5s$	82	+2.81	+2.93	± .013
5.....	*V* I $3d^44s-3d^44p$	60	−1.00	−1.02	± .010
6.....	*Mn* I $3d^64s-3d^64p$	54	+1.73	+1.75	±0.0096

in Table 3. The second column contains the element and transition array; the fourth column, the quantities $\bar{\Delta}_{1n}$; and the fifth and sixth

columns the computed values of Δ_{1n} with their mean errors. The agreement of the Δ's with the mean values and the smallness of the mean error speak well for the consistency of the results.

The values of $F'(R_i\lambda_j)_n$ were next increased by the addition of the value of Δ_{1n} to reduce the other five tables to the scale of the first. Next, all entries of Tables 1–6 with the same values of R and λ were averaged. We then incorporated the remaining transition arrays into the combined table by computing the mean value of Δ_{1n} for each table, adding this quantity to the entries $F'(R_i\lambda_j)_n$ and averaging as before. The final calibration is given in Table 4 and represents the material from 37 transition arrays. The table gives a value of

$$\log X_0'' = \log X_0 + \Delta_1 , \tag{11}$$

where the subscript 1 refers to the array *Ti* II $3d^3 - 3d^24p$, for every pair of values of R and λ, from $R = -3$ to $R = +8$ and from λ 2800 to λ 6800.

The calibration contained in Table 4 involves the assumption that the quantities Δ_1 are constant with wave length and hence implies that N_a, the total number of atoms above the photosphere, is independent of wave length. If the general opacity of the solar atmosphere varies with wave length, the position of the effective photosphere will rise or fall, and the numbers of atoms will also vary. To test for this variation and at the same time to impose a general check on the calculations, we have employed Allen's measures of equivalent widths in an independent calibration for the region $\lambda\lambda$ 4000–6600. Values of $\log X_0$ were obtained for each unblended line in Allen's "Intensity Table" from the tabulated equivalent widths and the curve of growth. We then computed mean values of $\log X_0$ for each Rowland intensity and for wave-length intervals of 400 A, to make the results correspond with the multiplet calibration. The results are given in Table 5. We examined the constancy of Δ_1 as a function of wave length by computing mean values of this quantity from Tables 4 and 5. The resulting values are plotted against the wave length in Figure 1. The straight line, which was fitted to the plotted points by least squares, obeys the relation

$$\Delta_1 = 2.72 - 0.230\,\lambda , \tag{12}$$

where λ is in units of 1000 A. This law corresponds very nearly to a λ^3 opacity variation. It must be remembered, of course, that the relation (12) may be due in part to systematic wave-length errors between the two calibrations.

TABLE 4

MEAN VALUES OF LOG X_0'' AS A FUNCTION OF R AND λ

R	Wave Length				
	2800–3200	3200–3600	3600–4000	4000–4400	4400–4800
+8	+1.90 (1)*	+1.22 (4)	+1.19 (2)	+0.77 (3)	.....
+7	+2.06 (1)	+1.53 (4)	+1.24 (2)	+0.45 (2)	+0.50 (1)
+6	+1.51 (1)	+0.92 (5)	+0.83 (2)	+0.88 (3)	+0.53 (2)
+5	+0.44 (1)	+0.48 (8)	+0.21 (4)	+0.03 (7)	+0.49 (3)
+4	+0.87 (2)	+0.46 (8)	+0.19 (7)	+0.15 (8)	−0.04 (4)
+3	+0.45 (3)	+0.06 (9)	−0.56 (6)	−0.40 (8)	−0.51 (9)
+2	−0.09 (4)	+0.06 (10)	−0.69 (10)	−0.84 (9)	−0.91 (10)
+1	−0.45 (3)	−0.42 (10)	−1.05 (11)	−1.11 (11)	−0.82 (8)
0	−0.69 (5)	−0.90 (5)	−1.51 (5)	−1.67 (8)	−1.23 (11)
−1	−1.33 (4)	−1.42 (5)	−1.34 (4)	−2.27 (6)	−1.69 (9)
−2	−1.28 (2)	−1.33 (4)	−1.42 (4)	−2.13 (5)	−1.82 (6)
−3	.....	−1.64 (5)	−1.42 (3)	−2.15 (1)	−2.25 (3)

R	Wave Length				
	4800–5200	5200–5600	5600–6000	6000–6400	6400–6800
+8	+0.89 (1)	.....	−0.54 (1)	.....	+0.37 (1)
+7	+0.74 (1)	+0.46 (1)	.....	−0.07 (1)	.....
+6	+0.64 (1)	+0.18 (2)	−0.15 (1)	−0.36 (2)	+0.04 (1)
+5	+0.51 (2)	−0.21 (2)	−0.72 (1)	−0.69 (1)	−0.26 (1)
+4	+0.11 (3)	−0.59 (3)	−0.55 (1)	−0.82 (1)	−0.68 (1)
+3	−0.52 (7)	−0.32 (4)	−0.69 (1)	−0.61 (2)	.....
+2	−0.73 (6)	−0.78 (4)	−1.35 (7)	−0.86 (2)	.....
+1	−1.11 (4)	−1.56 (2)	−1.38 (4)	−1.55 (3)	−1.03 (3)
0	−1.43 (7)	−1.36 (6)	−1.85 (8)	−1.59 (3)	−1.40 (2)
−1	−1.52 (6)	−1.72 (7)	−1.88 (6)	−2.09 (7)	−2.31 (1)
−2	−2.00 (4)	−1.75 (8)	−2.01 (5)	−1.94 (5)	−2.70 (1)
−3	−1.99 (6)	−2.19 (6)	−2.97 (3)	−1.15 (1)	−2.49 (2)

* Numbers within parentheses refer to the number of tabular entries included in each average.

Possible systematic differences between the two calibrations as a function of Rowland intensity should be revealed in the averages of log X_0 and log X_0'' for each Rowland intensity from −1 to +6 over the wave-length range from 4000 A to 6400 A. The two sets of values

TABLE 5

VARIATION OF LOG X_0, OBTAINED FROM EQUIVALENT WIDTHS AND THE CURVE OF GROWTH, AS A FUNCTION OF R AND λ

R	Wave Length						
	4000–4400	4400–4800	4800–5200	5200–5600	5600–6000	6000–6400	6400–6800
+6.....	+2.80	+2.09	+2.26	+2.10	+1.38	+0.87	+1.37
+5.....	+2.23	+1.84	+1.88	+2.04	+0.76	+0.70	+1.10
+4.....	+1.82	+1.49	+1.79	+1.61	+0.73	+0.52	+0.82
+3.....	+1.58	+1.22	+1.21	+1.16	+0.42	+0.36	+0.53
+2.....	+1.02	+0.86	+0.85	+0.72	+0.18	+0.13	+0.27
+1.....	+0.62	+0.44	+0.39	+0.28	−0.07	−0.14	0.00
0.....	+0.08	−0.10	+0.03	−0.15	−0.39	−0.45	−0.44
−1.....	−0.42	−0.50	−0.31	−0.50	−0.61	−0.60	−0.52

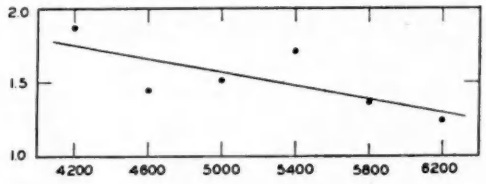

FIG. 1.—Mean values of Δ_1 as a function of wave length

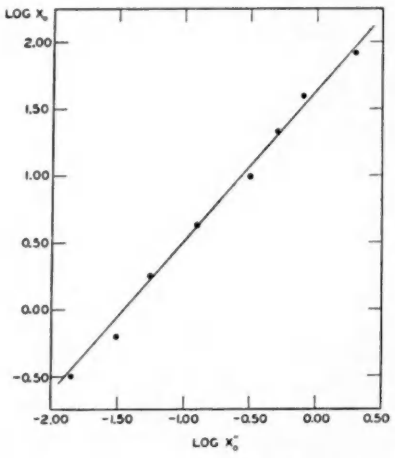

FIG. 2.—Relation between mean values of log X_0 and log X_0'' for each Rowland in tensity from −1 to +6.

were plotted one against the other. The straight line passing through the points in Figure 2 gives the relation

$$\log X_0 = 1.62 + 1.12 \log X_0'' . \qquad (13)$$

The equivalent-width calibration is somewhat steeper than that derived from the multiplet strengths. This result may possibly arise from systematic errors in the curve of growth, particularly in the flat portion, where, for a given value of $\log W/\lambda$, a small displacement in the curve may produce a disproportionately large change in $\log X_0$.

TABLE 6

FINAL SMOOTHED CALIBRATION, CORRECTED FOR OPACITY VARIATION

R	WAVE LENGTH									
	3000	3400	3800	4200	4600	5000	5400	5800	6200	6600
+8.....	4.21*	3.47	+3.17	+2.97	+2.74	+2.71	+2.18	+1.32	+1.57	+1.68
+7.....	3.84	3.18	+2.84	+2.62	+2.44	+2.40	+1.92	+1.11	+1.32	+1.43
+6.....	3.45	2.89	+2.50	+2.27	+2.14	+2.09	+1.65	+0.90	+1.08	+1.19
+5.....	3.08	2.60	+2.17	+1.92	+1.84	+1.78	+1.39	+0.70	+0.83	+0.94
+4.....	2.71	2.31	+1.83	+1.57	+1.54	+1.47	+1.12	+0.49	+0.59	+0.70
+3.....	2.34	2.02	+1.49	+1.22	+1.24	+1.16	+0.85	+0.29	+0.34	+0.45
+2.....	1.95	1.73	+1.16	+0.87	+0.94	+0.85	+0.59	+0.08	+0.09	+0.21
+1.....	1.59	1.43	+0.82	+0.51	+0.64	+0.54	+0.32	−0.12	−0.16	−0.03
0.....	1.22	1.14	+0.49	+0.16	+0.34	+0.23	+0.06	−0.33	−0.40	−0.28
−1.....	0.85	0.85	+0.15	−0.20	+0.05	−0.08	−0.20	−0.53	−0.65	−0.52
−2.....	0.47	0.56	−0.18	−0.55	−0.25	−0.39	−0.47	−0.75	−0.90	−0.77
−3.....	0.10	0.27	−0.52	−0.90	−0.56	−0.70	−0.73	−0.96	−1.14	−1.01

* The tabular entries are $\log X_0$.

As the final step in the calibration, the values of $\log X_0''$ in Table 4 were corrected by the addition of appropriate values of $-\Delta_1$ derived from equation (12). We have no means of ascertaining whether the relation (12) is valid on the violet side of λ 4000, but we adopt this assumption for lack of a better one. We then smoothed the values of $\log X_0$ thus derived by the graphical process of plotting R against $\log X_0$ for each wave-length interval separately and representing each set of points by a straight line, which was computed by least squares. The final calibration is contained in Table 6 and is shown graphically in Figure 3.

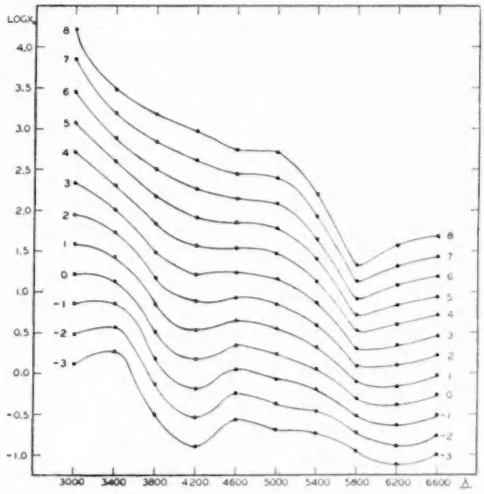

FIG. 3.—Smoothed calibration of Rowland's scale in terms of log X_0 as a function of R and λ.

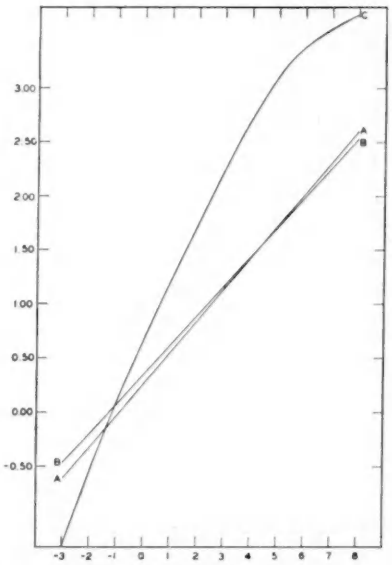

FIG. 4.—Comparison of present calibration with that of Russell, Adams, and Moore. Curve A represents log X_0, averaged over all wave lengths, as a function of Rowland intensity for a temperature of 4500°; curve B is a similar plot for a temperature of 5740°; curve C shows the variation of log A (determined by Russell, Adams, and Moore) with R. The ordinate units of B and C are arbitrary.

It is interesting to compare the present calibration with the earlier one of Russell, Adams, and Moore. If we plot Rowland intensity against mean log X_0, averaged over all wave lengths, we obtain a curve that may be assumed to correspond with the Russell-Adams-Moore plot of R against their log A. The curves are shown in Figure 4. Curve A represents the calibration adopted in the present investigation with an assumed temperature of 4500°; curve B shows a similar calibration for a temperature of 5740°, uncorrected, however, for opacity variation, while C is the curve of Russell, Adams, and Moore. The ordinate units are arbitrary, since we are concerned here only with the slopes of the various curves. Curves A and B are considerably less steep than curve C. Also the small difference in slope between A and B shows that the type of calibration considered here is relatively insensitive to the choice of temperature.

HARVARD OBSERVATORY
October 1939

SOLAR ERUPTIONS

R. G. GIOVANELLI

ABSTRACT

Observations of 268 solar eruptions made with a spectrohelioscope during the period June, 1937, to December, 1938, have been analyzed to show the relative distributions of intensities and areas. A simple photometer for the measurement of eruption intensity is described.

The width of the *Hα* line during eruptions is constant for small intensities but increases rapidly when the intensity becomes equal to, and exceeds that of, the continuous spectrum. There appears to be no appreciable vertical velocity of the eruption itself. Approximately 20 per cent of the eruptions eject eruptive prominences, and, assuming that this is caused by *Lα* radiation pressure, the width of *Lα* is found to be approximately six times that of *Hα* when measured in velocity units.

The position of eruptions in the chromosphere is discussed, and it is concluded that, in general, eruptions are confined to the levels in which the normal bright hydrogen occurs.

OBSERVATIONS

The observations used for the following discussion have been made by the author with the spectrohelioscope of the Commonwealth Solar Observatory. Surveys of the sun's disk have been made throughout days of sunshine at intervals of approximately half an hour, except during eruptions and periods of considerable solar activity, when the observations were continuous. As far as possible, the program of observations following the discovery of an eruption consisted of (1) a sketch of related spot group and eruption, (2) measurement of area, (3) estimate of intensity, (4) measurement of width of the eruptive *Hα* line, and (5) examination of the eruptive area and its surroundings for velocities of bright or dark hydrogen. These were repeated as often as was felt desirable during the eruption.

The area measurements are affected by the following: (*a*) poor seeing conditions, (*b*) the narrowness of eruptions, (*c*) the diffuse edges of many eruptions, (*d*) slight changes of focus owing to temperature, and (*e*) the impossibility, under existing arrangements, of bringing the measuring graticule into contact with the image. It seems that an error of at least 20 per cent may be expected in the area estimates.

The intensity or brightness of an eruption was estimated by eye on an arbitrary scale. As a large number of eruptions occurred dur-

ing June and July, 1937, it was not long before a fairly consistent set of intensities, on a scale from 1 to 5, was being used. Moreover, it was soon found possible to subdivide each division into three, e.g., 2; 2.3; 2.7; 3. Actually the maximum intensity recorded has been 4.3. Since the intensity was measured by eye on an arbitrary scale, it is evident that, over a period of 18 months, without any standard of intensity, there were bound to be slight variations, possibly systematic, in intensity estimates. Any one observation may have been in error by 0.3, or possibly 0.6, units; but it is not considered probable that an estimate should have been in error by one whole unit. The intensity is disturbed by bad seeing or by a lens slightly out of focus, as mentioned above, and also by the presence of cirrus clouds or sky haze, which reduces the intensity of the image and blurs it by scattering.

TIME OF MAXIMUM INTENSITY

For twenty-four eruptions the times of commencement and maximum intensity were observed. The following summary of these may be made. (*a*) The mean time for an eruption to reach its maximum brightness was 7 minutes. (*b*) For half the eruptions the intervals between commencement and maximum were 4 minutes or less. (*c*) The mean interval for eruptions of importance 1 was 4 minutes, as against 11 minutes for eruptions of importance 2. It must be remembered that the mean duration of eruptions of importance 1 is only 21 minutes, as compared with a mean life of 38 minutes for eruptions of importance 2.[1] (*d*) There was a tendency for the interval to increase with increased brightness, i.e., the brighter the eruption the longer was the time required to reach that brightness.

DISTRIBUTION OF INTENSITIES AND AREAS

It is of interest to find how intensities of eruptions vary with areas. M. Waldmeier has already stated[1] that intensities are more or less proportional to areas, but he has not supplied figures to support this. In Table 1 the observed intensities are given under ranges of the area. It is clear that the intensity increases with the area. It is seen that Waldmeier's statement receives support from these ob-

[1] Waldmeier, *Zs. f. Ap.*, **16**, 276, 1938.

servations, although the variations for individual cases are considerable.

In the reports published in the *Bulletin for Character Figures of Solar Phenomena* the importances of eruptions are given on a scale of 1 to 3. It was recommended[2] that, in order to preserve uniformity, the "importance" should be determined by its area alone, and for these purposes a small eruption was to be called of importance 1, a

TABLE 1

INTENSITIES AND AREAS OF ERUPTIONS

Area	25	75	125	175	225	275	325	375	450	750	All
Occasions.....	19	65	30	13	14	16	6	15	6	5	189
Mean intensity	1.3	1.7	2.3	2.3	2.5	2.3	2.4	2.7	2.6	3.9	2.1

NOTE.—Areas are given in units of one-millionth of the sun's disk.

TABLE 2

IMPORTANCE AND AREAS OF ERUPTIONS

Importance	Number of Eruptions Used	Mean Area	Waldmeier's Mean Areas
1.....	78	106	120
2.....	66	326	380
3.....	4	800	1020

medium-sized eruption of importance 2, while very large eruptions were to be of importance 3. With the exception of the suggestion that eruptions of importance 3 should have an area of 750-millionths of the sun's disk, the estimate of importance was thus left largely to the observer. Hence, it is of interest to determine the mean areas for eruptions of given importance. These are shown in Table 2, together with the only other similar table previously published.[1] The mean areas given by Waldmeier are about 1.15 times those obtained at Mount Stromlo.

It is desirable to determine the numbers of eruptions occurring with different intensities. In Table 3 the eruptions have been sepa-

[2] *Bulletin for Character Figures of Solar Phenomena*, No. 31, 1935.

rated into groups of the same importance, and the number with the given observed intensity has been listed. However, as the maximum intensity may have occurred some time before the discovery of the eruption, this is not a true distribution of intensities. To allow for this, suppose provisionally that the intensity of an eruption increases linearly to a maximum during a time α and then decreases linearly to zero during a time β. Let i and I be the maximum and the observed

TABLE 3

DISTRIBUTION OF INTENSITIES

Intensity (I)	Numbers Observed			Numbers Observed (Smoothed)		Calculated Distribution		Mean		
	Importance			Importance		Importance		Importance		
	1	2	3	1	2	1	2	1	2	3
4.3	.....	1	2	.....	1	.....	2	.....	1.5	2
4.0	1	2	1	1	2.5	4	5	2.5	4	1
3.7	5	4	1	3	5	10	10	6.5	7.5	1
3.3	2	4	.....	5	8.5	13	17	9	12.5	.....
3.0	9	18	.....	7	10.5	15	16	11	13	.....
2.7	9	3	.....	10	10.5	19	11	14.5	10.5	.....
2.3	8	9	.....	15	9	27	4	21	6.5	.....
2.0	25	12	.....	20	7	29	.....	24.5	3.5	.....
1.7	24	5	.....	22	5	15	.....	18.5	2.5	.....
1.3	16	.....	.....	21	3	.....	.....	10.5	1.5	.....
1.0	23	1	.....	18	1	.....	.....	9	0.5	.....
0.7	10	2	.....	10	.....	.....	.....	5	.....	.....

intensities, and $f(i)$ and $F(I)$ the true and the observed numbers of eruptions with these intensities. Then it may be shown that

$$F(I) = \frac{1}{\alpha + \beta}\left[\alpha f(I) + \sum_{i>I} \frac{\beta \delta i f(i)}{i}\right],$$

where δi is the smallest measured increment of intensity, i.e., $\delta i = \frac{1}{3}$. This is the number given in the column "Number Observed (Smoothed)" in Table 3.

Now, for eruptions of importance 1 mean values are

$$\alpha = 4 \text{ min.}; \qquad \beta = 17 \text{ min.}$$

For eruptions of importance 2

$$\alpha = 11 \text{ min.}; \qquad \beta = 27 \text{ min.}$$

The evaluations of $f(i)$ can thus be made, starting, for eruptions of importance 1, from $I = 4, \Sigma = 0$, giving $f(4)$. The value of $f(4)$ may then be substituted in the formula for $f(3.7)$, and the process continued until $f(i)$ falls to zero. The values obtained are designated "Calculated Distribution" in Table 3 and have been reduced so that the total calculated number and the observed number are equal. The foregoing procedure, however, probably produces an overcorrection. If the intensity-time plot had been rectangular, the observed distribution would have been the same as the true one. Thus, the actual distribution probably lies between the two, and so the mean of these two values is adopted and tabulated on the right of Table 3. The noteworthy points are: (1) There is a wide range of scatter in intensity within any one importance group. (2) The maximum number of occurrences takes place as follows:

Importance	Intensity
1	2.0
2	3.0
3	4.3

This shows a progressive increase with importance.

It has recently been felt desirable to calibrate the scale of intensities used in the foregoing observations and also to provide a more quantitative measurement of the intensity of an eruption. One type of photometer for the measurement of intensity with a spectrohelioscope has already been described by Newton and Woolley.[3] In this the intensity of a flocculus is measured by comparing it with a photometer field placed immediately above the flocculus. As eruptions frequently have the appearance of bright points or lines on a darker background, it seems more satisfactory to compare them with a similar photometer image, as described below.

A is a motor head lamp (Fig. 1), run, with a transformer, from the A.C. mains. The light passes through a red filter, *B*, chosen to match

[3] *M.N.*, **96**, 5, 1935.

Hα, and then through an optical wedge, *C*. The light is then focused by a lens, *D;* and after passing through a diaphragm, *E*, to reduce scattered light, the filament is focused onto a slit, *F*. This cuts off all but a very small part of the filament of the lamp. A thin piece of unsilvered glass, *G*, at 45° to the beam reflects a part of the light into the eyepiece, *H*, which is equidistant optically from *F* and the second slit of the spectrohelioscope. Most of the light coming from the second slit passes through *G*, and the filament image appears superimposed on the solar field. This creates a fairly good "artificial

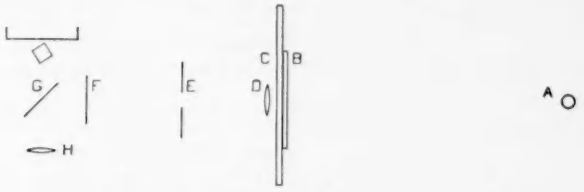

FIG. 1.—Schematic diagram of eruption photometer

eruption" the intensity of which may be varied by using the wedge. Newton and Woolley's method[3] for determining the scattering from one wave length to another is used. Suppose the grating removes the fraction α of the light of any particular wave length and scatters it in directions proper to other wave lengths; then α may be readily determined from the known central intensity of *Hα* (12 per cent), as compared with the value measured with the eruption photometer. The increase of intensity due to the artificial eruption is measured in terms of the continuous spectrum; to obtain the true intensity of the flocculus this has to be increased by a factor of $1/(1 - \alpha)$, since α is the fraction of the excess of floccular intensity over *Hα* which has been removed by scattering, and to this has to be added the initial corrected intensity of the *Hα* background, i.e., 12 per cent.

The optical wedge used obeyed the law

$$I = I_0\, 0.10^{-0.054x},$$

where x was measured in millimeters, over about 5 cm and was found satisfactory in the range of brightness. The whole photometer is extremely simple in operation and, as it reproduces eruption condi-

tions fairly satisfactorily, may be recommended with confidence for eruption photometry.

For the calibration of intensities the intensity of an eruption was first estimated by eye and then measured with the photometer, the intensity of the continuous spectrum background 2.6 A from the center of *Hα* being determined immediately afterward. Not many observations have yet been made, but it has been thought worth while to include them to give a quantitative idea of the foregoing scale of intensities. Mean values are given in Table 4.

TABLE 4

CALIBRATION OF INTENSITY SCALE

Intensity	1	2	3	4
Percentage of continuous spectrum	36	76	117	158

WIDTH OF THE ERUPTIVE *Hα* LINE

On many occasions during eruptions the width of the *Hα* line has been measured. To do this the line-shifter was rotated toward the violet until the eruption just disappeared, and the position was noted. The same procedure was followed on the red side of the line, and the position of the center of *Hα* was also obtained. The scale being calibrated in units of kilometers per second, the width was also given in terms of that unit, although whether or not the entire width is due to Doppler effect need not concern us here. The settings of the line-shifter were usually reproducible to within 3 km/sec. In nearly all cases the intensity of the eruption was estimated at the same time. The widths of *Hα* are grouped under intensities in Table 5. It will be noticed that the width, which is more or less constant for values of I up to $I = 2.3$, begins to increase for $I = 2.7$ (which corresponds to about 105 per cent of the continuous spectrum) and increases rapidly thereafter. The increase thus begins when the central intensity becomes approximately equal to the neighboring continuous spectrum.

VELOCITIES OF ERUPTIONS

It is of importance to decide whether an eruption is stationary in the chromosphere or whether it rises, as do eruptive prominences.

During all the author's observations no eruption has been observed on the disk in which there was a definite displacement by velocity of the position of maximum intensity. Moreover, by the courtesy of Dr. C. W. Allen, the author has been permitted to examine several spectra and microphotometer tracings of eruptions made by him at the observatory on which also, although there is a dark reversal in the center of the bright line, it is quite clear that during these eruptions there was no appreciable displacement of the eruptive line. Actually, the dark reversal produces a flatter line and

TABLE 5

WIDTH OF ERUPTIVE *Hα* LINE

Intensity	1	1.3	1.7	2	2.3	2.7	3	3.3	3.7	4	4.3
Number of observations....	9	10	23	21	16	14	20	11	8	4	1
Mean width (km/sec).....	82	74	86	84	85	91	105	123	124	192	

makes accurate visual measurements of any very small displacements difficult. Further evidence on the stationary state of eruptions is obtained from the width observations previously mentioned. If we assume that the emission line is symmetrical—in the wings, at any rate—then the mean of the blue and red edges of *Hα* gives a measure of the velocity. The distribution of velocities as determined in this way is given in Table 6, where the probable error of a determination is about 3 km/sec. The results vary considerably but show a recessive mean of 3.4 km/sec. If this represents a true velocity, it indicates that any velocity is, on the average, inward.

On one or two occasions the brightest part of the eruption was not observed quite at the center of *Hα*; on these occasions, however, it was clearly seen that a dark marking, due to an overlying prominence, was superimposed on the eruption; and because of a vertical velocity, its absorption line was removed to one of the sides of *Hα*, thus distorting the eruptive line. Perhaps where displacements of the *Hα* emission line have been previously reported, phenomena of this type may have occurred.

OBSERVATIONS OF OTHER LINES

The following lines were, at one time or other, observed to be affected during eruptions:

Hydrogen	$H\alpha$	$H\beta$	$H\gamma$
Sodium	D_1	D_2	....
Magnesium	b_1	b_2	b_4
Iron (neutral)	$\lambda 5269.7$	....	....
Iron (ionized)	$\lambda 5018.6$	b_3	....
Helium	D_3	....	....

In all elements other than hydrogen the effect during eruptions is very weak, and the observations are most incomplete. Even so, a

TABLE 6

VELOCITIES OF ERUPTIONS

	Velocity (Km/Sec)	Number of Occurrences	Total
Approach	11	1	
	9 –11	0	
	6½– 8½	1	35 approach
	4 – 6	5	
	1½– 3½	12	
	–1 – 1	39	11 zero
Recessive	1½– 3½	26	
	4 – 6	24	
	6½– 8½	15	
	9 –11	3	92 recessive
	11½–13½	2	
	14 –16	4	
	16½–18½	3	
	19	3	

Mean of approach velocities..... −2.1 km/sec
Mean of recessive velocities..... +5.9 km/sec
Mean velocity..... +3.4 km/sec

few generalizations may be made. (1) In all elements except helium an increase in radiation was observed. With the D_3 helium line, not usually visible in the solar spectrum, the effect produced was an absorption. (2) The effects in the foregoing lines can be observed only when the $H\alpha$ intensity is high. (3) The position and shape of the eruption in other lines is that of the brightest parts of $H\alpha$. (4) The eruptions can be observed only in the very center of the line. Since

these lines are all much narrower than $H\alpha$, any slight velocity would have displaced the emission into the wings or even into the continuous spectrum. From (4) it is clear that, in these cases at least, the elements concerned had no appreciable vertical velocity.

ERUPTIONS AND ERUPTIVE PROMINENCES

In view of the foregoing conclusions it is of interest to review opinions on the nature of eruptive prominences. Of early workers, Young has said:

> In a few instances the gaseous eruptions in the neighbourhood of a spot are so powerful and brilliant that with a spectroscope their forms can be made out on the background of the solar surface in the same way that the prominences are seen at the edge of the sun. In fact, there is probably no difference at all in the phenomena, except that only prominences of most unusual brightness can thus be detected on the solar surface.[4]

Abetti expressed the opinion[5] that "the bright flocculi are, as a rule, eruptive prominences," while McCrea[6] has recently come to a similar conclusion. Fox,[7] on the other hand, stated that eruptions were the bases of eruptive prominences. Pettit remarked[8] that, in general, no markings appear on disk plates (presumably spectroheliograms) in the region of eruptive prominences and, with McMath, further supported this view[9] in objecting to Kiepenheuer's theory of eruptive prominences, pointing out that eruptive prominences may be widely distributed over the disk, while eruptions are limited to spot zones.

Since eruptions have no vertical velocities, the remarks of Young, Abetti, and McCrea seem, in general, to be without support. It will be shown below that there might be exceptional occasions, however, in which their views are valid. With the other observers the differences in opinion lie in confusing two distinct types of eruptive prominence. (*a*) The first type commences as a quiet prominence and for some, as yet unknown, reason acquires a velocity outward and rapidly disintegrates. This is the type most frequently examined by Pettit. (*b*) The second type is that described by Fox, i.e., a type as-

[4] *The Sun*, p. 135, rev. ed., 1904.
[5] *Handb. d. Ap.*, **4**, 121.
[6] *Observatory*, **62**, 16, 1939.
[7] *Ap. J.*, **28**, 253, 1908.
[8] *Pub. Yerkes Obs.*, **3**, 205.
[9] *Ap. J.*, **88**, 244, 1938.

sociated with eruptions. It is possible that some of these correspond to those listed by Pettit as "surges."

When observed on the limb, an eruptive prominence shoots out with high velocity and in the course of an hour usually disintegrates, but at times parts of the prominence may be seen turning over and falling back into the sun. In twenty cases since the beginning of March, 1938, when this matter was first given attention, eruptions have been seen on the disk, and strong absorption markings with high approach velocities have been found in the neighborhood. These markings are of a quite different type from those described by Hale,[10] which usually show approach velocities at one end and recessive velocities at the other and take the form of neat curved lines. The dark markings referred to above, however, occupy a wide irregular area. Usually they are first seen devoid of accompanying recessive dark markings; but the latter, equally irregular in shape, soon appear, while the approach markings decrease in intensity and disappear after an interval of about half an hour. It is quite apparent that these masses of dark hydrogen are really eruptive prominences, ejected from the eruption proper and strongly absorbing the wave lengths corresponding to the Doppler velocities. This view is completely verified by the observation of five of these eruptions on the disk but near the limb, in which the dark hydrogen showing velocities traveled to and passed beyond the limb, continuing outward to appear as eruptive prominences. Additional evidence, if necessary, was obtained in the case of the eruption of December 19, 1938 (to be discussed later), which was situated right on the limb of the sun. Although not in vertical motion itself, a prominence was observed to be expelled from a neighboring area and to reach a height of 65,000 km before disintegrating. In ten further cases approaching dark flocculi, obviously eruptive prominences in projection, were observed without any eruption but near active spots. In one of these it was subsequently discovered that a radio fadeout had occurred 25 minutes previously, indicating that an eruption had probably taken place around this center. It seems that in these cases the eruption had died down before the observations were made, leaving only the eruptive prominence projected on the disk.

[10] *Ap. J.*, **71**, 55, 1930.

It is quite conclusive that this second type of eruptive prominence does exist and is expelled from eruptions. During the period March–December, 1938, 112 eruptions were observed, of which 21, or 19 per cent, gave rise to eruptive prominences. What, then, is the cause of

TABLE 7

ERUPTIONS PRODUCING ERUPTIVE PROMINENCES IN PROJECTION

DATE	TIME (E.A.S.T.)	IMPORTANCE	AREA	INTENSITY	VELOCITY OF PROMINENCE (KM/SEC)		REMARKS
					Mean	Maximum	
1938							
Mar. 17	1254–1256	1	.....	.....	48	184	.....
Apr. 11	1538–1546	1	.....	0.7	.....	97	Prominence extending over limb
May 6	1527–1542	1	.....	.....	.....	120	.....
June 1	1105–1147	1	.....	1.3	.....	187	Same
July 13	1005–1007	1	100	2.7	.....	210	.....
15	0936–0946	1	80	2.3	.....	115	.....
Aug. 1	0907–0918	2	.....	.....	.....	400	Same
3	1046–1056	1	.....	1.7	38	120	.....
Sept. 23	1131–1139	1	130	3.7	.....	280	Same
24	1107–1110	1	.....	1.0	53	160	.....
Oct. 6	1606–1615	2	250	2.7	47	.....	.....
11	1040–1050	1	.....	.....	22	.....	.....
14	1630	2	.....	.....	.....	67	.....
19	1428–1430	1	.....	.....	.....	220	.....
19	1537–1640	2	360	2.3	29	63	.....
Nov. 2	1431–1437	1	120	1.3	.....	92	.....
11	0955–1003	2	240	1.7	.....	81	.....
21	0855–0913	1	.....	.....	33	.....	.....
24	1023–1038	1	120	1.7	.....	320	.....
Dec. 7	1247–1250	1	.....	3.3	.....	330	Same

this special phenomenon accompanying some eruptions? It might have been expected that the chance of producing eruptive prominences would have been greater for the eruptions of greater intensity. In Table 7 are given the eruptions, together with area, importance, intensity, and velocity, of the accompanying prominence. The mean area is 175, compared with a mean for all eruptions of 188, showing that the chance of producing an eruptive prominence is independent of the importance, or area, of the eruption. Again, the

mean intensity is 2.0, compared with a mean observed intensity of 2.1 for all eruptions. None of these eruptions was observed at its beginning, but that does not seem sufficient to account for this result: the chance of producing a prominence is independent of area and intensity. Remembering that the other type of eruptive prominence arises from an existing prominence, it seems probable that the presence of a low-lying prominence is essential before the second type of eruptive prominence can be produced, and that when the conditions of position of prominence and eruption are suitable, the eruption will give rise to an eruptive prominence. It is rare for an eruptive prominence to arise from the eruption itself, but there is usually a gap of about 10,000 km between the dark markings and the eruptions.

The prominence velocities given in Table 7 represent the resultant of Doppler velocity measurements and movement at right angles to the line of sight. Let us see if the velocity of the prominence is affected by area or intensity of the eruption. The mean of the maximum velocities of prominences associated with eruptions of importance 1 is 187 km/sec, while with eruptions of importance 2 it is 153 km/sec, a result showing no appreciable effect of area. However, when the maximum velocities are compared with *Hα* intensity, there is a definite tendency toward an increase in velocity with intensity. If the velocity of 320 km/sec, occurring on November 24, 1938, be omitted on the assumption that the eruption had been of greater intensity before it was first observed, the velocities fall into two groups: (*a*) small velocities (average, 114 km/sec) for intensities 2.3 and less; (*b*) high velocities (average, 271 km/sec) for intensities 2.7 and more. This is exactly the same division of intensities as has been found to influence the width of *Hα*. It is thus probable that these prominences are expelled by the mechanism of Kiepenheuer's theory,[11] i.e., the light-pressure of Lyman radiation from the eruption, for with greater intensity, the width of *Hα*, and presumably *Lα*, would be greater, and consequently the velocity of the prominence would be high.

If it be accepted that these prominences are ejected by radiation pressure of *Lα*, the observations may be used to estimate the relative widths of *Hα* and *Lα*. However, as in many of these cases the maxi-

[11] *Zs. f. Ap.*, **15**, 53, 1937.

mum intensities were not observed and in most of the *Hα* widths were not determined, this estimate can only be made indirectly.

The distribution of intensities among eruptions has been given in Table 3; and, by using the mean widths of *Hα* given in Table 5, the relative numbers of eruptions expected to have maximum *Hα* widths in given ranges were obtained. The distribution of prominence velocities was smoothed for comparison purposes. Now, if to a given *Hα* width there always corresponds a definite *Lα* width, if we neglect the inverse-square effect, and if, in the foregoing cases, there has been no other mechanism acting to increase the velocities of the prominences, then, corresponding to a given *Hα* width, there will be a definite prominence velocity. By a direct comparison between the two foregoing distributions this relationship has been determined. It may be expressed by

$$\text{Velocity} = 6.2\ (\tfrac{1}{2}\ H\alpha \text{ width} - 25)\ ,$$

when the *Hα* width is expressed in velocity units.

The width of *Lα*, then, in velocity units is approximately six times that of *Hα*. It may be pointed out that the theory of radio fadeouts advanced by Martyn, Munro, Higgs, and Williams[12] required a width of *Lα* of approximately this amount. The constant in the preceding expression would be interpreted as representing the distance from the edge of the *Lα* line at which radiation pressure is just sufficient to balance gravity.

POSITION OF ERUPTIONS IN THE CHROMOSPHERE

It has previously been pointed out[13] that, where the base of an eruption is obscured by the limb, radio fadeouts have not been observed, while fadeouts can and do occur in association with eruptive prominences whose bases are on the visible side of the limb. This is taken to indicate that the eruptions causing these prominences are at no great height above the chromosphere.

Again, on several occasions eruptions have been observed projecting over both umbra and penumbra of sunspots. There has been no detectable discontinuity or change in the appearance of the erup-

[12] *Nature*, **140**, 603, 1937.

[13] Giovanelli, *Ap. J.*, **88**, 204, 1938.

tions at these places, and hence the eruption lies at a higher level than umbra or penumbra.

To confirm these statements, a watch was kept for an event on the edge of the sun which could unhesitatingly be classed as an eruption proper on the limb. Such an eruption was observed on December 19, 1938. In height, the eruption was 10,000 km, half of which projected beyond the edge of the hydrogen chromosphere; this is considerably greater than the usual width of 3,000 km. Now, the height of the chromosphere is about 8,000 km, so that the center of the eruption was about 8,000 km above the reversing layer. The intensity of the eruption, which seemed uniform throughout its height, brightened considerably from 11^h05^m, when first observed, to a maximum value of 3 at 11^h08^m. By 11^h19^m the intensity had decreased to 1.7. The eruption itself showed no tendency whatever to rise, but at 11^h07^m there was observed the ejection of an eruptive prominence fainter than the normal *Hα* disk, which reached a height of 65,000 km. The base of this prominence did not quite touch the eruption, a gap of about 10,000 km separating them. The whole sequence of events was so similar to that observed during an eruption on the disk that it was felt that no mistake in identity could have been made.

Since eruptions generally appear as brightenings in already bright hydrogen flocculi, and as the latter usually occur in or just above the normal hydrogen chromosphere, we may derive the following conclusions about the general nature of eruptions. (1) Eruptions take place in bright hydrogen flocculi. As they show no vertical velocity, they do not leave their original position during their existence. (2) Approximately one-fifth of the eruptions give rise to eruptive prominences whose intensities are less than that of the center of *Hα*. These do not usually touch the eruption itself but are separated by a gap of 10,000 km or more. If these be ejected by radiation pressure of *Lα*, it appears that the width of *Lα* must be about six times that of *Hα*, when measured in velocity units. (3) The brightness in *Hα* is of the same order as the continuous spectrum in the neighborhood of *Hα*. The width of the eruptive *Hα* line, which is more or less constant for lower intensities, increases rapidly when the intensity becomes equal to and exceeds that of the continuous spectrum.

This discussion seems to give fairly definite conclusions as to the

general conditions of velocities and positions of the eruptions in the chromosphere. However, it must be realized that exceptions are possible. To illustrate this, on March 14, 1939, at 10^h15^m E.A.S.T., there was observed to grow, most probably from an active group which had then passed 3° behind the limb, a brilliant prominence whose maximum intensity reached 90 per cent of the continuous spectrum. It reached a maximum height of 84,000 km at 10^h33^m and attained a maximum area equal to 400-millionths of the sun's disk. By 10^h42^m it had shrunk and completely disappeared. In all respects it seemed similar to the great surges described by McMath and Pettit.[14] This prominence must surely have been classed as an eruption had it been situated on the sun's disk, for the intensity was equal to that of the average eruption. According to a recently developed formula,[15] an eruption of such intensity and area would not have been expected to produce a complete radio fadeout; yet it would probably have caused a weakening in *E*-echoes; and this is precisely what happened. It must be concluded, then, that this eruptive prominence, or surge, was indeed an eruption. Unless the apparent rise of the eruption was due to an upward transfer of luminescence—a phenomenon whose existence is at present doubtful—this represents an exception to the general rule that eruptions have little or no vertical velocity, for the mean velocity recorded was 78 km/sec. From the evidence previously presented, it must be deduced that such eruptions are rare.

COMMONWEALTH SOLAR OBSERVATORY
CANBERRA, AUSTRALIA
July 1939

[14] *Ap. J.*, **85**, 296, 1937.

[15] Giovanelli and Higgs, *Terr. Mag.*, **44**, 181, 1939.

SOME CORRECTIONS TO DREYER'S CATALOGUES OF NEBULAE AND CLUSTERS*

DOROTHY CARLSON

ABSTRACT

Corrections to Dreyer's catalogues compiled from Mount Wilson plates and other photographic sources; 330 objects are to be dropped from the *New General Catalogue* (Table 1*a*) and 250 from the two *Index Catalogues* (Table 1*b*). Positions of 49 objects are corrected (Table 3), and the existence of 23 doubtful ones is confirmed (Table 4).

The Mount Wilson collection of photographs made with the 100-inch and 60-inch reflectors includes about two thousand extra-galactic nebulae occurring in Dreyer's *New General Catalogue* and about seven hundred in the *Index Catalogues*, in addition to a considerable number of galactic nebulae and clusters. In the course of identifying and classifying these objects, various lists of corrections to Dreyer's catalogues have been consulted, and a new list has been compiled from the Mount Wilson plates. The publishing of the Mount Wilson list offers an opportunity to bring together the more authentic corrections from all sources.

Experience demonstrates the great reliability of corrections derived from photographs in comparison with those derived from visual observations. Consequently, the corrections included in the present list are, in general, restricted to photographic sources. However, Dreyer's own corrections, assembled for the most part from visual observations, have been freely consulted; and a supplementary list (Table 2) has been formulated containing objects which Dreyer proposed to remove from the catalogues, although no photographic evidence is available for confirmation. The lists of corrections, although extensive, are far from complete, and additions will accumulate for a long time to come.

The sources for the present compilation, together with the symbols by which they are represented in the tables, are as follows:

W Mount Wilson photographs.

L *Publications of the Lick Observatory*, **13**, 1918.

* *Contributions from the Mount Wilson Observatory, Carnegie Institution of Washington*, No. 626.

R *Heidelberg Veröffentlichungen*, **9**, 1926. Reinmuth attempted to describe the 4445 objects north of Decl. = −20° in John Herschel's general catalogue, as they appeared on camera plates or, occasionally, on plates taken with the 27-inch reflector. Uncertainties, in general, are restricted to small, compact nebulae described as nebulous stars, for which the small scale employed was not entirely satisfactory. The effects are illustrated in Table 4, which contains nebulae not found by Reinmuth but found on Mount Wilson plates in their catalogued positions.

Hel *Helwan Observatory Bulletins*, Nos. 9, 15, 21, 22, and 30. Reports of a survey of nebulae between Decl. 0° and −45°, made with the Helwan reflector.

H *Harvard Annals*, **88**, No. 1, 1930. A catalogue of 2778 nebulae in the region of the Virgo Cluster; includes a list of 39 identical nebulae and one of 94 missing NGC and IC objects.

D I Notes following the NGC, *Memoirs R.A.S.*, **49–50**, 212, 1888.

D II Notes and corrections to the NGC (following *First Index Catalogue*), *Memoirs R.A.S.*, **51**, 225, 1895.

D III Notes and corrections to the NGC (following *Second Index Catalogue*), *Memoirs R.A.S.*, **59**, 186, 1908.

D IV Dreyer's own corrections to the NGC resulting from the revision of Sir William Herschel's three catalogues of nebulae, *Memoirs R.A.S.*, **73**, 37, 1912–13.

The other symbols in the tables are those used by Dreyer with the addition of "nf," meaning "not found." Tables 1*a* and 1*b* contain listed numbers which, on the evidence of photographic plates, should be removed from the *New General Catalogue* and the *Index Catalogues*, respectively. Table 2 is a compilation, from Dreyer's notes, of missing nebulae which have not been checked by photography. Table 3 gives a few corrections to catalogue positions where the errors are more than 5′; and Table 4, nebulae not found by Reinmuth and other observers, but which have been found on Mount Wilson plates in the catalogued positions.

TABLE 1*a*

OBJECTS TO BE STRICKEN FROM THE *New General Catalogue*

NGC	
18	** W
30	** W, R
46	* R
56	No trace of nebulosity, W, L. "vF, pL, pmE, ph, = neb Wolf XIII No. 112; neb Wolf XIII No. 111 np 9′," R. However, Wolf XIII No. 112 is 1^m6 f and 5′ s of Dreyer position of 56 and is pL (1′.7 in diam) instead of eL as Herschel has described it.
82	* W
84	* W
90	* W
153	= NGC 151, W, D II
156	** W
158	nf, W
160	= NGC 162, W. In NGC, h39 sp should read h32 sp. NGC 162 is merely a better position of NGC 160 and is listed as such by Schultz. R mistakes a star for 162.
171	nf, W, D IV, R
207	"Nothing shown here, but 4′ s of IC 41 there is a neb, pF, S, E 90°," Hel
313	** R
358	4 st, 10–11.5, in parallelogram, R
370	nf, W, R
372	*** W, R
408	* W, R
421	nf, R
531	nf, plate not good, R
552	= IC 110?, R
553	= IC 111?, R
603	*** W, R, D III
607	** W, D II, R, Hel
616	** R
618	nf, R, D I, D II
674	= NGC 697?, R
728	*** R
730	* W
737	*** W, D II, R
747	nf, Hel
757	nf, Hel
760	** W
763	nf, Hel
771	50 Cas, nebulous?, R
843	*** R
952	nf, R
983	nf, R
1040	= NGC 1053, R
1059	** R, D I, D II
1141 1142	** R
1210	nf, Hel
1240	* R
1251	** R
1269	nf, Hel
1276	** W
1312	* ?, R
1318	nf, W, Hel
1340	= NGC 1344, W, D III
1367	= NGC 1371, W
1369	nf, W, Hel
1378	** W, Hel
1429	* W
1436	nf, Hel
1442	= NGC 1440, R, D I, D IV
1443	nf, W
1458	nf vis, Hel
1488	** R
1551	= NGC 1550, R, D I, D IV
1724	*** R
1746 1750 1758	vL Cl, R
1757	nf, R, D I, D II
1781	= NGC 1794, R, D III
1908	nf, R
1909	nf, R
1927	nf, R, D I
1988	* R, D I
1990	nf, by Curtis on 2 hr. exp. (L, 13), who suggests that Herschel was here misled by the radiance about the bright star, or that he observed the similar nebulosity, IC 434, south of ζ Ori instead.
2045	BD+12°884, no nebulosity, W, R
2061	No Cl, Hel
2167	"No nebulosity found around BD−6°1412," Hel
2189	nf, R
2330	= IC 458?, R, D II, D IV
2334	= IC 464?, R, D II, D IV
2361	= NGC 2359, Hel
2386	*** W
2387	* R
2390	* W, R
2391	nf, W, R
2404	* W
2471	* R
2492	* R
2515	** R
2542	No nebulosity, W
2597	nf, R
2643	= IC 2390, R
2653	gp of st, W
2703	nf, Hel
2705	nf, Hel
2707	nf, Hel
2727	"No nebula in this position which is near BD−2°2766," Hel
2741	nf, W, R

TABLE 1*a*—*Continued*

NGC	
2786	nf, R
2816	nf, R
2829	2 neb and *, W
2837	nf, Hel
2847	gp of st, W
2879	nf, W, Hel
2971	nf, W
2984	= IC 556?, R
3000	** W, R
3002	** W
3004	** W
3063	** R
3123	nf, R
3129	nf, R, D I
3148	BD+51°1585, R, L
3174	= NGC 3144, R, D IV
3194	= NGC 3155, R, D IV
3210	* R
3218	= NGC 3183, R, D I, D IV
3234	nf, R, D I
3284	* R, D IV
3291	* W
3317	** W, Hel
3342	* R
3345	** W, D I, D IV
3371	* W, R
3373	* W, R
3397	= NGC 3329, R, D I, D IV
3484	nf, R, D IV
3494	nf, W
3497	= NGC 3528, R, D IV
3498	*** R
3500	= NGC 3465, R, D IV
3544	= NGC 3571, Hel
3560	* R
3575	nf, R
3604	= NGC 3611, R
3616	nf, R, D III
3632	= NGC 3626, W, R, D IV
3643	= NGC 3645, W, R
3647	Nest of nebulae, W
3712	* R
3730	= NGC 3732, W
3760	= NGC 3301, W, R, D I, D II
3793	= NGC 3786, W
3797	= NGC 3788, W
3804	= NGC 3794, W, R, D IV
3807	nf, R
3852	= NGC 3848, R
3874	** R
3899	= NGC 3912, R
3924	nf, R
3927	nf, R
3939	nf, R
3950	* W
3980	= NGC 3977, W
3984	nf, R, D III
4007	= NGC 4005, W, R, D IV
4028	nf, R
4042	= NGC 4032?, R, D II

NGC	
4055	"pF–cF, cS, iR, glbM; in Dreyer's place no pB neb found," R
4099	nf, R, D IV
4107	* R, H, D III
4113	nf, R, D III
4119	nf, R, H, D III
4139	nf, R
4140	nf, R
4153	nf, R
4154	* R
4167	= NGC 4163?, R
4208	= NGC 4212, W, R, H, D IV
4209	nf, W, R
4223	= NGC 4241, R, H, D IV
4228	= NGC 4214, W, R, D I, L
4265	= NGC 4263, W, D III
4297	nf, R, H
4315	nf, W, H
4317	* R
4322	= NGC 4323, W, H
4327	nf, H
4338	= IC 3247?, R
4345	* W
4354	= NGC 4351, W, H
4357	= NGC 4381, R, D IV
4364	nf, R
4366	= NGC 4370, W
4367	nf, H, D III
4368	nf, W, R, H
4397	*** W, D III, H
4398	* W, D III, R, H
4407	= NGC 4413, W, H, L
4409	= NGC 4420, W, h, R
4426 / 4427	**R, D III
4437	= NGC 4417, W, R
4443	* W, D III, R, H
4447	= NGC 4446, W, H
4471	* W, R, H
4505	= NGC 4496, W
4508	nf, H, R
4512	= NGC 4521?, R
4549	nf, R
4554	nf, H, D III
4560	nf, R, D III
4577	= NGC 4543?, R
4582	* R
4604	nf, Hel
4610	= NGC 4470, W, R, D IV
4624	= NGC 4636?, R
4629	** R
4637	nf, H; =NGC 4647?, R
4664	= NGC 4665, W, D IV, R
4667	nf, R, H, D I, D III, L
4706	nf, Hel
4729	nf, Hel
4730	nf, Hel
4752	* R
4766	*** W, L
4797	nf, R, D III

TABLE 1*a*—*Continued*

NGC	
4804	= NGC 4802, R, Hel
4882	= NGC 4886, W
4884	= NGC 4889, W, R
4910	nf, R
4913	nf, R, D III
4960	nf, R
4962	nf, R, D IV
4979	= IC 4198, R, D IV
5003	nf, R
5008	nf, R
5067	** R
5106	* R, D I
5111	= NGC 5110, R
5113	= NGC 5109, R, D I, D IV
5160	** R, D I
5200	** R
5242	nf, W
5268	* R
5310	* R
5317	nf, R
5390	= NGC 5371, W, R
5404	** R
5428	** W, Hel
5429	** W, Hel
5432	** W, Hel
5435	** W, Hel
5467	* W
5527	* W
5588	** R, D I
5648	* W
5699	= NGC 5706, R, D IV
5703	= NGC 5709, R, D IV
5704	nf, R
5819	= NGC 5808, R
5841	nf, W, R
5865	nf, W, D IV
5871	nf, W
5877	*** R
6002	nf, R
6049	nf, L
6064	= NGC 6052, R, D IV
6125	= NGC 6130, R
6199	nf, R
6354	4 st, Hel
6430	chain of 4 st, R
6431	nf, R
6466	= NGC 6478, W
6481	** W
6499	** R, L
6550	= NGC 6548, W, D III
6605	No Cl, R
6625	No Cl, R
6647	No Cl, R
6660	= NGC 6661, W, D II, R
6682	No Cl, R
6724	No Cl, R
6728	No Cl, R
6737	No Cl, R
6749	No Cl, R
6773	No Cl, R
6795	No Cl, R
6828	No Cl, R
6837	No Cl, R
6839	No Cl, R
6843	No Cl, R
6847	nf, R, D I
6873	** R
6895	No Cl, R
6896	nf, R
6901	= IC 5000?, R
6904	No Cl, R
6933	** W, R, L
6947	nf vis. (twice), Hel
6952	= NGC 6951, W, D III
6965	* W, R, Hel
6966	** W, Hel
7011	No Cl, R
7028	nf, R
7043	nf, R
7071	= NGC 7067?, R
7122	* R
7150	nf, R
7161	** R
7186	7 F st, R
7202	nf, Hel
7210	nf, R, D I
7234	No Cl, R
7255	nf vis. (twice), Hel
7326	** W, L
7327	* W, L
7333	** W, R
7338	** W
7350	* W, R
7403	nf, W, R
7431	nf, W
7438	No Cl, R
7439	nf, R, L
7447	* R, D I, D II
7472	nf, R, D II
7477	4 st, R, D II
7504	* R
7526	3 F st in line, R
7555	nf, R, D I
7560	** W, R
7561	* W, R
7565	* R
7574	nf, R
7575	* W, R
7581	= NGC 7541, W, R
7605	= NGC 7583, R
7614	nf, R
7739	nf, R
7748	nf, L
7791	** R
7804	** R, D I, D II
7815	nf, R

TABLE 1*b*

OBJECTS TO BE STRICKEN FROM THE *Index Catalogues*

IC	
1	** W
39	= NGC 178, Hel
47	nf, Hel
89	= NGC 446, R
117	= NGC 558, W
191	= NGC 794, R
280	gp of st, W
281	= NGC 1177, W, R
324	= NGC 1331, W, Hel
339	* W, Hel
394	nf, W
487	= NGC 2494, R
532	nf, Hel
587	BD−1°2334, W
629	= NGC 3312, W
684	= NGC 3644, W, R
689	= NGC 3661, R
765	** W
788	= NGC 4405?, W, H
793	= NGC 4445, W, R, H
805	= NGC 4611, W, H
811	= NGC 4663, W
820	= NGC 4676?, R
839	= NGC 4851?, R
847	= NGC 4974, R, D III
958	nf, W
973	nf, W
974	nf, W
1026	* W
1098	* W
1126	= NGC 5952, R
1148	= NGC 6020?, R
1171	nf, W
1175	nf, W
1179	= NGC 6054, W
1184	** W
1190	nf, W
1282	nf, W
1306	nf, W
1307	nf, W
1312	= NGC 6892?, R
1316	= IC 5000; Decl. of 1316 is wrong, of 5000 correct, W
1325	= NGC 6927, W, R
1326	= NGC 6928, W
1363	nf, W
1441	= NGC 7240, W
1450	* W
1457	* W
1511	= NGC 7767, R
1538	nf, W
1539	= NGC 70, W, R
1547	nf, W
1556	nf, W, Hel
1658	= NGC 444, R
1686	= NGC 499, R
1710	= NGC 575, R
1712	= NGC 584, W, R
1751	= NGC 741, R
1765	= NGC 783, R
1766	= NGC 785, W, R
1851	nf, $1^h\ 50^m$ exp., L
1871	nf, W
1983	nf, W
2040	nf, Hel
2041	nf, Hel
2048	nf, Hel
2077	= NGC 1608, R
2091	gp of F st, W
2092	** W
2107	= NGC 1707, R
2133	nf, W
2154	** W
2173	= NGC 2291, W
2232	= NGC 2543, W, R
2262	
2266	
2270	
2272	
2273	
2274	nf, L. Curtis remarks (L, 13): "I
2275	am unable to identify any of these
2276	objects. IC 2274 appears to be 3
2277	small stars almost in contact.
2278	Most of the others appear to be
2279	simply very faint stars. The re-
2280	gion was carefully checked."
2281	
2284	
2289	
2290	
2291	
2408	* W
2410	= NGC 2667, W, R
2413	* W
2424	= NGC 2704, R, D IV
2425	nf, Hel
2460	nf, W
2500	nf, W
2509	* W
2528	* W
2571	= NGC 3223, W, Hel
2579	= NGC 3251, R, D III
2605	nf, W
2609	? = NGC 3404, Hel
2610	nf, W
2611	* W
2658	* W
2659	* W
2662	* W
2663	nf, W
2664	* W

TABLE 1*b*—*Continued*

IC	
2726	* W
2728	* W
2731	* W
2865	* W
2866	* W
2868	= IC 698, W
2970	*** W
3009	nf, H
3011	= NGC 4124, W, H
3018	nf, may be neb 30′ s of Frost's published position for IC 3018, H
3026	* W
3027	nf, a defect on the plate where it was originally found by Frost, H
3035	= NGC 4165, W, H
3042	= NGC 4178, W, H
3045	nf, H
3048	** W, H
3050	= NGC 4189, W, H
3051	= NGC 4193, W, H
3056	nf, may be neb 1° s of Frost's published position for IC 3056, H
3059	nf, W
3064	= NGC 4206, W, H
3070	* W, H
3071	nf, H
3072	nf, H
3076	nf, H
3083	nf, H
3085	* W, H
3086	nf, H
3087	** W, H
3088	* W, H
3090	** W, H
3098	= NGC 4235, W, H
3102	= NGC 4241, H
3103	* W, H
3113	= NGC 4246, W, H
3114	nf, H
3117	nf, H
3123	* H
3124	* W, H
3129	* W, H
3130	nf, H
3132	= IC 3131, H
3133	nf, H
3139	* W, H
3150	nf, H
3158	* W, H
3160	* W, H
3161 3162	**W, H
3163	** W, H
3181	= NGC 4286, W
3182	gp of 3 st, W, H
3183	* H
3190	* W, H
3191	nf, H
3223	* H
3245	nf, a defect on the plate where it was originally found by Frost, H; ** W
3254	= NGC 4336, H
3256	= NGC 4342 = III 95
3260	= NGC 4341 = III 96 NGC 4343 = III 94 = h 1223. Nos. assigned according to Decl., in which the differences are greater than in R.A., W
3257	nf, W, H
3265	* H
3266	= NGC 4353, H
3273	= NGC 4356, H
3279	* H
3281	nf, H
3307	* W; = IC 3301, H
3310	* W, H
3318	* W, H
3319	= NGC 4390, W, H
3320	= NGC 4390, W, H
3333	* W, H
3339	= NGC 4411, H
3343	nf, H
3350	* W, H
3352	nf, H
3354	* W, H
3356	* W; found by H
3366	nf, W, H
3398	* W; found by H
3400	nf, W, H
3404	nf, H
3408	* H
3414	= H II 26?, nf NGC 4453 18!8, R
3417	* W; = NGC 4470, H
3420	* W, H
3423	nf, W, H
3426	* W, H
3427	= NGC 4482, W, H
3431	* W; found by H
3438	= NGC 4492, H
3447	* W; found by H
3449	** W
3452	= NGC 4497, W, H
3455	nf, W
3463	** W, H
3464	* W
3477	* W
3485	* W, H
3493	* W, H
3504	nf, H
3519	nf, W; found by H
3524	** W, H
3537	** W, H
3538	nf, W
3544	** W, H
3553	** W

TABLE 1*b*—*Continued*

IC	
3566	nf, W, H
3569	= NGC 4561, W
3572	* W, H
3577	** W, H
3584	* W, H
3588	* W; = NGC 4571, H
3594	* W
3601	nf, a defect on the plate where it was originally found by Frost, H
3607	* W; found by H
3616	nf, W; = IC 3612, H
3647	* W; found by H
3648	nf, H
3675	= NGC 4625, W
3676	* W, H
3688	= NGC 4633, W, H
3706	* W
3708	= NGC 4654, W, H
3712	= IC 3690, W; nf, H
3722	* H
3725	= IC 3721, H
3739	nf, H
3743	* H
3760	= IC 815, H
3764	= IC 816, H
3790	* W, H
3792	nf, W, H
3797	nf, H
3801	nf, W, H
3804	= NGC 4711, R
3823	** W
3901	* W
3964	* W
3999	* W, Hel
4015	= NGC 4893, R
4016	= NGC 4893, R
4136	nf, Hel
4156	nf, W
4190	nf, W
4192	nf, W
4211	* W
4338	= NGC 5334, W, Hel
4376	*** Hel
4412	= NGC 5594, R
4471	= NGC 5697, R
4493	= NGC 5747, R
4551	= NGC 5964?, R
4586	= NGC 6014, W
4613	= NGC 6196, R
4616	= NGC 6197?, R
4622	nf, W
4625	= NGC 6240, W, R
4626	nf, W
4643	= NGC 6301, R
4657	nf, W
4700	= NGC 6595, R, Hel
4895	= NGC 6822, W
5029	nf vis, Hel
5031	nf vis, Hel
5057	* W
5058	* W, Hel
5061	*** W, Hel
5082	= NGC 7010, R
5127	= NGC 7102, W, R
5153	nf, W
5155	nf, W
5159	* W
5228	= NGC 7302, W, Hel
5251	* W
5260	nf, Hel
5264	nf, Hel
5265	= IC 1459, W, Hel
5294	nf, Hel
5308	** Hel
5311	* W
5313	nf, Hel
5366	nf, 2^h exp., L
5386	= NGC 7832, R

TABLE 2

NEBULAE NOTED BY DREYER AS MISSING (NOT INCLUDED IN TABLES 1*a* AND 1*b*)

Dreyer II:

NGC	846	988	1458	2531	5881	5926
	874	1174	2652	5834	5884	7045
						7157

Dreyer III:

NGC	58	1575	3704	6465	7157	IC	106
	395	1592	4279	6526	7254		136
	422	1619	4722	6556	7520		165
	458	1689	4740	6588	7522		453
	465	2054	4802	6607	7655		468
	644	2203	4817	6608	7730		507
	716	2491	5357	6668	7761		717
	859	2589	6082	6678	7776		823
	866	2674	6206	6762	7813		1115
	885	2757	6294	6797	7829		1227
	1205	2869	6328	7021			1243
	1327	3103	6398	7105			1247
	1448	3295	6403	7112			1281
	1523	3322	6450	7134			1300
							1463

Dreyer IV:

NGC 1613 = NGC 1611
3110 = 3122

TABLE 3

CORRECTIONS TO DREYER'S POSITIONS

NGC	48	R.A. −7′.4*, W, D III	NGC	3307	N.P.D. −4′.9, W
	49	R.A. −5′.7, W, D III		4024	R.A. −7′.9, W, D III
	51	R.A. −5′.2, W, D III		4046	$11^h\ 55^m.9$, 87° 16′, W
	150	R.A. +7′.2, W, D III		4186	R.A. +9′.4, W
	178	R.A. +22′.7, W, D III		4301	$12^h15^m.3$, 84° 40′, W
	739	5′.9 np NGC 740, W		4392	1′.7 p NGC 4389, not f, W
	1188	R.A. +8′.9, W, D III		4482	R.A. −6.9, W, D III
	1191	R.A. +5′.8, W, D III		4799	$12^h40^m.2$, 86° 28′, L
	1192	R.A. +6′.5, W, D III		4840‡	NGC correct, W
	1331	10^s p NGC 1332, W		5070	1′ sf NGC 5077, W
	1350	$3^h25^m.6$, 124° 6′ (1860), W		5480	R.A. −21′.5, W
	1373	N.P.D. −5′, W		5481	R.A. −23′.1, W
	1382	R.A. +12′.2, W		5669	R.A. −8′.1, W, D III
	1394	R.A. +6′.6, W, D II		6555	$18^h1^m.6$, 72° 30′, W, D III
	1416†	NGC correct, W		6579§	NGC correct, W
	1422	R.A. −12′, W, D III		6580§	NGC correct, W
	1455	R.A. −11′, L		7361	R.A. −26′, W
	1489	R.A. −8′.2, W, D III		7451§	NGC correct, W
	1518	R.A. −14′, W, D III	IC	148	N.P.D. −19′.8, W
	1521	R.A. −14′, W, D III		346	$3^h35^m.4$, 108° 44′, W, D III
	1640	R.A. +21′, W, D II		1077	N.P.D. −5′.2, W, D III
	1744	R.A. −8′.6, W, D III		1254	R.A. −5′.3, W
	2653	N.P.D. −10′, L		2168	N.P.D. −30′, W
	2977	$9^h29^m.7$, 14° 30′, R		5195	3′.4 ssf NGC 7242, W
	3143	N.P.D. −4′.7, W, D III			

* Value of $\Delta\alpha \cos\delta$; $\Delta\alpha$ = correction to catalogue R.A. reduced to minutes of arc.

† Howe's correction (D III) to NGC not confirmed.

‡ Wolf's correction (D III) to NGC not confirmed.

§ Bigourdan's correction (D III) to NGC not confirmed.

TABLE 4

NEBULAE WHICH HAVE BEEN REPORTED NOT FOUND, BUT WHICH APPEAR ON MOUNT WILSON PLATES IN CATALOGUE POSITIONS

NGC	373	** R; neb + *, W
	1402	? a *, Hel; Sa neb, W
	2536	Knot in s arm of NGC 2535?, R; SBc neb, W
	2827	=IC 2460?, R; Reinmuth describes the correct neb but it is not = IC 2460, no neb there, W
	4320	nf by Frost, D III; SBc_p neb, W
	4465	nf by Schwassman, D III; SBa neb, W
	4467	nf by Schwassman, D III; E4 neb, W
	4637	= NGC 4647?, R; nf, H; the S, F neb v close f NGC 4638 was probably the one observed at Birr; Schwassman really measured 4638 instead of 4637 that he records, W
	4673	neb * 13, R; E1 neb, W
	4792	doubtful, D III; E3 neb, W
	4853	neb *, R; neb, W
	5373	neb *, R; E0 neb, W
	5615	v doubtful, R; SBa neb, W
	5867	* 14.5, not nebulous, R. Reinmuth observed a star but not the object found by Lord Rosse, which is 1'.5 ssp of NGC 5866, W
	6359	neb *, R; E1 neb, W
	6549	3 st, mag. 14, in line, R; SBa neb, W
	6927	identif. doubtful, R; SBa neb, W
	7325	? neb *, R; SBc neb, W
	7336	nf, L; SBb neb, W
	7340	nf, L; E2 neb, W
	7353	nf, R; SBc neb, W
	7682	eeF pL neb s 9', R; SBab neb, Reinmuth refers to a group of stars, W
IC	3672	= IC 809, H; S0 neb, W

This work has been carried out under the general direction of Dr. Hubble, to whom I am indebted for advice and assistance, sometimes in the search for an elusive photograph and sometimes in settling a difficult question of identity.

CARNEGIE INSTITUTION OF WASHINGTON
MOUNT WILSON OBSERVATORY
December 1939

NOTES

RELATIVE POPULATIONS OF 2^1S AND 2^3S STATES OF HELIUM IN THE ORION NEBULA*

ABSTRACT

The observed equivalent width of λ 3889 of *He* I produced by the Orion nebula, together with the absence of λ 3965, leads to a lower limit for the ratio of populations of the 2^3S and 2^1S states of $N_3/N_1 \geq 25$. This is considerably in excess of the values calculated by Struve and Wurm on the assumption of strict metastability for both levels, and thus points toward a shorter mean life for 2^1S than for 2^3S. The matter may be complicated, however, by the selective absorption by the nebula of the light from the Trapezium stars.

Breit and Teller[1] find that, under conditions similar to those to be expected in a gaseous nebula, the 2^1S level of *He* I should have a much shorter mean life than the 2^3S level. It is therefore of interest to examine briefly the observational data bearing on this point. The line $2^3S - 3^3P$ λ 3889 has been observed in absorption in all the stars of the Trapezium, and, from its character and displacement, it must originate in the surrounding nebula. Observations are most numerous for the brightest Trapezium star (ϑ'C Orionis), in which the line is found to have a total absorption of 0.20 A.[2] No lines arising from the 2^1S level have been observed, although a careful search has been made for them. The line $2^1S - 4^1P$ λ 3965 is well placed for observation on spectrograms taken primarily for λ 3889, a number of which have been secured with the 32-inch Schmidt camera arrangement at the coudé spectrograph of the 100-inch telescope. These plates, of excellent quality, have a linear dispersion of 10.2 A/mm, and it may be rather conservatively estimated that the total absorption of λ 3965 cannot exceed 0.01 A. Similarly, the line $2^1S - 3^1P$ λ 5016 has not been found, although, owing to certain technical difficulties, the observations in this part of the spectrum are less satisfactory than those at shorter wave

* *Contributions from the Mount Wilson Observatory, Carnegie Institution of Washington*, No. 625.

[1] *Ap. J.*, **91**, 215, 1940.

[2] *Pub. A.A.S.*, **9**, 274, 1939.

lengths. Nevertheless, the equivalent width of λ 5016 probably cannot exceed 0.02 A.

The preceding data permit the calculation of a lower limit for the ratio N_3/N_1, where N_3 and N_1 signify the populations of the 2^3S and 2^1S states, respectively. On the linear portion of the curve of growth a transition having the oscillator strength f and arising from a level whose population is N cm^{-3} will produce a total absorption A_λ given by

$$A_\lambda \propto NLf\lambda^2,$$

where L is the path length through the absorbing material. (The geometry of the problem, as in the case of interstellar lines, justifies the neglect of emission into the beam.) The values of f for λ 3889 and λ 3965 are 0.052 and 0.063, respectively.[3] Hence a lower limit for N_3/N_1 is given by

$$\frac{N_3}{N_1} \geq \frac{0.2}{0.01} \cdot \left(\frac{3965}{3889}\right)^2 \cdot \frac{0.063}{0.052} = 25.$$

This result is to be compared with the calculations of Struve and Wurm,[4] who derived approximate values of N_3/N_1 for different temperatures and dilution factors on the assumption that both 2^1S and 2^3S were strictly metastable. Their data show that N_3/N_1 has only a rather weak dependence upon the dilution factor and does not differ very greatly from the Boltzmann distribution for a given temperature. In fact, it may be estimated that N_3/N_1 would not exceed approximately 12 and 6 for $T = 10^4$ and $T = 2.5 \times 10^4$, respectively, even for very small dilution factors. Hence, unless the value of T appropriate to the Orion nebula is appreciably less than 10,000°, the observational evidence must be considered as offering support to the theoretical work of Breit and Teller. The difficulty is that the Orion nebula is known to absorb selectively the light of the stars within it.[5] Thus, for example, if the reddening produces an excess in the radiation density in the infrared, relative to that in the

[3] Hylleraas, *Zs. f. Phys.*, **106**, 395, 1937.

[4] *Ap. J.*, **88**, 84, 1938; see Table 4.

[5] Baade and Minkowski, *Mt. W. Contr.*, No. 572; *Ap. J.*, **86**, 123, 1937.

blue-violet, the transition $2^1s - 2^1P$ λ 20582 will occur with greater relative frequency than is accounted for in the calculations of Struve and Wurm. Since 2^1P connects directly with the ground state, 1^1S, the net result will be a depopulation of 2^1S, with little or no effect upon 2^3S. Unfortunately, this possibility seems to make the astrophysical evidence for a shorter mean lifetime for 2^1S than for 2^3S rather uncertain.

O. C. WILSON

CARNEGIE INSTITUTION OF WASHINGTON
MOUNT WILSON OBSERVATORY
January 1940

NOTE ON THE POINT-CONVECTIVE MODEL FOR THE SUN

ABSTRACT

The internal temperature, density, and mass distributions of the sun have been calculated on the basis of the point-convective model, using tables of Strömgren and the Kramers' opacity law, $\kappa = \kappa_1 \rho / T^{3.5}$. These tables are more extensive than Cowling's and are useful for investigations into the energy production of main-sequence stars more massive than the sun.

In his paper on "Energy Production in Stars," H. A. Bethe[1] quotes values for the central temperature and central density of the sun which were found by the present author on the basis of the point-source convective model. It seems worth while to publish this calculation in more detail and for its own intrinsic interest. Its significance for a quantitative discussion of the nuclear sources of energy in main-sequence stars will be pointed out elsewhere.[2]

For the model under consideration the central regions must be in convective equilibrium, and they will therefore consist of polytropic cores of index $n = 1.5$[3] surrounded by "point-source envelopes." In the envelope the standard equation of radiative equilibrium will be valid. For given M, R, L, μ, and κ_1, the envelope equation may be numerically integrated inward from the surface of the star subject

[1] *Phys. Rev.*, **55**, 450, 1939.

[2] H. A. Bethe and R. E. Marshak, "Progress Reports in Physics," *Physical Society of London*, 1939.

[3] If we neglect radiation pressure, an assumption justifiable for the sun.

to the boundary conditions $\rho = 0, T = 0, M_r = M$ at $r = R$. Assuming that $M = M_\odot$, $R = R_\odot$, $L = L_\odot$, $\mu = 1$ (corresponding to the theoretically computed hydrogen content of about 35 per cent by weight[4]), Strömgren[5] has performed the integration with the following values of log κ_1:

$$24.99,\ 24.89,\ 24.79,\ 24.69,\ 24.59,\ 24.49,\ 24.39\ .$$

From his tables it is seen that for large values of κ_1, $\rho \to \infty$, $T \to \infty$ as $r \to 0$ (the "centrally condensed" solutions); for the smaller values of κ_1, $M_r = 0$ at $r > 0$ (the "collapsed" solutions). The physically significant temperature-density distribution corresponds to some intermediate value of $\kappa_1 = \kappa_1^0$.

To find this distribution we shall assume that the energy is being produced entirely within the convective core and that the outer radiative envelope (where the luminosity has of course been taken as constant and equal to the total luminosity) must be fitted to this convective core.[6] This fitting can be performed by standard methods.[7] It is found that at the interface between the point-source envelope and the polytropic core we have the values

$$\xi' = 1.22\ ; \qquad \theta'_{3/2} = 0.776\ ; \qquad R' = 1.23 \times 10^{10}\ ;$$
$$T' = 15.8 \times 10^6\ ; \qquad \rho' = 34.7\ .$$

$\theta_{3/2}$ is the Emden function of index $3/2$ and ξ the "normalized" distance. Further, at the center we have

$$T_c = 20.4 \times 10^6\ ; \qquad \rho_c = 50.8\ .$$

Also for $\mu = 1$ it is found that $\log_{10} \kappa_1^0 = 24.708$. The close agreement between these values of $R'/R_\odot$, T'/T_c, ρ'/ρ_c and the values of the same quantities computed in the general case by Cowling[8] (by a

[4] Cf. B. Strömgren, *Zs. f. Ap.*, **7**, 22, 1933. Strömgren employed the standard model to compute the hydrogen content. However, it is not expected that the "point-source" values (at least for negligible radiation pressure) will differ appreciably from Strömgren's values; this is due to the insensitive dependence in the mass-luminosity formula of the average molecular weight on the energy-source concentration.

[5] These tables were made available through the kindness of Professor Gamow.

[6] S. Chandrasekhar, *Introduction to the Study of Stellar Structure*, pp. 222–228, 1939.

[7] *Ibid.*, pp. 351–355.

[8] *M.N.*, **96**, 42, 1936 (cf. also n. 6).

somewhat different technique) is excellent. It is worthy of note that an application of Strömgren's semiempirical method[9] to determine κ_1^0 leads to precisely the same result.

Table 1 gives the temperature, density, and mass distributions for the sun in the region of radiative equilibrium. The values of these quantities in the convective core can be found simply by the use of tables of the Emden function of index 1.5. The superiority of Table 1

TABLE 1

$t=\log_{10}\left(\frac{1}{r}-\frac{1}{R_\odot}\right)$	$\log_{10} T$	$\log_{10} \rho$	$M_r/M_\odot$
0.40 −12.....	5.977	7.862−10	1.000
0.50 −12.....	6.077	8.186−10	0.999
0.60 −12.....	6.176	8.510−10	0.998
0.70 −12.....	6.276	8.834−10	0.996
0.80 −12.....	6.375	9.157−10	0.991
0.90 −12.....	6.475	9.478−10	0.980
0.00 −11.....	6.573	9.794−10	0.961
0.10 −11.....	6.670	0.102	0.927
0.20 −11.....	6.764	0.399	0.871
0.25 −11.....	6.810	0.541	0.833
0.30 −11.....	6.855	0.676	0.791
0.35 −11.....	6.898	0.803	0.735
0.40 −11.....	6.939	0.923	0.675
0.45 −11.....	6.978	1.035	0.610
0.50 −11.....	7.015	1.137	0.540
0.55 −11.....	7.051	1.228	0.470
0.60 −11.....	7.083	1.307	0.400
0.65 −11.....	7.113	1.374	0.334
0.70 −11.....	7.140	1.433	0.274
0.75 −11.....	7.165	1.483	0.221
0.80 −11.....	7.188	1.522	0.174
0.825−11.....	7.199	1.538	0.155

over the Cowling table[10] lies in the fact that values of T and ρ are given at much closer intervals in the region of radiative equilibrium just outside the convective core. This is important when one wishes to find the temperature-density distribution of more massive stars than the sun on the point-convective model; one may use a homology transformation on the sun and then correct for radiation pressure by means of a perturbation calculation.

R. E. MARSHAK

UNIVERSITY OF ROCHESTER

[9] *Zs. f. Ap.*, **2**, 343, 1931; $\kappa_1 = \kappa_1^0$ when $d^2M_r/dt^2 = 0$ for $M_r = M_\odot/2$.

[10] See Cowling, *op. cit.*, Appendix.

ON THE NUMBER OF BALMER LINES IN EARLY-TYPE STARS

The quantum number of the last Balmer line clearly seen on spectrograms obtained with the quartz Cassegrain spectrograph of the McDonald Observatory,[1] on Eastman Process emulsion, has been plotted against spectral type in Figure 1. The absolute magnitudes

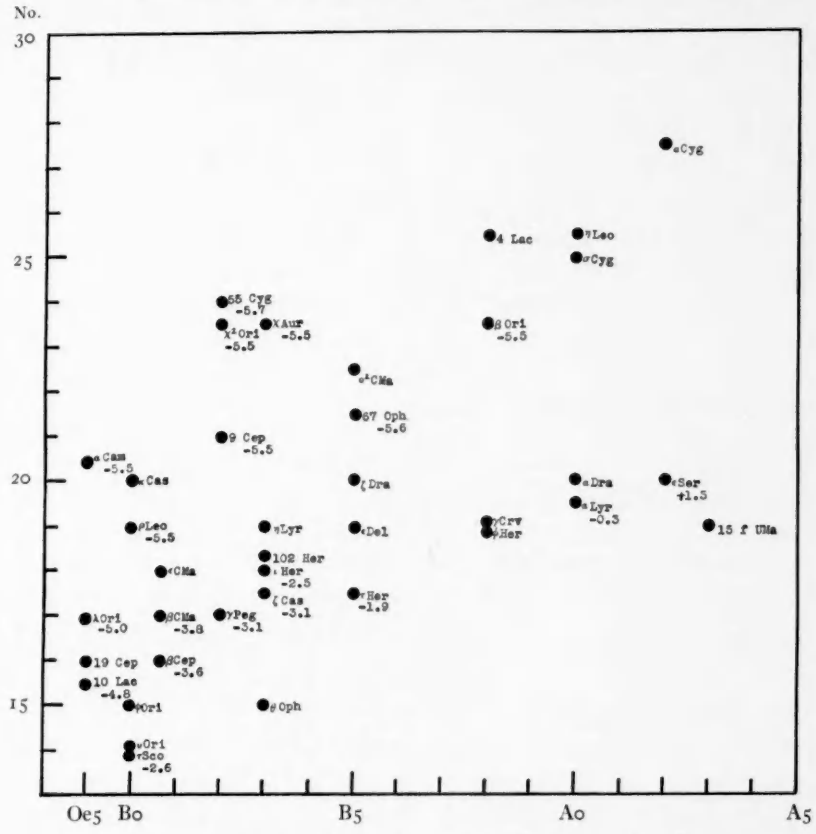

FIG. 1.—The ordinate gives the number of Balmer lines as a function of spectral type.

determined by E. G. Williams[2] from his spectral types and luminosity groups (ML) are shown, where available, below the name of each star. The absolute magnitudes of α Lyrae and ε Serpentis are based

[1] O. Struve, *Ap. J.*, **90**, 699, 1939. [2] *Ap. J.*, **83**, 333, 1936.

upon trigonometric parallaxes. The spectral classes are essentially those of the *Henry Draper Catalogue*, corrected in accordance with Struve's sequences.[3] The correlation between the number of Balmer lines and the absolute magnitude, within each spectral subdivision, is very conspicuous. Stars having appreciable rotational broadening were not used.

An interesting feature of the observations is the fact that the apparent widths of the last few Balmer lines in supergiants are always quite small. This is conspicuous in α Cygni, but the effect is also present in the B2 supergiant 55 Cygni, where H_{23} and H_{24} are surprisingly narrow.[4] On the other hand, the higher members of the two *He* I series, $2^1P - n^1D$ and $2^3P - n^3D$, are distinctly diffuse in 55 Cygni. It would appear, therefore, that Stark broadening is appreciable in supergiant B stars. The apparent sharpness of the H lines must be due to the confluence of the wings, which permits us to discern only the central cores of fairly strong broadened lines.

A. Unsöld
O. Struve

McDonald Observatory
and
Yerkes Observatory
August 1939

NOTE ON ROSS 22

The faint star Ross 22 was suspected to be a white dwarf (or a subdwarf) on the basis of the early spectral type, F, as determined from four plates[1] and from the large published motion, 0".77 per year. Dr. Van Maanen now informs the writer that he found no evidence of motion for this star; the plates available at the Yerkes Observatory confirm this conclusion and show that the published motion was due to a defect. The star should therefore be dropped from the writer's list.

G. P. Kuiper

March 13, 1940

[3] *Ap. J.*, **78**, 73, 1933.

[4] Struve designated these lines as "sharp" in his list of wave lengths of B stars (*ibid.*, **90**, 722, 1939).

[1] *Ap. J.*, **90**, 269, 1940.

REVIEWS

Tabelle der Hauptlinien der Linienspektren aller Elemente. By H. KAYSER. 2d ed. by R. RITSCHL. Berlin: Julius Springer, 1939. Pp. viii+269. Rm. 28.50.

Since the appearance of the first edition[1] of this table in 1926 many new measurements of wave lengths have been published, especially in the ultraviolet and infrared regions of the spectrum. The ultraviolet limit has been extended from 124 to 32.75 A, but the infrared limit of the first edition, 90,850 A for *Na* I, has been retained in the new edition. Dr. Ritschl points out that improvements in the photographic technique have produced a vast increase in the number of lines between 7000 and 12,000 A, as well as in the ultraviolet, but that there is only a relatively small increase on the infrared side of 12,000 A. All wave lengths are given in international angstrom units. Those longer than 2000 A are given for air; those shorter than 2000 A are given for vacuum. Most wave lengths are given to 0.01 A, but there are still many for which the precision of measurement warrants the use of only one decimal place.

Dr. Ritschl points out that "the confusion concerning the data on intensities, which had already been discussed in the first edition, has become rather worse," especially because of the tendency to increase the range of estimated intensities to many thousand units. "All intensities are crude estimates which have a meaning only in narrow spectral regions and only within a single spectrum." Astrophysicists will find it difficult to understand why the experimental physicists have given so little attention to the problem of accurate intensities.

OTTO STRUVE

Tafeln und Aufgaben zur harmonischen Analyse und Periodogrammrechnung. By K. STUMPFF. Berlin: Julius Springer, 1939. Pp. vii+174. Unbound, Rm. 36; bound, Rm. 39.60.

This volume contains a collection of tables and numerical examples supplementing the same author's book, *Grundlagen und Methoden der Periodenforschung*, which was reviewed in this *Journal*, **87**, 216, 1938.

[1] See review in *Ap. J.*, **65**, 133, 1927.

Physical Meteorology. By JOHN G. ALBRIGHT. New York: Prentice-Hall, Inc., 1939. Pp. xxvii+392. $5.35.

The author has presented in this book the material which he has, for a period of ten years, been presenting in a course in meteorology at Case School of Applied Science. He has emphasized the physical aspects of meteorology, and the book presupposes a knowledge of the principles of physics. One chapter on the principles of heat is included because of its frequent application in the study of the atmosphere. The book is divided into twenty chapters. The last of these, on atmospheric optics, occupies twenty-six pages. The book should be of interest to astronomers.

The Concepts of the Calculus. By CARL B. BOYER. New York: Columbia University Press. Pp. vii+346. $3.75.

The author gives a suggestive outline of the development of the basic concepts of calculus from their incipiency in antiquity to their final formulation in modern times. There are eight chapters: (i) Introduction, (ii) "Concepts in Antiquity," (iii) "Medieval Contributions," (iv) "A Century of Anticipation," (v) "Newton and Leibniz," (vi) "The Period of Indecision," (vii) "The Rigorous Formulation," (viii) Conclusion.

MICROFILM SETS OF PERIODICALS

The Committee on Scientific Aids to Learning, President Conant of Harvard, chairman, has made a grant to cover the cost of making a microfilm master-negative, on the most expensive film, of sets of volumes of scientific and learned journals.

This permits the nonprofit Bibliofilm Service to supply microfilm copies at the sole positive-copy cost, namely, 1 cent per page for odd volumes, or a special rate of $\frac{1}{2}$ cent per page for any properly copyable ten or more consecutive volumes.

The number of pages will be estimated on request to American Documentation Institute, Offices of Science Service, 2101 Constitution Avenue, Washington, D.C.

ERRATUM

On page 312 of Volume **90,** second line of the footnote, *read* NaO *instead of* N_2O.